

“The Nonperturbative laws of QCD in Experiments (Part II)”

S.S. Shimanskiy (JINR, Dubna)



ров, А. А. Богуш, Л. М. Томильчик, Н. М. Шумейко). Она сыграла большую роль в становлении и укреплении теоретической, а впоследствии и экспериментальной физической школы в Белоруссии.

Слушателям школы, а среди них было достаточно много молодежи, предлагалась разнообразная программа. Она охватывала исследования в области высоких и низких энергий, неускорительной физики, новые тенденции в квантовой теории поля. Были и необычные для таких школ лекции по нанотехнологиям, новым материалам и квантовым технологиям. За восемь рабочих дней можно было познакомиться с последними экспериментальными результатами, полученными на ускорителях

RHIC, HERA, тэватроне, DESY, а также с перспективой проведения в будущем исследований на LHC.

Заметный интерес аудитории вызвали лекции ректора школы Н. Русаковича (о 50-летии ОИЯИ и программе ATLAS), И. Мешкова (ускорители вчера, сегодня, завтра). С большим вниманием были прослушаны лекции по синтезу сверхтяжелых элементов (М. Иткис), об информационных технологиях (В. Иванов) и изучении структуры сплошных сред с помощью рассеяния нейтронов (А. Белушкин). Запомнилось яркое выступление молодого исследователя из Бельгии Ф. Морттата (исследования на детекторе CMS).

Много докладов было сделано белорусскими учеными. Доклад Л. М. Томильчика был посвящен

Гомель (Белоруссия), 25 июля – 5 августа. VIII Международная школа-семинар «Актуальные проблемы физики микромира»



Gomel (Belarus), 25 July – 5 August. VIII International school-seminar «Actual Problems of Microworld Physics»

VIII International Physics School in Gomel

The traditional school-seminar «Actual Problems of Microworld Physics» was held on 25 July – 5 August in Gomel (Belarus). The history of this school dates back to 1971. Its initiators were physicists from JINR (N. N. Bogoliubov, V. G. Kadyshevsky, A. N. Sissakian, I. A. Savin, N. B. Skachkov) and Belarus (F. I. Fedorov, A. A. Bogush, L. M. Tomilchik, N. M. Shumeiko). It has played an important role in establishing and strengthening the theoretical and, later, experimental physics school in Belarus.

The school attendees, who were largely young scientists, were offered a comprehensive programme. It included

research in high- and low-energy physics, nonaccelerator physics, modern trends in quantum field theory. Quite unusual for such schools, there were also lectures on nanotechnologies, new materials and quantum technologies. Over a period of eight working days, the students of the school had an opportunity of getting acquainted with the recent experimental results obtained at the accelerators RHIC, HERA, Tevatron, DESY, as well as with the prospects of conducting future research at the LHC.

Great interest was shown by the audience in the lectures of School Rector N. Russakovich (on JINR's 50th anniversary and the ATLAS programme) and I. Meshkov (accelerators of yesterday, today and tomorrow). Lectures on



HIGH p_T ISSUES at SPD



1. Diquark properties.
2. The Confinement laws.
3. Nature of the spin effects.
4. The Deuteron spin structure.
5. FSI (with s,c -quarks participation).
6. Nature of CsDBM.
7. np dilepton production anomaly.
8. Exotic states.
9. Subthreshold J/Ψ production.

...

CsDBM investigation

Исследования на коллайдере ОИЯИ ($\sqrt{s_{NN}} < 10 \text{ GeV}$).

Шиманский С.С.

18.08.2006

1. Физическая программа.

Детали физической программы будут опубликованы. Предварительно эти вопросы докладывались и обсуждались на семинарах в ОИЯИ (ЛВЭ, ЛТФ и ЛЯП), а также в ИФВЭ (г.Протвино, 2-е совещание по поляризационной программе на У-70) и в ПИЯФ(г.Санкт-Петербург,XL зимняя школа ПИЯФ). Здесь изложены только выводы.

Физическая программа может быть разделена на две части:

- 1) поиск и исследования горячей кварк-глюонной фазы (ГКГФ) (вкраплений кварк-глюонной плазмы) образующейся в ядро-ядерных взаимодействиях;
- 2) исследование холодной кварк-глюонной фазы (ХКГФ) с использованием процессов в области больших p_T и поляризованных пучков.

Исследования ХКГФ непосредственно связаны в вопросами структуры нуклонов в области доминирования валентных夸克ов, кора NN -взаимодействия и свойств холодной ядерной материи при плотностях в несколько раз превосходящих обычную. Все эти вопросы имеют решающее значение для построения теории эволюции звезд и предсказания свойств материи в центре звезд. Программа исследований по пункту 2) может быть сделана уникальной, если предусмотреть в проекте коллайдера

The first QCD Phase Diagram

EXPONENTIAL HADRONIC SPECTRUM AND QUARK LIBERATION

N. Cabibbo and G. Parisi, Phys. Lett. B59 (1975) 67

The exponentially increasing spectrum proposed by Hagedorn is not necessarily connected with a limiting temperature, but it is present in any system which undergoes a second order phase transition. We suggest that the "observed" exponential spectrum is connected to the existence of a different phase of the vacuum in which quarks are not confined.

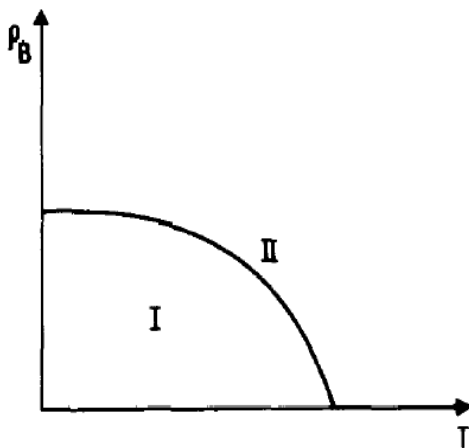


Fig. 1. Schematic phase diagram of hadronic matter. ρ_B is the density of baryonic number. Quarks are confined in phase I and unconfined in phase II.

Curious “warnings” in the paper:

These results do not take into account the presence of ghosts.

The true phase diagram may actually be substantially more complex, due to other kinds of transitions,

RHIC Physics: 3 Lectures*

Larry McLerran

Physics Department PO Box 5000 Brookhaven National Laboratory Upton, NY 11973 USA

September 13, 2003

+ CERN Yellow
Report
2007-005, p.75

The Evolving QCD Phase Transition

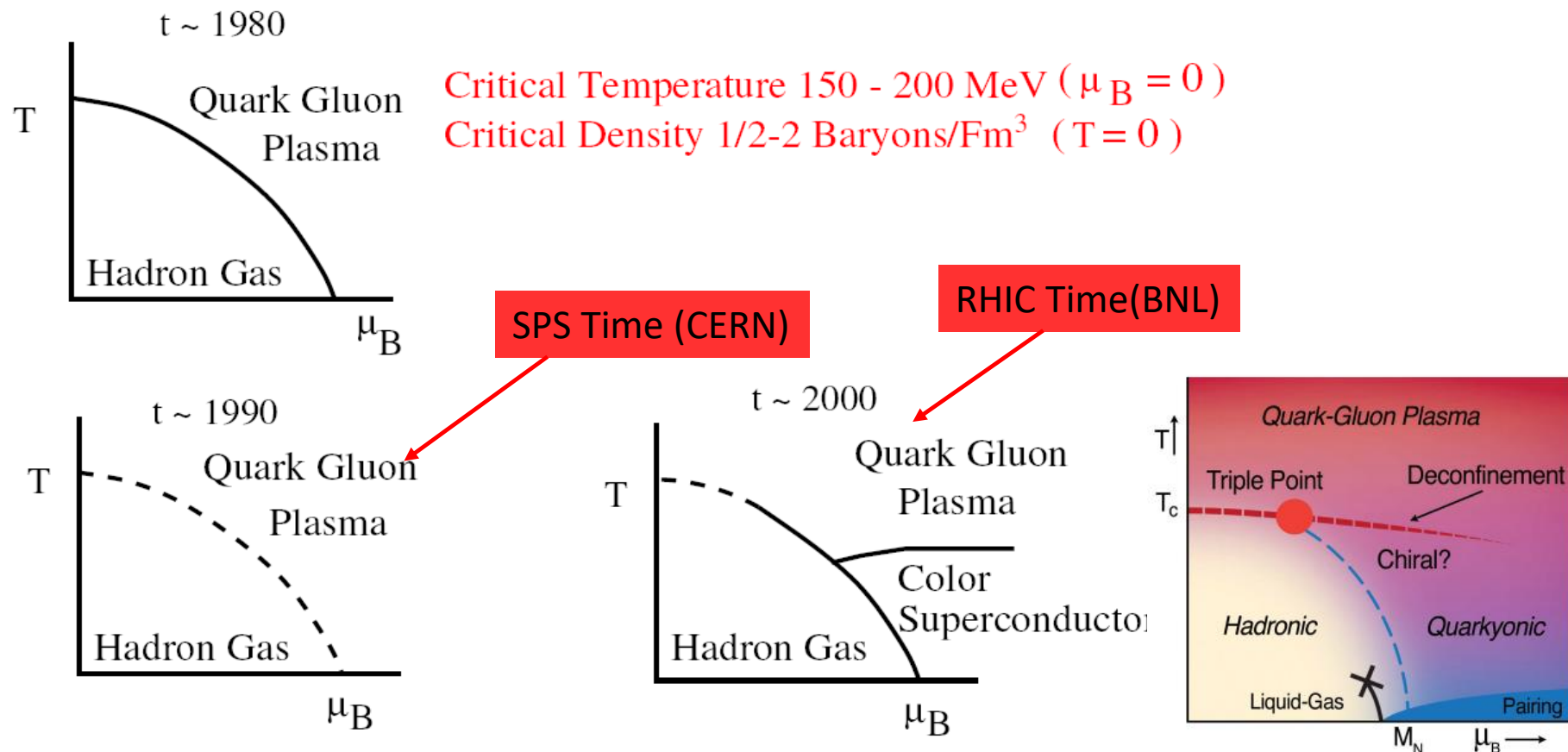
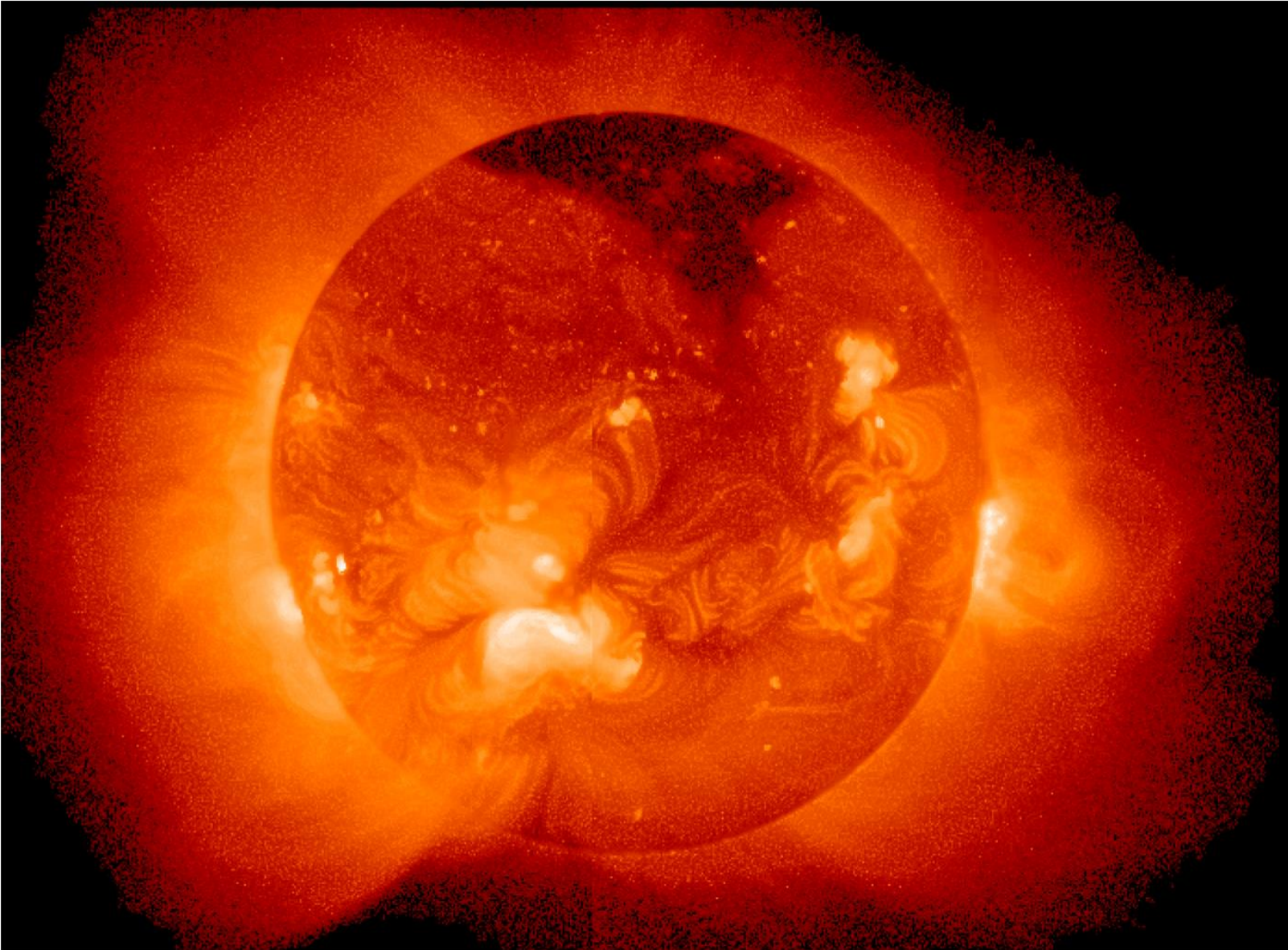


Figure 4: A phase diagram for QCD collisions.

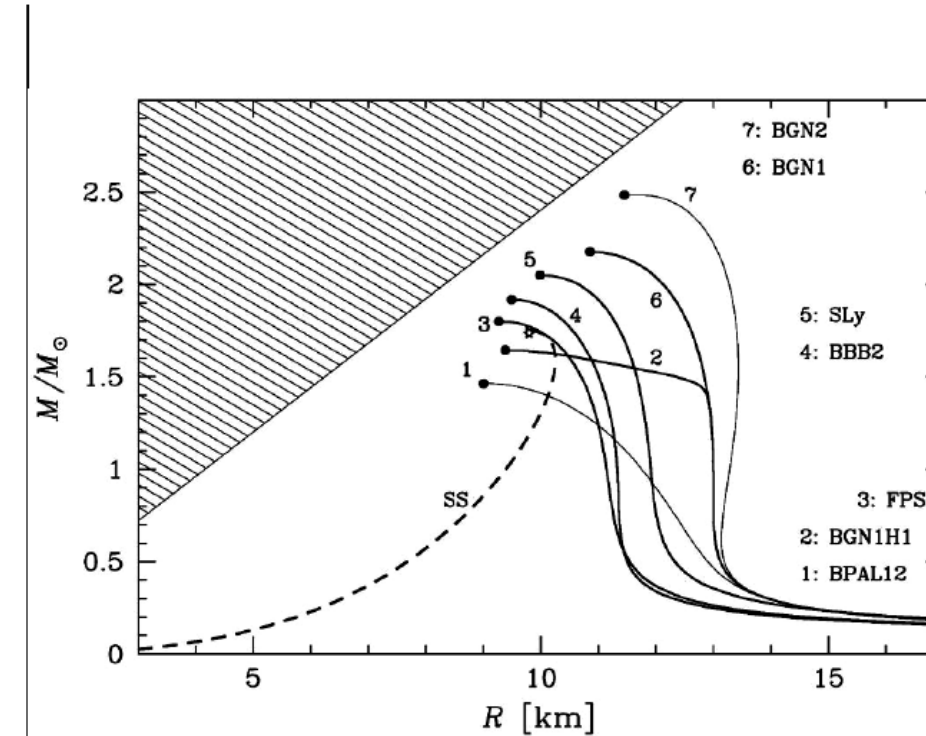
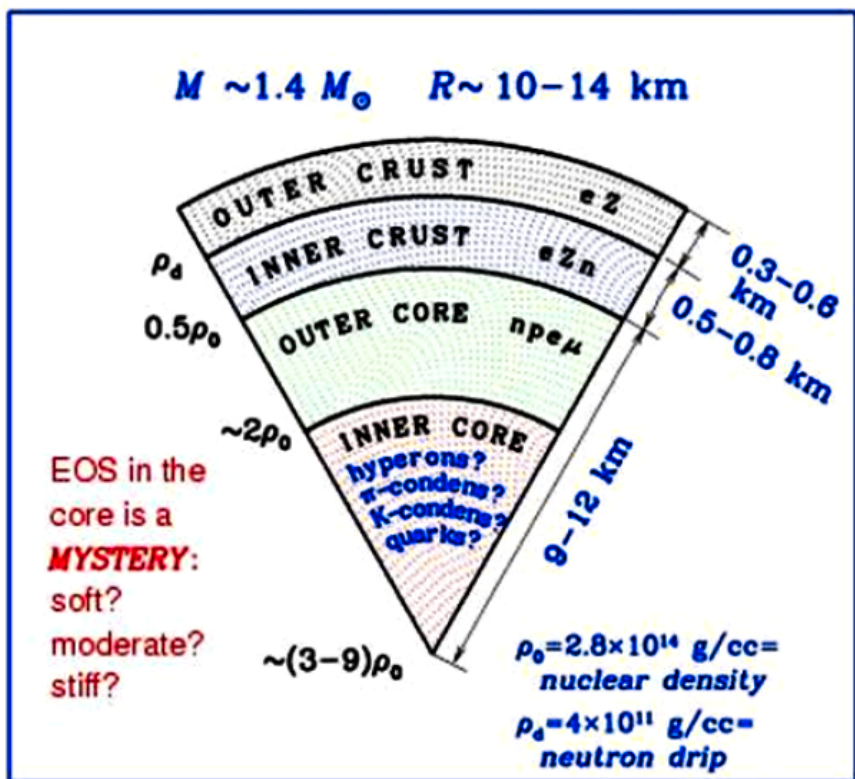
Temperature at the centre of the Sun $\sim 15\,000\,000$ K



A medium of 170 MeV is more than 100 000 times hotter !!!

Remnants of the collapse: Neutron stars

NS internal structure is determined by equation of state which is poorly known



Summary of advanced nuclear burning

Advanced Nuclear Burning Stages
(e.g., 20 solar masses)

Fuel	Main Product	Secondary Products	Temp (10 ⁹ K)	Time (yr)
H	He	¹⁴ N	0.02	10 ⁷
He	C,O	¹⁸ O, ²² Ne s- process	0.2	10 ⁶
C	Ne, Mg	Na	0.8	10 ³
Ne	O, Mg	Al, P	1.5	3
O	Si, S	Cl, Ar K, Ca	2.0	0.8
Si	Fe	Ti, V, Cr Mn, Co, Ni	3.5	1 week

FRIDOLIN WEBER*, ALEXANDER HO†, RODRIGO P. NEGREIROS‡,
PHILIP ROSENFIELD§

$$H \sim 10^{16} \text{ Gs}$$

$$E \sim 10^{19} \text{ V/cm}$$

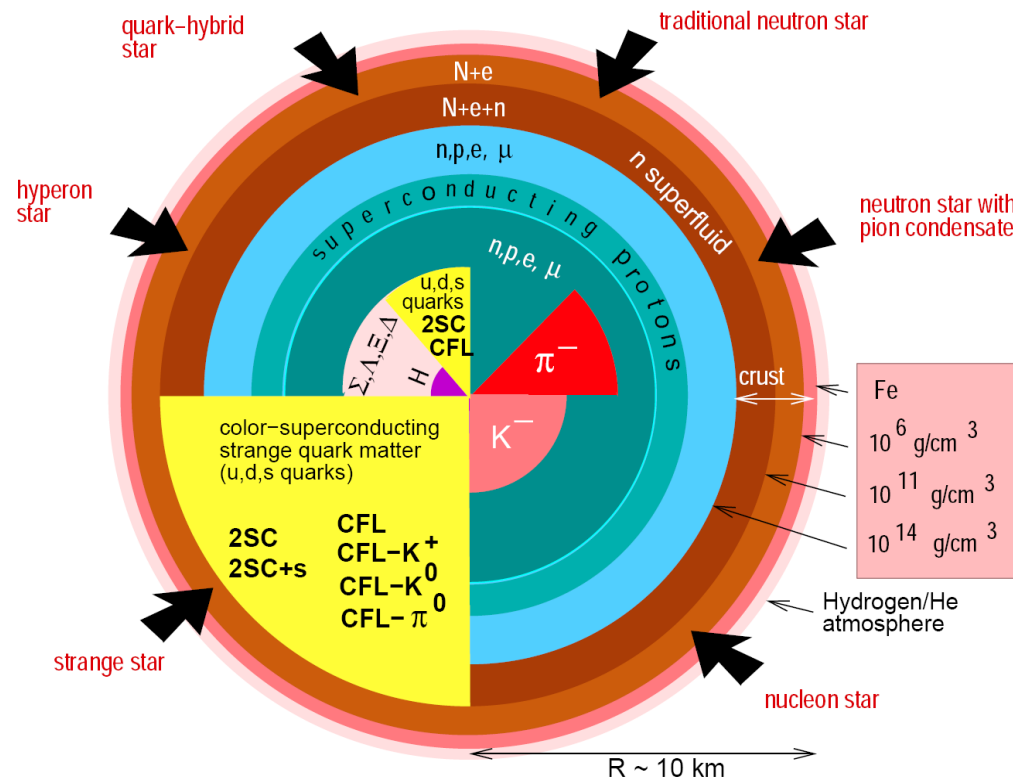


Fig. 1. Competing structures and novel phases of subatomic matter predicted by theory to make their appearances in the cores ($R \lesssim 8 \text{ km}$) of neutron stars⁴.

significant range of chemical potentials and strange quark masses⁵¹. If the strange quark mass is heavy enough to be ignored, then up and down quarks may pair in the two-flavor superconducting (2SC) phase. Other possible condensation patterns

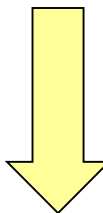
color-superconducting
strange quark matter
(u,d,s quarks)

K. Rajagopal and F. Wilczek, *The Condensed Matter Physics of QCD*, At the Frontier of Particle Physics / Handbook of QCD, ed. M. Shifman, (World Scientific) (2001).
M. Alford, Ann. Rev. Nucl. Part. Sci. **51** (2001) 131.

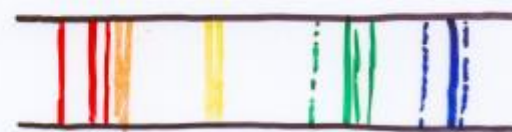
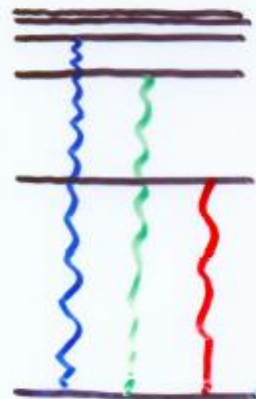
F. Close

Structure of Matter

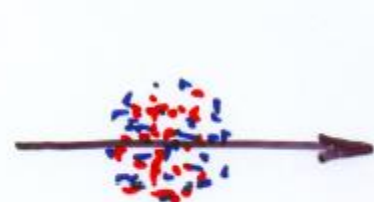
Two ways that structure is revealed:



1. SPECTRA



2. SCATTERING FROM "HARD" CENTRES



True from atoms to particles....

The Beginning

ON THE FLUCTUATIONS OF NUCLEAR MATTER

D. I. BLOKHINTSEV

Joint Institute for Nuclear Research

Submitted to JETP editor July 1, 1957

J. Exptl. Theoret. Phys. (U.S.S.R.) 33, 1295-1299 (November, 1957)

It is shown that the production of energetic nuclear fragments in collisions with fast nucleons can be interpreted in terms of collisions of the incoming nucleon with the density fluctuations of the nuclear matter.

1. INTRODUCTION

THE motion of nucleons in nuclei can result in short-lived tight nucleon clusters, in other words, in density fluctuations of nuclear matter. Since such clusters are relatively far removed from the other nucleons of the nucleus, they become atomic nuclei of lower mass in a state of fluctuating compression.

In their study of the scattering of 675-Mev protons by light nuclei, Meshcheriakov and coworkers^{1,2} observed recently certain effects which confirm the existence of such fluctuations, at least for the simplest nucleon-pair fluctuations, which lead to the formation of a compressed deuteron.

We recall in this connection reports in earlier works^{3,4} that high-energy nucleons can split nuclei into "supra-barrier" fragments, i.e., fragments with an energy much larger than their binding energy and the energy of the Coulomb barrier. However, there was a lack of quantitative experimental data on which to base the theoretical analysis.

Some authors related this curious process, without foundation, to hypothetical long-range nuclear forces. Others tried to connect it with nuclear many-body forces.

The experimental data on the emission of high-energy deuterons from light nuclei give support to the idea that "supra-barrier" fragments are produced also by direct collision of an incoming nucleon with a tight nucleon cluster that results from density fluctuations of the nuclear matter. We offer in the following a quantitative argument in favor of the production of fast deuterons and other "supra-barrier" fragments by such fluctuations.

Concerning the nuclear many-body forces, it should be noted that, according to existing estimates,⁵ there is no reason to believe that they are considerably stronger than the two-body forces. At the instant of dense clustering both paired and collective interactions may take place. However, at present there exists no experimental information which would allow an explanation of this interaction, or in particular allow a determination of the relative contributions of the paired and the collective interactions.

2. INTERACTION OF DEUTERONS WITH FAST PROTONS

It was shown experimentally^{1,2} that scattering of 675-Mev protons by deuterium produces, in addition to scattered nucleons, a small number of undestroyed deuterons of high energy (up to 660 Mev). This shows that in such collisions the nucleon imparts an appreciable fraction of its momentum to the deuteron as a whole.

КРАТКИЕ
СООБЩЕНИЯ
ПО
ФИЗИКЕ

January 1, 1971

№ 1 январь 1971

It is possible to obtain the record high energy
particle beams by means of accelerating
the heavy nuclei with large charges

АКАДЕМИЯ НАУК СССР

Ордена Ленина

Физический институт им. П.Н. Лебедева

МАСШТАБНАЯ ИНВАРИАНТНОСТЬ АДРОННЫХ СТОЛКНОВЕНИЙ И ВОЗМОЖНОСТЬ ПОЛУЧЕНИЯ ПУЧКОВ ЧАСТИЦ ВЫСОКИХ ЭНЕРГИЙ ПРИ РЕЛЯТИВИСТСКОМ УСКОРЕНИИ МНОГОЗАРЯДНЫХ ИОНОВ

А. М. Балдин

Пучки частиц высоких энергий до последнего времени получались исключительно на протонных и электронных ускорителях, т.е. при ускорении частиц, обладающих единичным зарядом. Ускорение частиц, обладающих зарядом большим единицы, как известно, в принципе дает возможность получить энергию ускоряемых частиц (при одинаковых параметрах ускорителя) большую, чем энергия протонов, в число раз, равное кратности заряда. Так, например, на Дубненском синхрофазотротце, рассчитанном на получение протонов с энергией 10 Гэв, можно получить ядра гелия с энергией 20 Гэв, а ядра неона (заряд 10 е) с энергией 100 Гэв. Возникает естественный вопрос, не получатся ли в результате столкновения с мишенью ядер, например, неона, обладающих энергией 100 Гэв, пучки вторичных частиц, полученные пока только на Серпуховском ускорителе? Утвердительный ответ на этот вопрос означал бы, что с помощью ускорения тяжелых ядер, обладающих более высоким зарядом, можно было бы сравнительно дешевым способом в короткие сроки получить пучки частиц рекордно высоких энергий.

Цель настоящей заметки - рассмотреть этот вопрос и сделать определенные предсказания.

Обычно на вопрос о возможности передачи большой энергии составным ядром отдельному (например, сво-

Выражаю глубокую благодарность С. Б. Герасимову,
А. Б. Говоркову и Г. Н. Флерову за обсуждение изложенных
соображений. Как мне стало известно, Г. Н. Флеров еще несколько лет назад высказывал мысль о возможных кумулятивных эффектах при соударении реалистических ядер.

Поступила в редакцию
11 ноября 1970 г.

Л и т е р а т у р а

1. Л. И. Седов. Методы подобия и размерности в механике. ГИТГЛ, Москва, 1957 г.
2. К. П. Станюкович. Неустановившиеся движения сплошной среды. ГИТГЛ, Москва, 1958 г.
3. J. D. Bjorken. Phys. Rev., 179, 1547 (1969).
4. В. А. Матвеев, Р. М. Мурадян, А. Н. Тахвелидзе. Сообщения ОИЯИ Р2-4578, 1969 г.
5. В. А. Матвеев, Р. М. Мурадян, А. Н. Тахвелидзе. Сообщения ОИЯИ Е2-4968, 1970 г.
6. Ю. Б. Бушнина, Ю. П. Горин, С. П. Денисов и др. Ядерная Физика, 10, 585 (1969).

The first introduction of the term “cumulative effect”

Выражая глубокую благодарность С. В. Герасимову, А. Б. Говоркову и Г. Н. Флерову за обсуждение изложенных сопротивлений. Как мне стало известно, Г. Н. Флеров еще несколько лет назад высказывал мысль о возможных кумулятивных эффектах при соударениях реликтнических ядер.

Поступила в редакцию
11 ноября 1970 г.

Л и т е р а т у р а

Jim Baggott HIGGS

The Invention and Discovery of the ‘God Particle’

Oxford University Press, 2012

FOREWORD

by Steven Weinberg

“Like many other theorists, I did not fully accept the existence of quarks until the 1973 work of David Gross and Frank Wilczek, and David Politzer. They showed that in the theory of quarks and strong nuclear forces known as quantum chromodynamics, the strong force gets weaker with decreasing distance”.

“Как и многие теоретики, я не вполне принимал существование существование кварков до 1973 года, до работы Дэвида Гросса, Фрэнка Вильчека и Дэвида Политцера. Они показали, что в теории кварков и сильных ядерных взаимодействий, называемой КХД , сильное взаимодействие становится слабее с уменьшением расстояния”.

ОБЪЕДИНЕННЫЙ
ИНСТИТУТ
ЯДЕРНЫХ
ИССЛЕДОВАНИЙ
Дубна



P1 - 5819



ЛАБОРАТОРИЯ ВЫСОКИХ ЭНЕРГИЙ

А.М. Балдин, Н. Гиордэнеску, В.Н. Зубарев,
А.Д. Кириллов, В.А. Кузнецов, Н.С. Мороз,
В.Б. Радоманов, В.Н. Рамжин, В.А. Свиридов,
В.С. Ставинский, М.И. Янута

НАБЛЮДЕНИЕ ПИОНОВ
ВЫСОКОЙ ЭНЕРГИИ
ПРИ СТОЛКНОВЕНИИ РЕЛЯТИВИСТСКИХ
ДЕЙТОНОВ С ЯДРАМИ

1971

The first experimental data

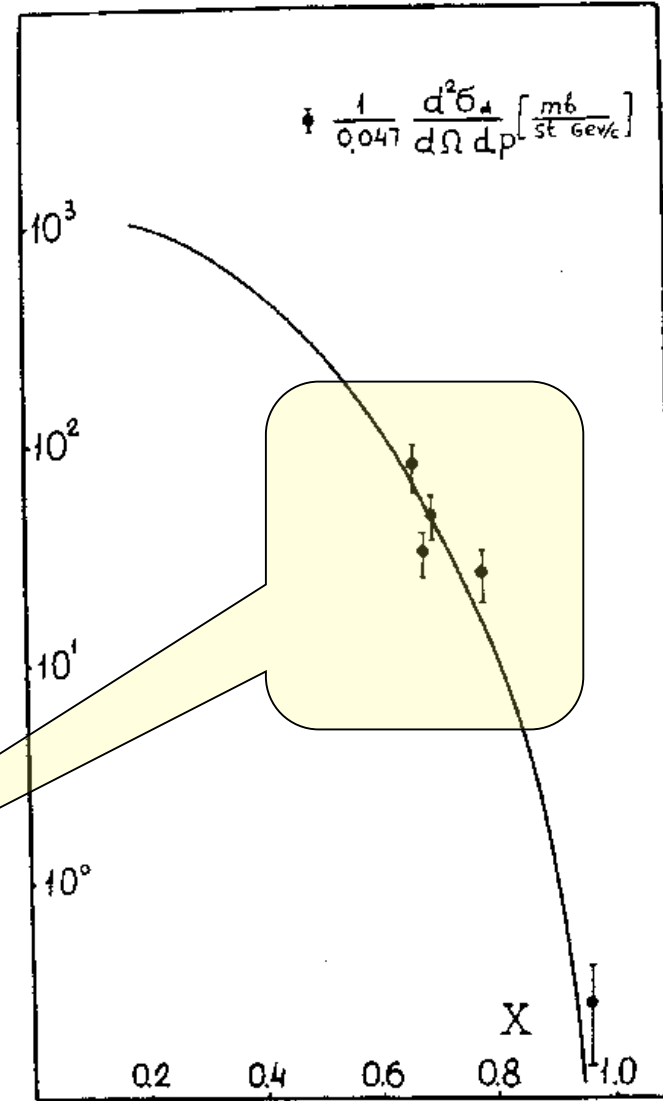
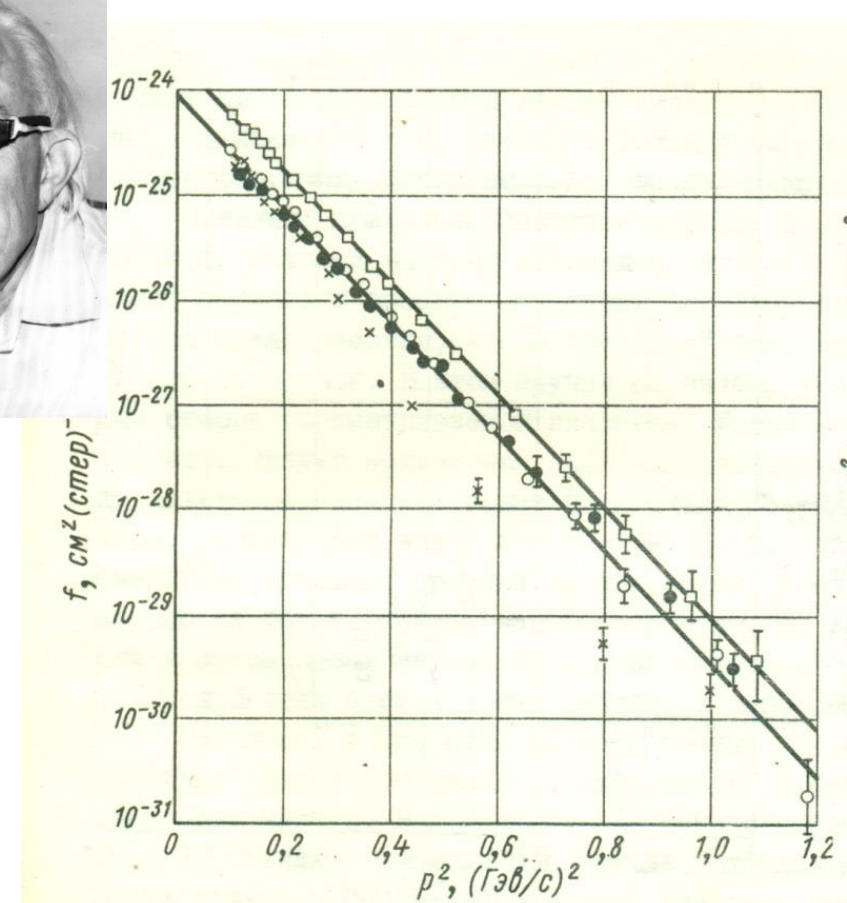
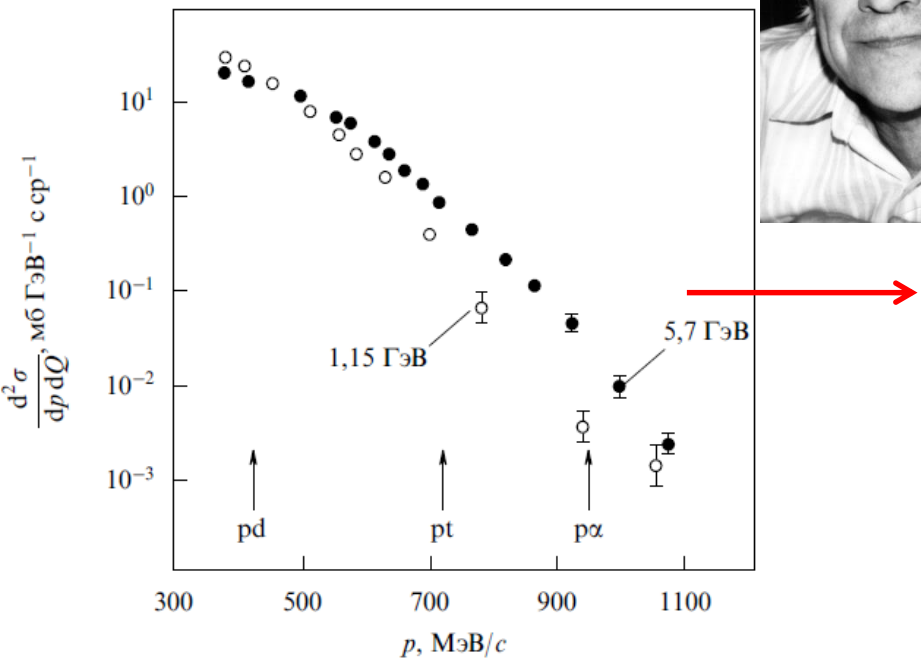
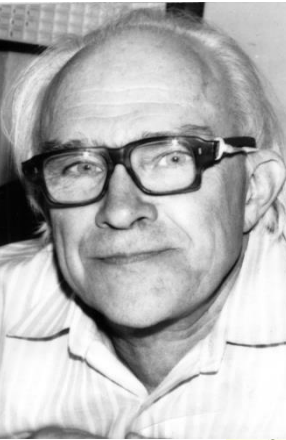


Рис. 3. Сравнение экспериментальных данных по сечению рождения пиона дейtronами с теоретической функцией, описывающей сечение рождения пиона протонами.

ITEP data for proton spectra (G.A.Leksin et al.)



На рисунках приведены спектры протонов, измеренные на ускорителе ИТЭФ под углом 137° в реакции $p+C \rightarrow p+X$ [2]. Стрелки показывают положения ожидавшихся квазиупругих максимумов для рассеяния на многонуклонных кластерах типа d, t, He . Присутствие в спектре частиц, за пределами ограничений кинематики $p\bar{p}$ взаимодействия ясно видно. Это были первые измеренные спектры протонов в кумулятивной области при начальных энергиях несколько ГэВ.

Баюков и др., Изв. АН СССР т.30, 1966, с.521

Рис. 6. Зависимость инвариантной функции от квадрата импульса вторичного протона, вылетающего из меди, облученной протонами с энергией 3,66 ГэВ \square ; из углерода, облученного протонами с энергией 1,15 ГэВ $*$; 3,66 ГэВ \diamond и 5,7 ГэВ \bullet

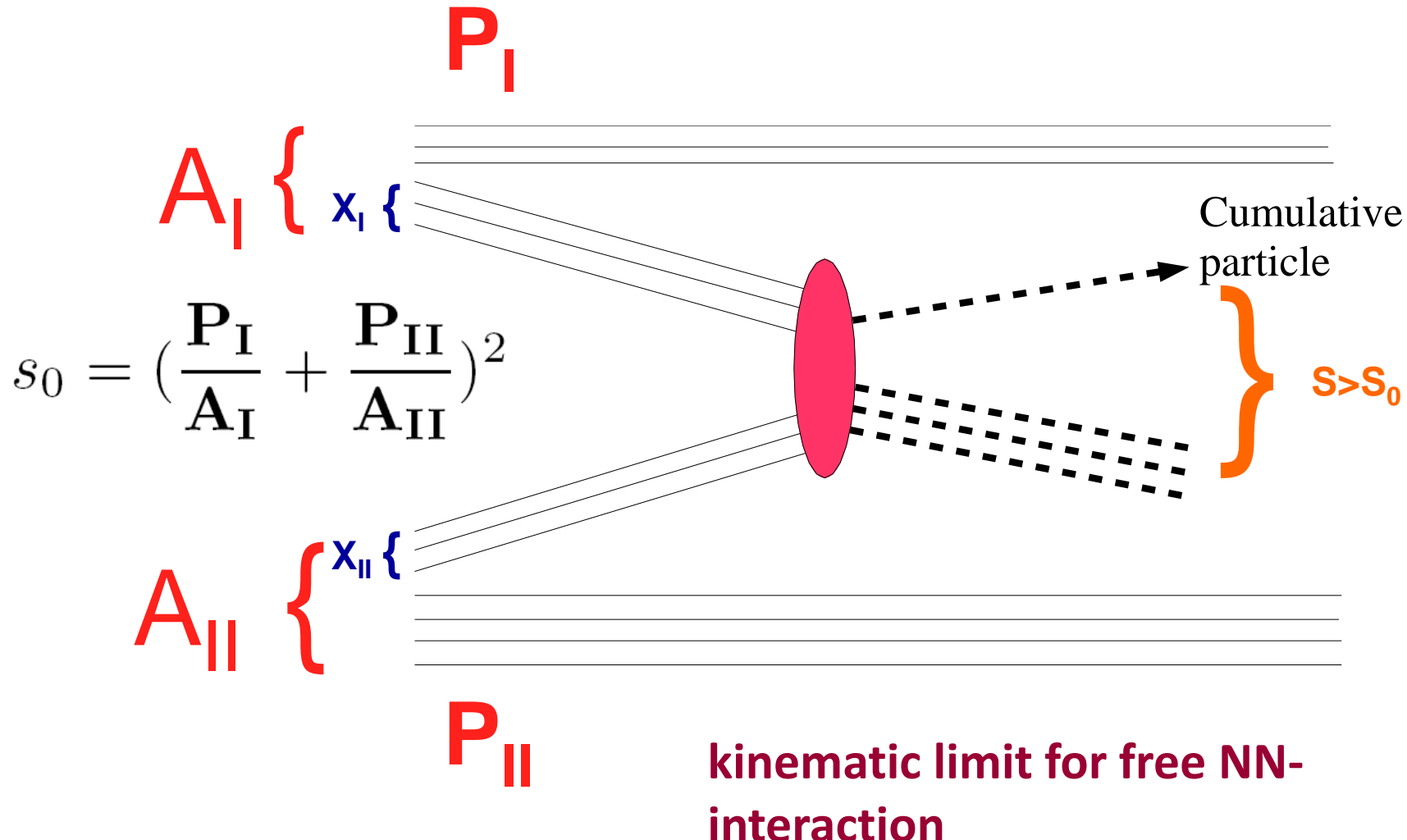
ЯФ т.18, с.1246, 1973

SPECTRA

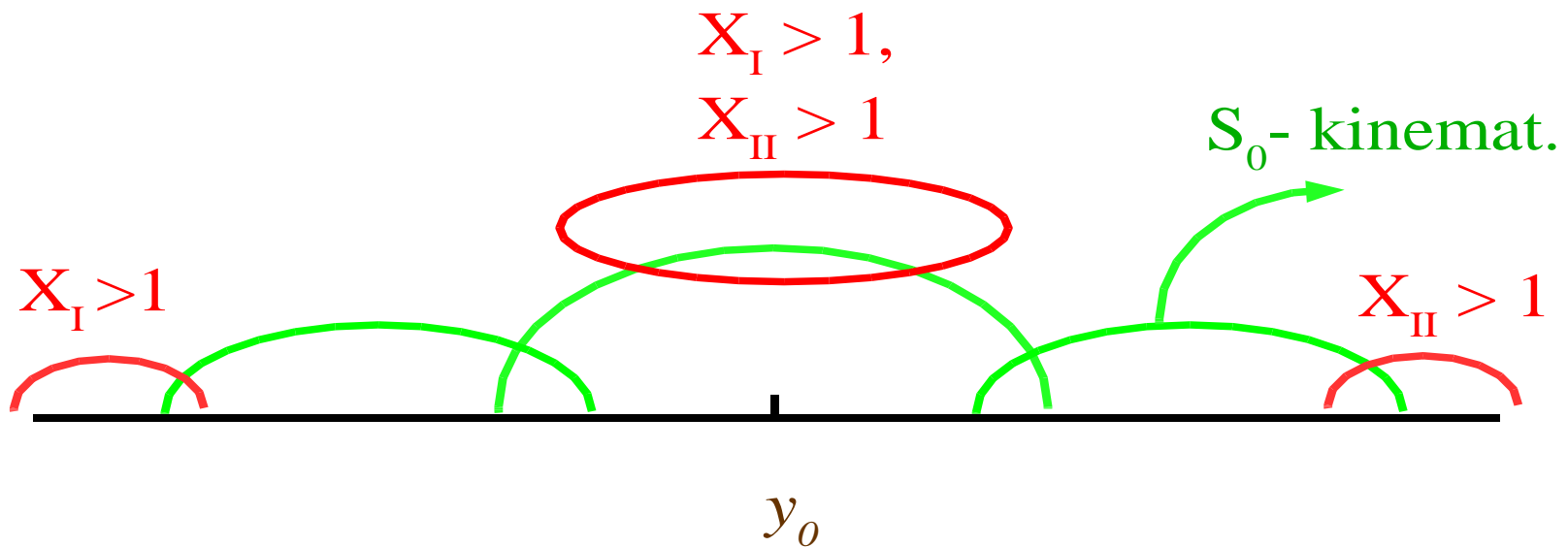
$$(X_I \cdot M_I) + (X_{II} \cdot M_{II}) \rightarrow m_c + [X_I \cdot M_I + X_{II} \cdot M_{II} + m_2]$$

Quark-parton model

$$(X_I \cdot P_I) + (X_{II} \cdot P_{II}) \rightarrow M(X_I, X_{II})$$



Cumulative kinematical region



Cumulative processes:

- 1) $X_I \leq 1$ and $X_{II} > 1$ } Fragmentation
- 2) $X_{II} \leq 1$ and $X_I > 1$ } regions
- 3) $X_I > 1$ and $X_{II} > 1$ Central region

ЕДИНЫЙ АЛГОРИТМ ВЫЧИСЛЕНИЯ ИНКЛЮЗИВНЫХ СЕЧЕНИЙ
РОЖДЕНИЯ ЧАСТИЦ С БОЛЬШИМИ ПОПЕРЕЧНЫМИ ИМПУЛЬСАМИ
И АДРОНОВ КУМУЛЯТИВНОГО ТИПА

В.С.Ставинский

Предложен единый алгоритм вычисления инклюзивных сечений рождения частиц с большими поперечными импульсами и адронов кумулятивного типа. Возможность единого описания этих процессов обусловлена введением нового аргумента — минимальной энергии сталкивающихся конституентов, необходимой для рождения наблюдаемой частицы. Проведено сравнение с экспериментальными данными.

Работа выполнена в Лаборатории высоких энергий ОИЯИ.

Unique Algorithm for Calculation of Inclusive Cross Sections of Particle Production with Big Transverse Momenta and of Cumulative Type Hadrons

V.S.Stavinskij

Unique algorithm is proposed for calculating inclusive cross sections of particle production with big transverse momenta and cumulative type hadrons. A possibility of unique description of these processes is due to introduction of a new argument — of minimal energy of colliding constituents needed for the production of observed particle.

The investigation has been performed at the Laboratory of High Energies, JINR.

Fragmentation regions

$$\mu + N_{min} \cdot m \rightarrow m_c + [N_{min} \cdot m + \Delta]$$

for $E_\mu \gg m_i, E_c$

$$X = N_{\min} = Q \cong \frac{(E_c - \beta_\mu \cdot P_c \cdot \cos \theta_c)}{m} + \dots \equiv X_I(X_{II}) \quad \text{Stavinsky (1970's)}$$

Common case for AA-collisions

V.S. Stavinsky JINR Rapid Communications N18-86, p.5 (1986)

$$(X_I \cdot M_I) + (X_{II} \cdot M_{II}) \rightarrow m_c + [X_I \cdot M_I + X_{II} \cdot M_{II} + m_2]$$

$$S_{\min}^{1/2} = \min(S^{1/2}) = \min[(X_I \cdot P_I + X_{II} \cdot P_{II})^{1/2}]$$

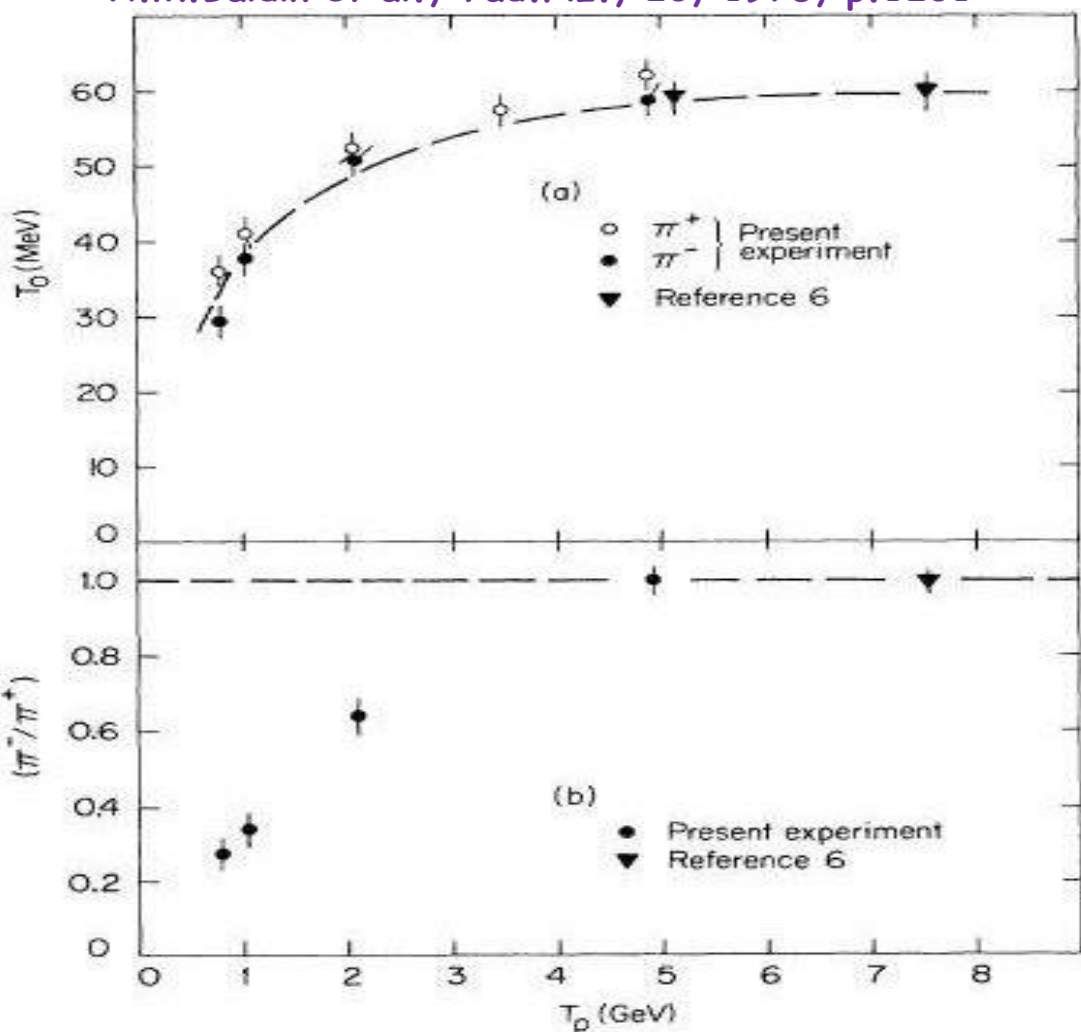


FIG. 1. Energy dependence of (a) T_0 parameter for pions, and (b) the π^-/π^+ ratio at 180° obtained by integrating each spectra up to 100 MeV for p -Cu collisions from 0.8 to 4.89 GeV. The dashed curve in both cases refers to the predictions of the "effective-target" model (Refs. 3 and 4).

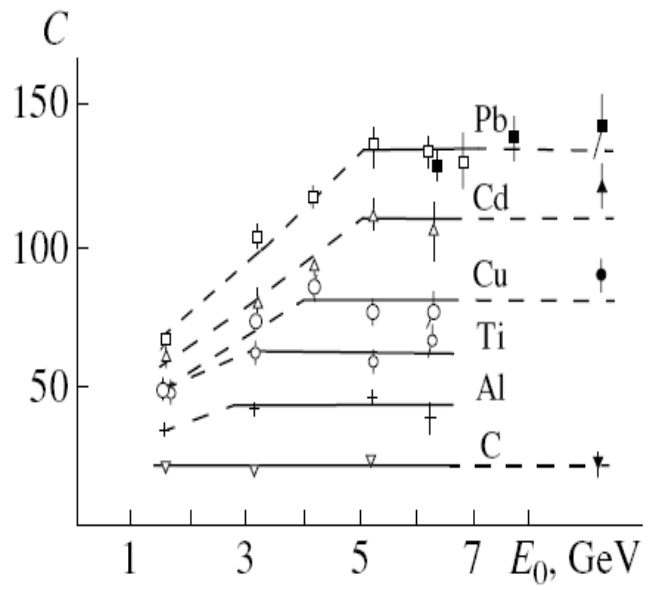


Fig. 3. The coefficient $C(T_0 = 125 \text{ MeV})$ in the parametrization of the invariant function $f = C \exp(-T/T_0)$ in the reaction $pA(C, \text{Al}, \text{Ti}, \text{Cu}, \text{Cd}, \text{Pb}) \rightarrow pX$ for a proton escape angle of 120° in the laboratory frame versus the incident-proton energy. The filled circles refer to the initial energy of 400 GeV.

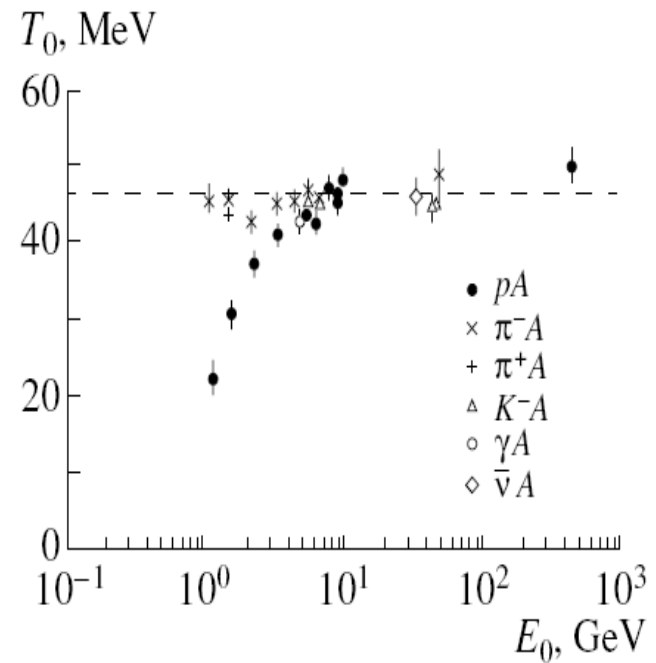
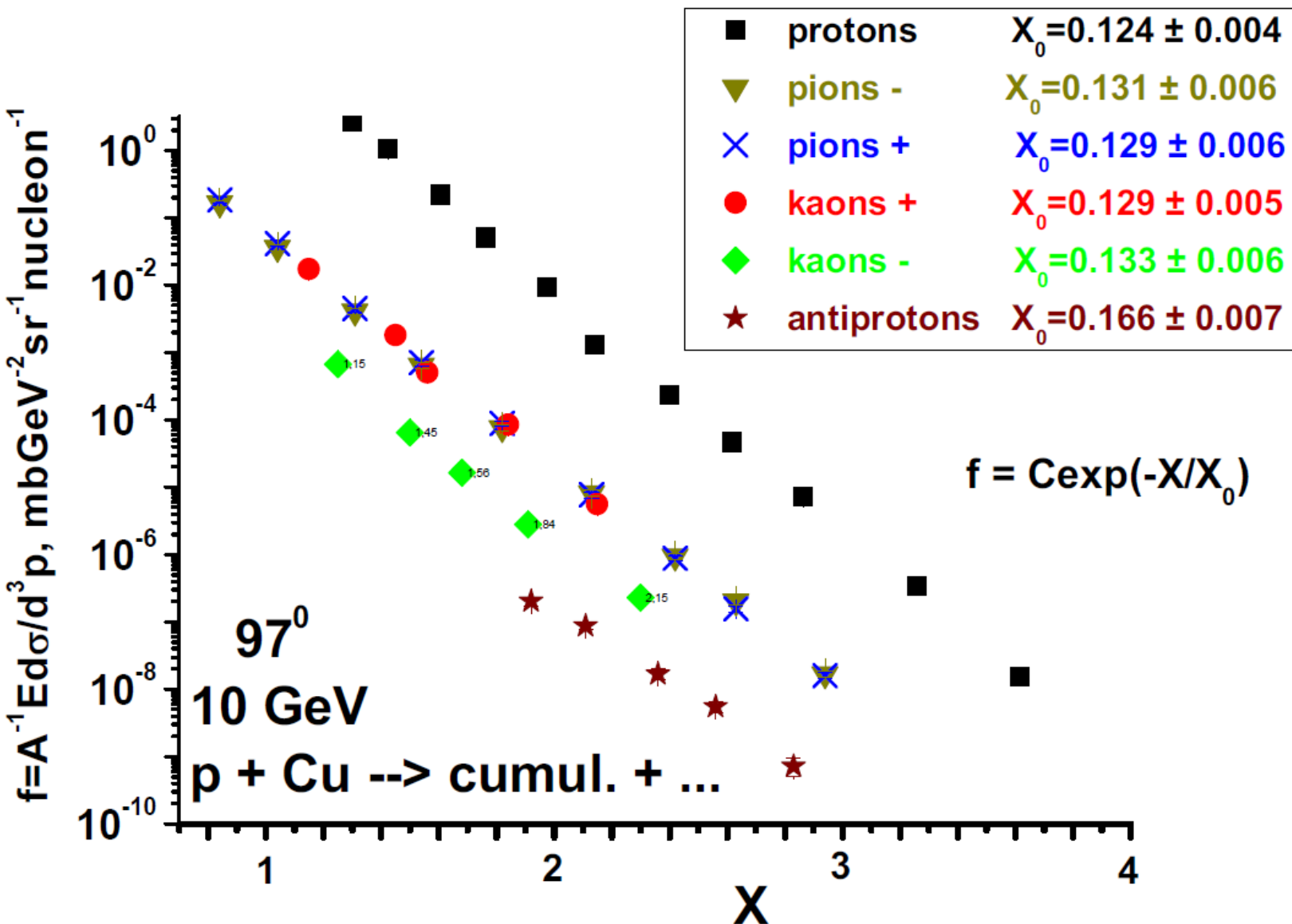


Fig. 5. Dependence of the slope parameter T_0 for the invariant function of the protons escaping under the action of $p, \pi^\pm, K^-, \gamma, \bar{\nu}$ with various energies E_0 ; the escape angle is 120° in the laboratory frame.



A - зависимость (1974-...)

$$\varepsilon \frac{d\sigma}{dp} (p + A \rightarrow \pi) \sim \begin{cases} A - \text{для тяжелых ядер} \\ A^{n>1} - \text{для лёгких ядер} \end{cases}$$

$$\varepsilon \frac{d\sigma}{dp} (p + A \rightarrow A') \sim \begin{cases} A^{5/3} - \text{для } d \\ A^2 - \text{для } t \end{cases}$$

В это же время группа Кронина обнаружила похожую сильную A-зависимость в процессах рождения частиц с большими p_T !!!

THEORIES

LARGE MOMENTUM PION PRODUCTION IN PROTON NUCLEUS COLLISIONS AND THE IDEA OF "FLUCTUATIONS" IN NUCLEI

V.V. BUROV

The Moscow State University, Moscow, USSR

and

V.K. LUKYANOV and A.I. TITOV

Joint Institute for Nuclear Research, Dubna, USSR

Received 27 January 1977

It is shown that in proton-nucleus collisions, the production of pions with large momenta can be explained by the assumption of the existence of nuclear density fluctuations ("fluctuations") at short distances of the nucleon core radius order, with the mass of several nucleons.

The purpose of this note is to realize the idea [4] that the cumulative effect is connected largely with a suggestion on the existence in nuclei of the so-called fluctuons. Earlier fluctuons were proposed [7] in order to understand the nature of the "deuteron peak" in the pA-scattering cross section at large momentum transfers [8] and also to interpret the pd-scattering cross section [9]. Compressional fluctuations of mass $M_k = km_p$ of nucleons in the small volume $V_\xi = \frac{4}{3}\pi r_\xi^3$ where r_ξ is the fluctuon radius were assumed.

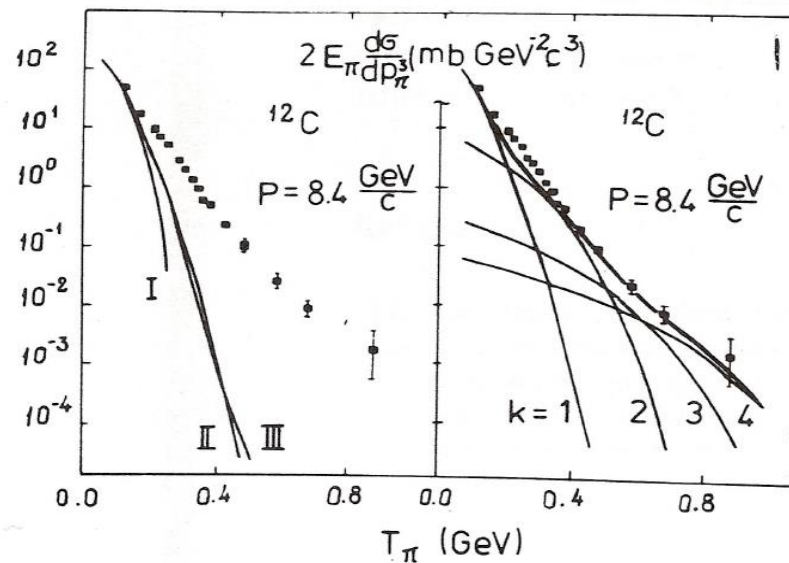


Fig. 1. (a) Calculations of the invariant pion production cross section for ^{12}C : I — for the free proton target; II — with fermi motion; III — the relativization effect. (b) The contributions of separate fluctuons with mass $M_k = km_p$ where k is the order of cumulativity.

Fluctons Probability inside nuclei

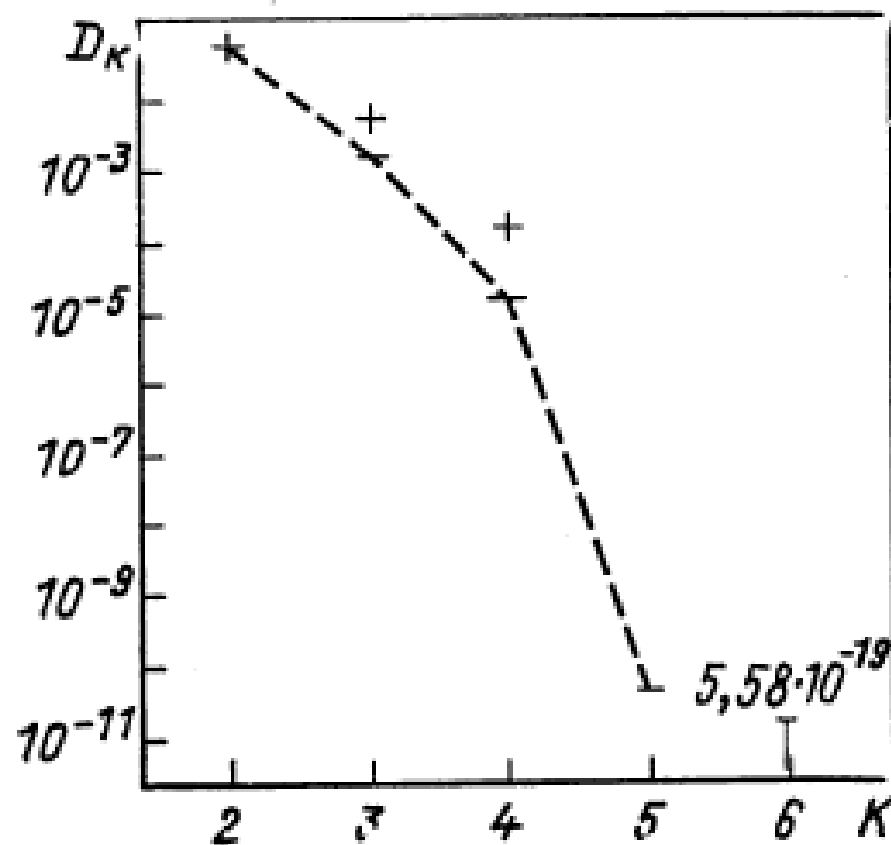


Рис. 19. Вероятность существования флюктонаов с k нуклонами в ядрах

D.I.Blokhintsev, A.V.Efremov, V.K.Lukjanov, A.I.Titov

JINR, Dubna

Abstract

The report summarizes the results of a series of works made recently in JINR, which explore the hypothesis about "fluctuons", i.e. multibaryon configurations of the mass $k m$ nucleon and correlation region of an order of elementary particles.

The probability of fluctuon-formation is calculated by the "quark bag" model. It is argued that the cumulative production is due to the hard scattering process (similar to high p_t hadron production) of beam particle partons with partons of a fluctuon considered as a hadron made of $3k$ quarks.

The model explains many qualitative and quantitative features of cumulative processes: The yield of cumulative hadrons, polarization of baryons, elastic and deep inelastic ed-scattering and so on. All this gives right to consider the cumulative processes as a new source of information about quark dynamics at small distance.

I. Fluctuons

It is as early as the fifties theoretists became interested in the appearance of "above-barrier fragments" /1/. The phenomenon consists in knocking out by protons of light nuclei (fragments) from heavier nuclei when the momentum transferred to a light nucleus is much larger than the binding energy of this nucleus.

At the same time, the hypothesis /2/ has been proposed that a large momentum can be transferred to a complex system of nucleons as a whole only when at the moment of collision with an incident particle a number of internuclear nucleons are inside a small volume, due to quantum fluctuations, and takes the momentum transfer as a unique particle with mass $M_k = km$ (m is the nucleon mass, k the number of nucleons in the group). A multi-nucleon formation of this type has recently been called as a "fluctuon".

1. Adjgirey L.S. et al. JETP, 23 (1957) 1185.
2. Blokhintsev D.I. JETP, 33 (1957) 1295.

* A report submitted to the XIX International Conference on High Energy Physics, Tokyo, 1978.

PHYSICAL REVIEW

A journal of experimental and theoretical physics established by E. L. Nichols in 1893

SECOND SERIES, VOL. 72, No. 1

JULY 1, 1947

On the Production of Mesotrons by Nuclear Bombardment

W. G. McMILLAN[†] AND E. TELLER

University of Chicago, Chicago, Illinois

(Received March 27, 1947)

Mesotron production by nuclear bombardment with fast, heavy particles has been investigated theoretically in a semi-quantitative way to determine the expected threshold energies, the cross sections, and their energy dependence. Whereas a treatment in which the target nucleons are assumed to be at rest predicts a requisite incident energy of ~ 210 Mev, the present treatment, based on the Fermi degenerate gas model, finds the threshold incident energy as ~ 95 Mev. The threshold is somewhat higher for positive than for negative mesotrons. The cross

section for single mesotron production, evaluated from the accessible volume in momentum space, is found to vary with the fractional excess energy, ϵ , as $\epsilon^{3.5}$ in the scalar or axial-vector theories; at low values of ϵ , a small difference in the energy dependence for negative and positive mesotrons arises from the necessity of giving the former a non-zero initial kinetic energy. For the pseudo-scalar and the polar-vector theories, the matrix element for mesotron emission is proportional to the momentum of the mesotron. This changes the power law to $\epsilon^{4.5}$.

INTRODUCTION

IN treatments of collisions between nuclei and high energy incident particles, it is often assumed as a first approximation that the constituent nucleons of the target nucleus may be considered as essentially free. For the case in which the desired result of the collision is the production of a mesotron (having rest-mass μ), the energy of the incident particle relative to the particular nucleon with which it collides must be at least μc^2 . If the nucleon has only the small velocity of the nucleus as a whole, nearly all the relative energy must be supplied by the incident particle; in the limit of zero-nucleon velocity this predicts for an incident proton or neutron a requisite energy just twice the rest-mass of the mesotron,¹ or about 210 Mev.

A more refined calculation should take account

of a possible contribution of the target-nucleon velocity to the relative energy, of any change in potential energy for the over-all process, and possibly also the effect of the inter-nucleonic forces. At least the first two of these refinements may be made rather easily. We shall use as our nuclear model the usual² degenerate Fermi gas mixture of protons and neutrons at zero temperature. Such a model is admittedly very crude, but will serve to determine orders of magnitude.

The limiting energy—the so-called “Fermi energy,” E_F —of the degenerate gas sets an approximate upper limit, p_F , to the permissible momenta of the target nucleons. Using this maximum momentum, directed anti-parallel to the path of the incident particle, it is readily seen that a lowering of the required incident energy is obtained. Furthermore, if the incident particle is captured without ejection of other nucleons its binding energy is released. However, since all the lowest states within the degenerate gas are filled

[†] Guggenheim Fellow, 1946-1947.

¹ We shall employ the value $\mu = 202$ electron masses (≈ 103 Mev), as recently determined by W. B. Fetter, Phys. Rev. 70, 625 (1946); see also D. J. Hughes, Phys. Rev. 71, 387 (1947).

² H. A. Bethe, Rev. Mod. Phys. 9, 82 (1937), ¶53A.

Antiproton discovery (1955)

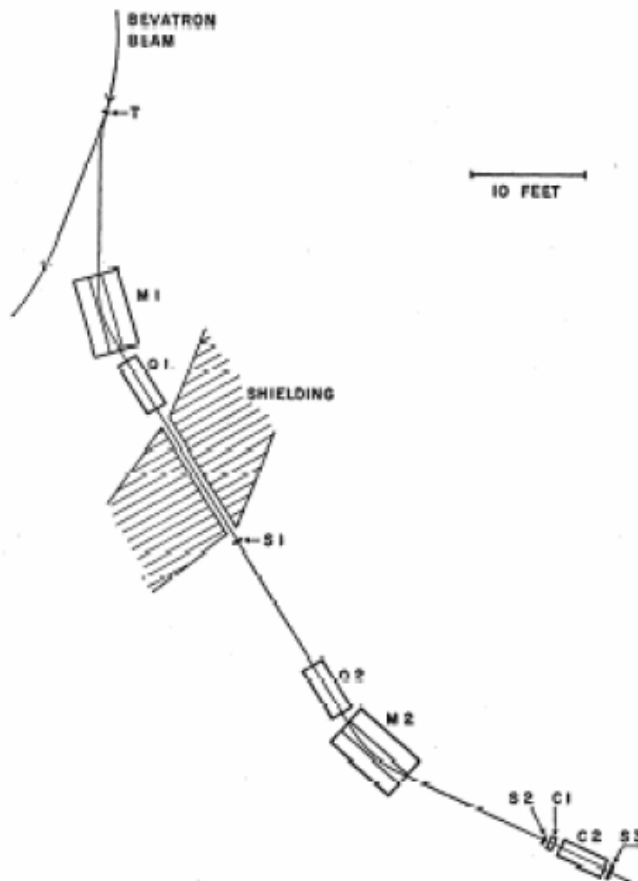
Threshold energy for antiproton (\bar{p}) production in proton – proton collisions

Baryon number conservation \Rightarrow simultaneous production of \bar{p} and p (or \bar{p} and n)

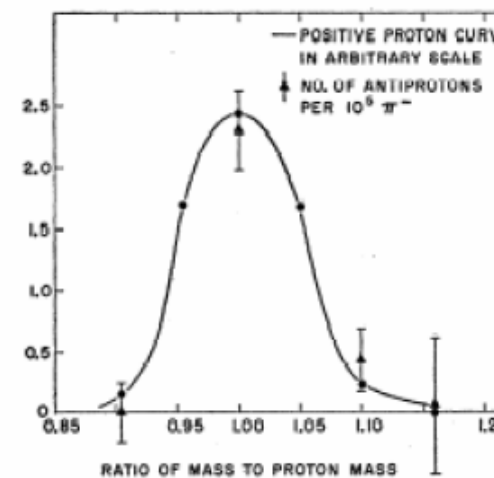
Example: $p + p \rightarrow p + p + \bar{p} + p$

Threshold energy ~ 6 GeV

“Bevatron”: 6 GeV
proton synchrotron in Berkeley



- build a beam line for 1.19 GeV/c momentum
- select negatively charged particles (mostly π^-)
- reject fast π^- by Čerenkov effect: light emission in transparent medium if particle velocity $v > c / n$ (n : refraction index) – antiprotons have $v < c / n$
 \Rightarrow no Čerenkov light
- measure time of flight between counters S_1 and S_2 (12 m path): 40 ns for π^- , 51 ns for antiprotons



For fixed momentum,
time of flight gives
particle velocity, hence
particle mass

Observation of Antiprotons*

OWEN CHAMBERLAIN, EMILIO SEGRÈ, CLYDE WIEGAND,
AND THOMAS YPSILANTIS

Radiation Laboratory, Department of Physics, University of
California, Berkeley, California

(Received October 24, 1955)

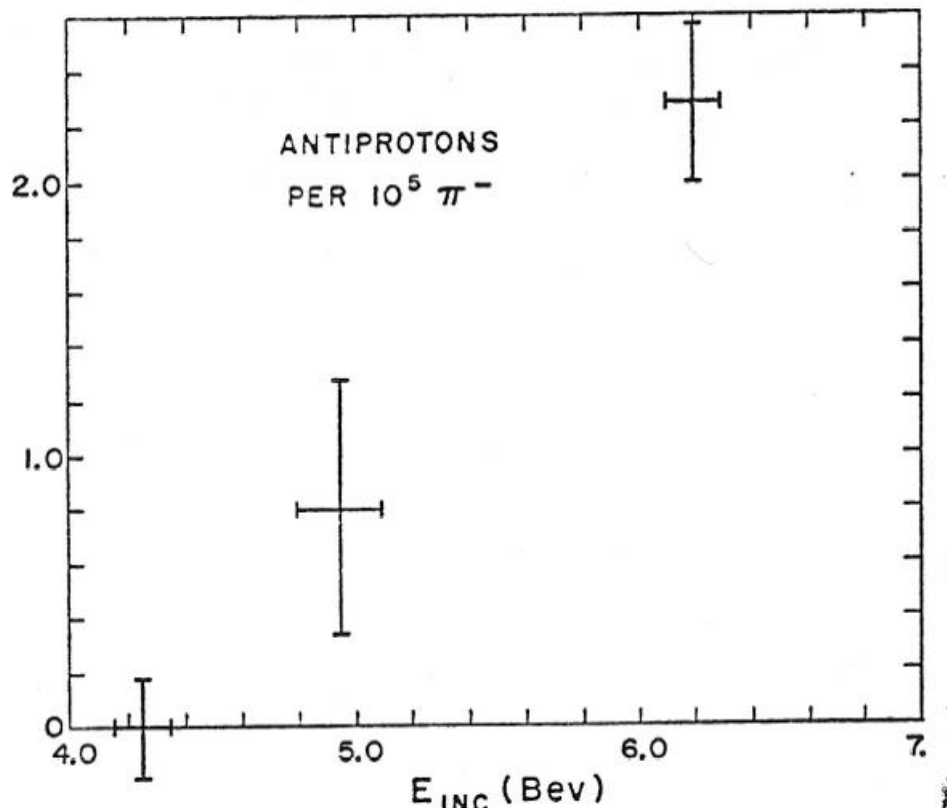


FIG. 5. Excitation curve for the production of antiprotons relative to meson production as a function of Bevatron beam energy.

**Subthreshold Antiproton Production in $^{28}\text{Si} + ^{28}\text{Si}$ Collisions
at 2.1 GeV/Nucleon**

J. B. Carroll,⁽¹⁾ S. Carlson,⁽¹⁾ J. Gordon,⁽¹⁾ T. Hallman,⁽⁴⁾ G. Igo,⁽¹⁾ P. Kirk,⁽⁵⁾ G. F. Krebs,⁽³⁾ P. Lindstrom,⁽³⁾ M. A. McMahan,⁽³⁾ V. Perez-Mendez,⁽³⁾ A. Shor,⁽²⁾ S. Trentalange,⁽¹⁾ and Z. F. Wang⁽¹⁾

⁽¹⁾*University of California at Los Angeles, Los Angeles, California 90024*

⁽²⁾*Brookhaven National Laboratory, Upton, New York, 11973*

⁽³⁾*Lawrence Berkeley Laboratory, Berkeley, California 94720*

⁽⁴⁾*Johns Hopkins University, Baltimore, Maryland 21218*

⁽⁵⁾*Louisiana State University, Baton Rouge, Louisiana 70803*

(Received 12 December 1988; revised manuscript received 16 February 1989)



We report on the first observation of subthreshold antiproton production in nucleus-nucleus collisions. This measurement was made for the system $^{28}\text{Si} + ^{28}\text{Si}$ at a bombarding energy of 2.1 GeV/nucleon (kinetic energy per NN pair in the c.m. frame ~ 850 MeV). A differential cross section $d^2\sigma/dPd\Omega$ of 80 ± 40 nb/sr (GeV/c) was measured for \bar{p} production at 1.9 GeV/c and 0° . This result is 3 orders of magnitude larger than that predicted by a calculation incorporating internal motion of the nucleons in the colliding nuclei.

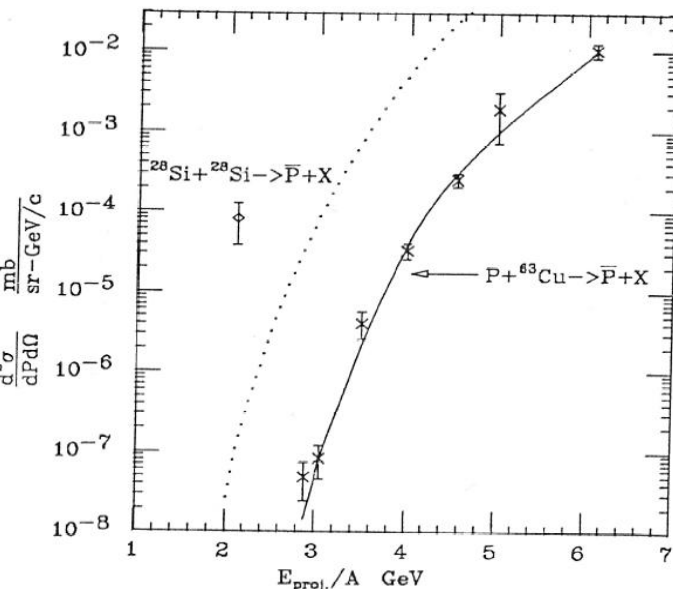


FIG. 3. Subthreshold antiproton production in $p + \text{Cu}$ collisions (\times) and a comparison with \bar{p} production in $\text{Si} + \text{Si}$ collisions (\diamond). Solid line is a calculation for $p + \text{Cu} \rightarrow \bar{p} + X$ incorporating a double-Gaussian distribution for the internal nuclear momentum (Ref. 11). Dotted line is the same calculation for $\text{Si} + \text{Si} \rightarrow \bar{p} + X$.

Forward K^+ Production in Subthreshold pA Collisions at 1.0 GeV

V. Koptev,¹ M. Büscher,² H. Junghans,² M. Nekipelov,^{1,2} K. Sistemich,² H. Ströher,² V. Abaev,¹ H.-H. Adam,³
 R. Baldauf,⁴ S. Barsov,¹ U. Bechstedt,² N. Bongers,² G. Borchert,² W. Borgs,² W. Bräutigam,² W. Cassing,⁵
 V. Chernyshev,⁶ B. Chiladze,⁷ M. Debowski,⁸ J. Dietrich,² M. Drochner,⁴ S. Dymov,⁹ J. Ernst,¹⁰ W. Erven,⁴
 R. Esser,^{11,*} P. Fedorets,⁶ A. Franzen,² D. Gotta,² T. Grande,² D. Grzonka,² G. Hansen,¹² M. Hartmann,² V. Hejny,²
 L. v. Horn,² L. Jarczyk,¹³ A. Kacharava,⁹ B. Kamys,¹³ A. Khoukaz,³ T. Kirchner,⁸ S. Kistryn,¹³ F. Klehr,¹²
 H. R. Koch,² V. Komarov,⁹ S. Kopyto,² R. Krause,² P. Kravtsov,¹ V. Kruglov,⁹ P. Kulessa,^{2,15} A. Kulikov,^{9,14}
 V. Kurbatov,⁹ N. Lang,³ N. Längenhan,⁸ I. Lehmann,² A. Lepges,² J. Ley,¹¹ B. Lorentz,² G. Macharashvili,^{7,9}
 R. Maier,² S. Martin,² S. Merzliakov,⁹ K. Meyer,² S. Mikirtychiantz,¹ H. Müller,⁸ P. Munhofen,² A. Mussgiller,²
 V. Nelyubin,¹ M. Nioradze,⁷ H. Ohm,² A. Petrus,⁹ D. Prasuhn,² B. Prietzschk,⁸ H. J. Probst,² D. Protic,² K. Pysz,¹⁵
 F. Rathmann,² B. Rimarzig,⁸ Z. Rudy,¹³ R. Santo,³ H. Paetz gen. Schieck,¹¹ R. Schleichert,² A. Schneider,²
 Chr. Schneider,⁸ H. Schneider,² G. Schug,² O. W. B. Schult,² H. Seyfarth,² A. Sibirtsev,² J. Smyrski,¹³
 H. Stechemesser,¹² E. Steffens,¹⁶ H. J. Stein,² A. Strzalkowski,¹³ K.-H. Watzlawik,² C. Wilkin,¹⁷ P. Wüstner,⁴
 S. Yashenko,⁹ B. Zalikhanov,⁹ N. Zhuravlev,⁹ P. Zolnierczuk,¹³ K. Zwoll,⁴ and I. Zychor¹⁸

K^+ -meson production in pA ($A = C, Cu, Au$) collisions has been studied using the ANKE spectrometer at an internal target position of the COSY-Jülich accelerator. The complete momentum spectrum of kaons emitted at forward angles, $\vartheta \leq 12^\circ$, has been measured for a beam energy of $T_p = 1.0$ GeV, far below the free NN threshold of 1.58 GeV. The spectrum does not follow a thermal distribution at low kaon momenta and the larger momenta reflect a high degree of collectivity in the target nucleus.

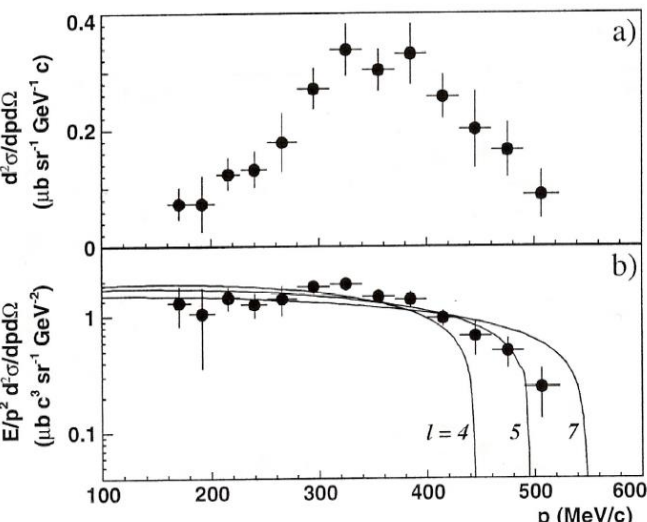


FIG. 2. (a) Double differential K^+ -production cross section for the $p(1.0 \text{ GeV})^{12}\text{C} \rightarrow K^+(\vartheta \leq 12^\circ)X$ reaction as a function of the K^+ momentum. (b) Same data plotted as invariant cross section. The error bars are purely statistical. The overall normalization uncertainty is estimated to be 10%. The solid lines describe the behavior of the invariant cross section within a phase-space approximation [Eq. (2)].

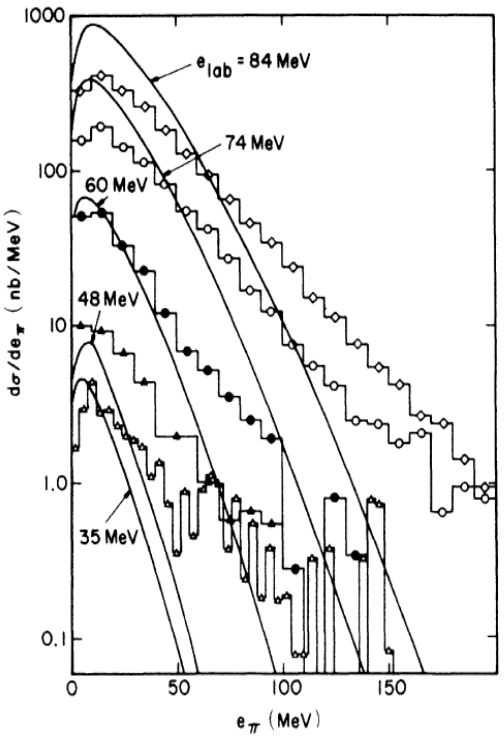


FIG. 2. Comparison of calculated and experimental spectra. The input π^0 absorption cross sections are those by the upper solid curve in Fig. 1. For the lower solid curve in that figure, the results shown here must be scaled down by a factor of about 2. The data are taken from Refs. 6 and 7 and the reaction $^{12}\text{C} + ^{12}\text{C}$ (upper four curves) and from Ref. 8 the reaction $^{14}\text{N} + \text{Ni}$ (open triangles).

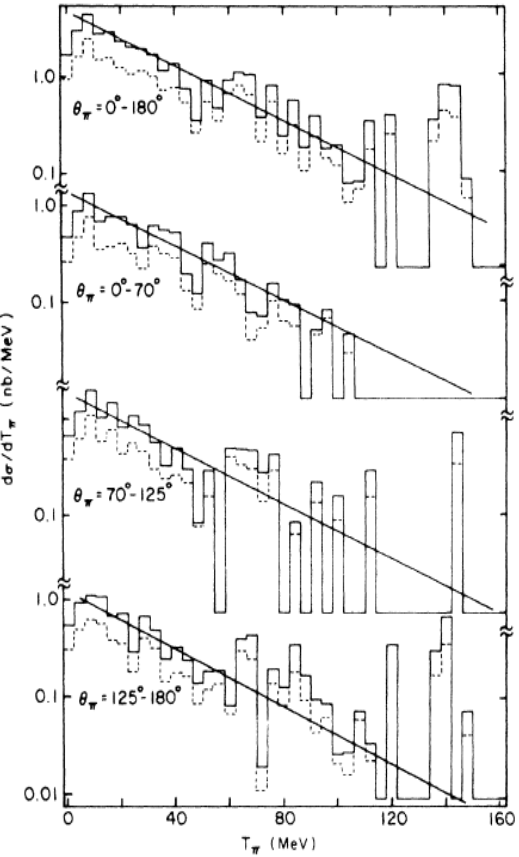


FIG. 3. Pion kinetic energy spectrum (solid histogram) in the laboratory frame for 35 MeV/nucleon $^{14}\text{N} + \text{Ni}$ integrated over all pion emission angles θ_π (top) and for various θ_π bins. For the meaning of the dashed histograms see the text. The straight lines represent an exponential with an inverse slope constant of 23 MeV.

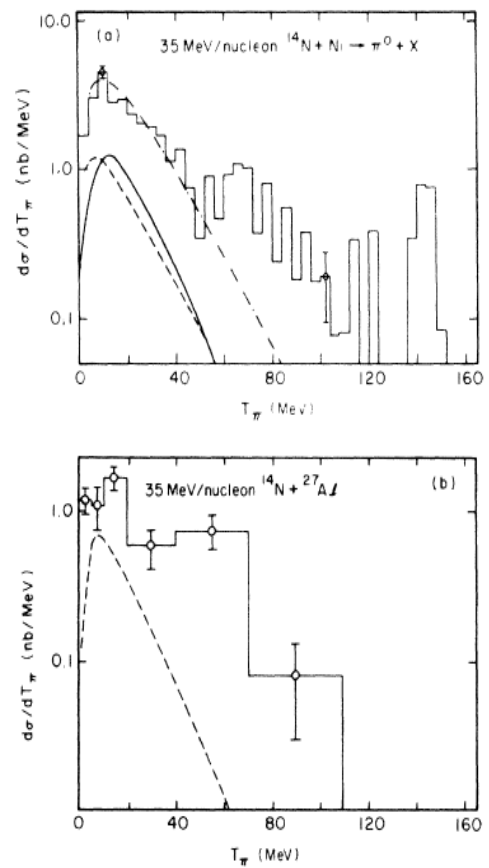


FIG. 4. Experimental pion kinetic energy spectra at 35 MeV/nucleon for the Ni and Al target. The spectrum for the Al target corresponds to the same measurements as shown in Ref. 6 but differs from the spectrum shown there by subtraction of the cosmic-ray background and use of the energy dependent conversion efficiency as discussed in the text (as compared to no cosmic subtraction and $\epsilon_c = 0.7$). The solid and dashed lines are predictions of Refs. 27 and 30, respectively. The dashed dotted line corresponds to a thermal spectrum (Ref. 20) with $T = 12.2$ MeV and is normalized to the data at low kinetic energies (10–60 MeV).

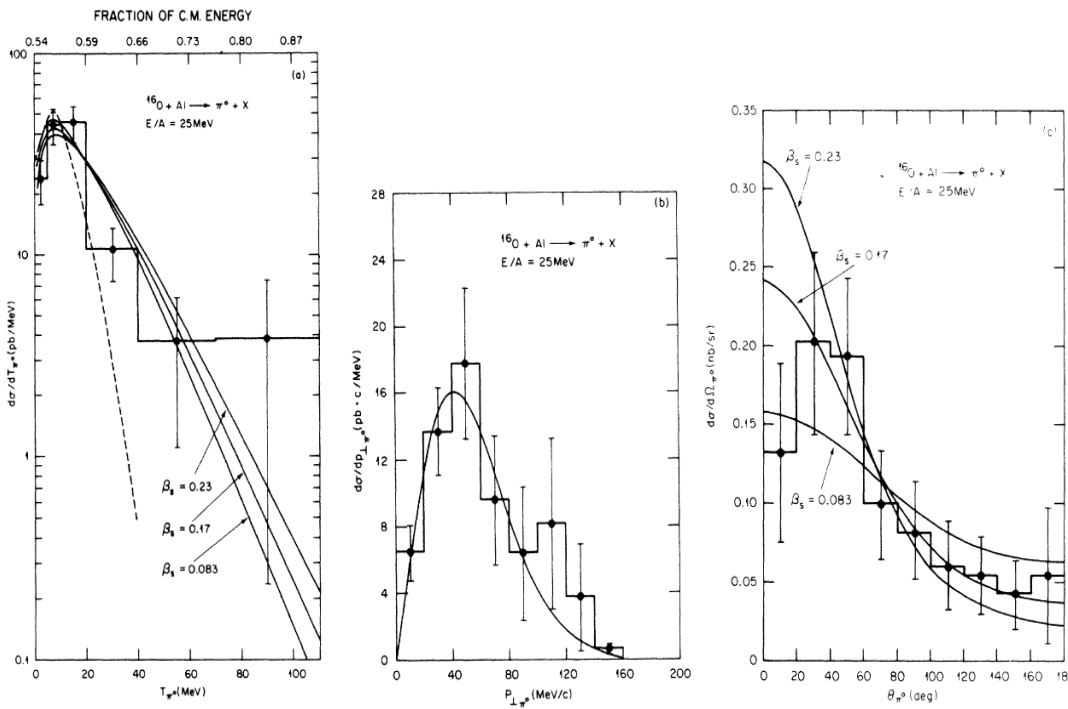


FIG. 2. (a) Laboratory kinetic energy distribution, (b) transverse momentum distribution, and (c) angular distribution for neutral pions observed in the reaction $E_{\text{lab}}/A = 25$ MeV $^{16}\text{O} + \text{Al} \rightarrow \pi^0 + \text{X}$. The dashed line in (a) is the prediction of Ref. 9 multiplied by a factor of 50. The solid line in (b) is a fit using Eq. (1) and yields $T = 11.6$ MeV. The solid lines in (a) and (c) are predictions of the simple thermal model discussed in the text with $T = 11.6$ MeV and source speeds $\beta_s = 0.083, 0.17$, and 0.23 . The legend at the top of (a) is the fraction of the c.m. energy required to produce a π^0 traveling at 0° in the laboratory.

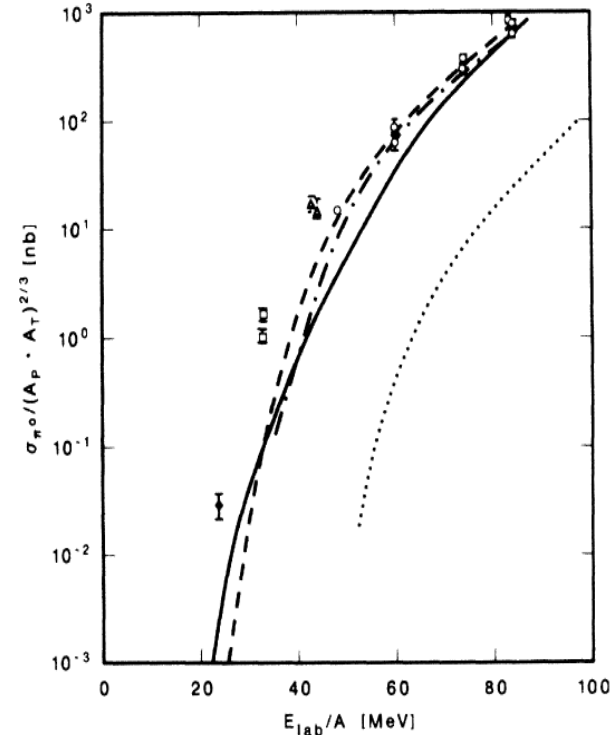


FIG. 3. Inclusive cross section for π^0 production, divided by $(A_p^{2/3} A_T^{2/3})$, where A_p and A_T are the projectile and target mass numbers, respectively, as a function of laboratory bombarding energy. (Open circles, Ref. 3; open triangles, Ref. 4; open squares, Ref. 2; closed diamond, present work.) The theoretical curves are from Ref. 8 (dotted line), Ref. 9 (long dashed line), Ref. 11 (dash-dot line), and Ref. 12 (solid line).

Celmer

Pion production: A probe for coherence in medium-energy heavy-ion collisions

J. Stachel, P. Braun-Munzinger, R. H. Freifelder,* P. Paul, S. Sen, P. DeYoung,[†] and P. H. Zhang[‡]
Department of Physics, State University of New York at Stony Brook, Stony Brook, New York 11794

T. C. Awes, F. E. Obenshain, F. Plasil, and G. R. Young
Physics Division, Oak Ridge National Laboratory, Oak Ridge, Tennessee 37831

R. Fox and R. Ronningen
*National Superconducting Cyclotron Laboratory, Michigan State University,
 East Lansing, Michigan 48824*
 (Received 19 November 1985)

The production of neutral pions has been studied in reactions of 35 MeV/nucleon $^{14}\text{N} + ^{27}\text{Al}, \text{Ni}, \text{W}$ and 25 MeV/nucleon $^{16}\text{O} + ^{27}\text{Al}, \text{Ni}$. Inclusive pion differential distributions $d\sigma/dT_\pi$, $d\sigma/d\Omega$, $d\sigma/dy$, $d\sigma/dp_\perp$, and $d^2\sigma/dy dp_\perp$ have been measured by detecting the two pion-decay γ rays in a setup of 20 lead glass Čerenkov detector telescopes. Special care was taken to understand and suppress background events. Effects of pion reabsorption are discussed and it is found that the cross sections presented here are substantially affected by such final state interactions. The comparatively large experimental cross sections and the shape of the spectral distributions cannot be accounted for in single nucleon-nucleon collision or statistical models; they rather call for a coherent pion production mechanism.

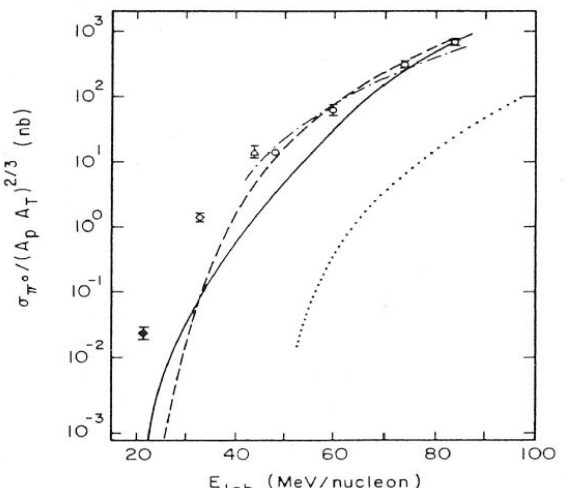


FIG. 13. Experimental integrated pion production cross sections divided by $(A_p A_T)^{2/3}$ for different beam energies. The different symbols signify $^{16}\text{O} + ^{27}\text{Al}, \text{Ni}, \text{W}$ (closed diamond, present data), $^{14}\text{N} + ^{27}\text{Al}, \text{Ni}, \text{W}$ (open diamond, present data), $^{40}\text{Ar} + ^{40}\text{Ca}$ (open triangle, Ref. 9), and $^{12}\text{C} + ^{12}\text{C}$ (open circles, Refs. 8 and 10). Also shown are results of a single nucleon-nucleon hard scattering model (Ref. 23) (dotted line), the extended phase space model (Ref. 27) (dashed line), a thermal model (Ref. 30) (solid line), and the bremsstrahlung model (Ref. 38) (dashed-dotted line).

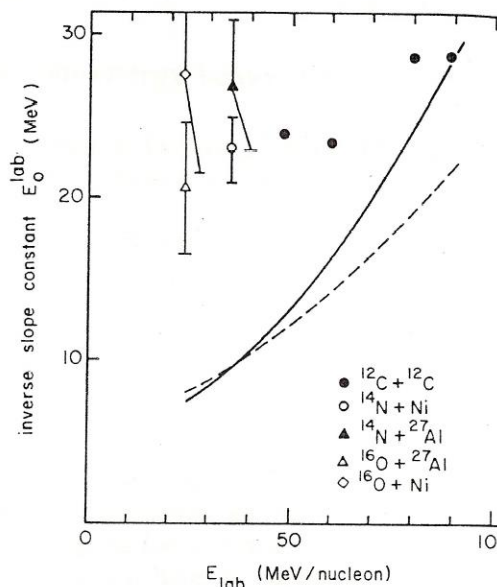


FIG. 14. Experimentally determined slope constants E_0 of pion kinetic energy spectra plotted as a function of beam energy/nucleon. For C + C spectra see Refs. 8 and 10. The solid and dashed lines correspond to predictions of Refs. 30 and 27, respectively. For details see the text.

A.A. Baldin's parameterization

Phys. At. Nucl. 56(3), p.385(1993)

$$\Pi = \frac{1}{2} (X_I^2 + X_{II}^2 + 2 \cdot X_I \cdot X_{II} \cdot \gamma_{I,II})^{\frac{1}{2}} = \frac{1}{2 \cdot m} \cdot S_{\min}^{\frac{1}{2}}$$

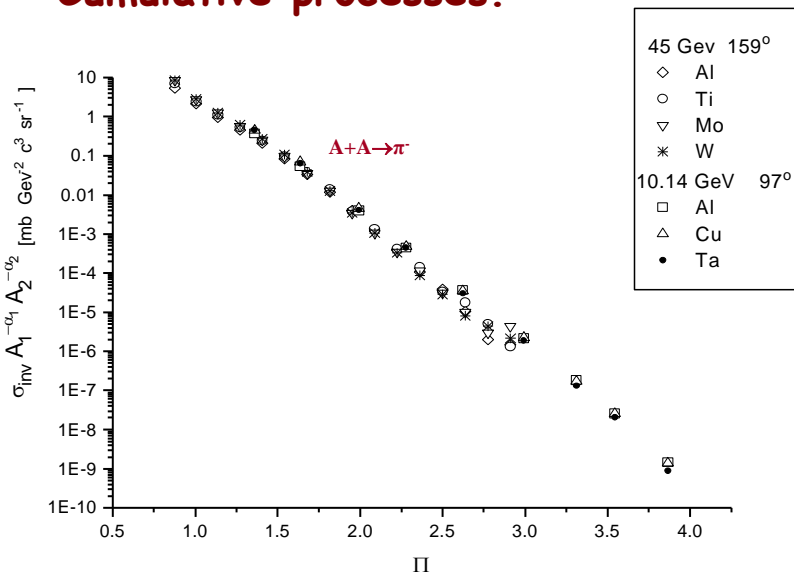
$$\gamma_{I,II} = \frac{(P_I \cdot P_{II})}{M_I \cdot M_{II}}$$

Inclusive data parameterization

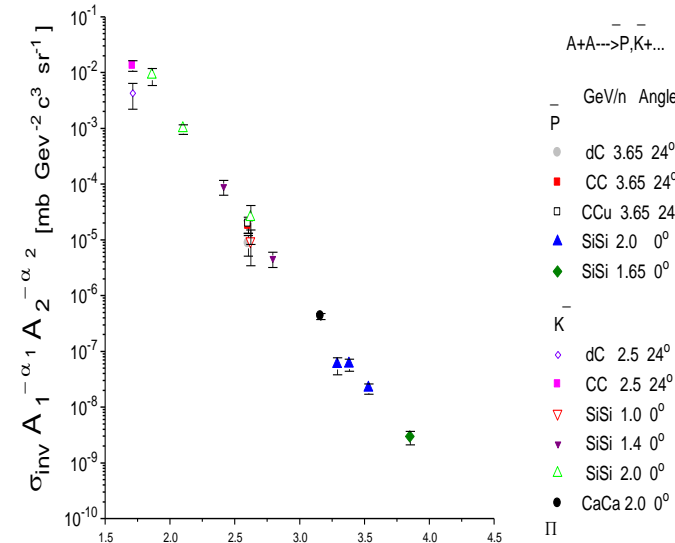
$$E \cdot \frac{d^3\sigma}{dp^3} = C_1 \cdot A_I^{\frac{1}{3} + \frac{X_I}{3}} \cdot A_{II}^{\frac{1}{3} + \frac{X_{II}}{3}} \cdot \exp(-\frac{\Pi}{C_2}),$$

$$C_1 = 2200 [mb \cdot GeV^{-2} \cdot c^3 \cdot sr^{-1}], C_2 = 0.127$$

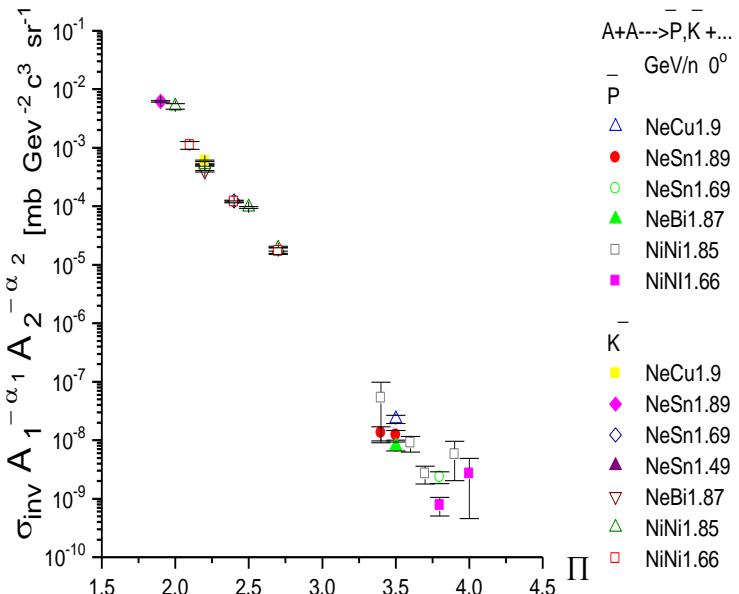
Cumulative processes.



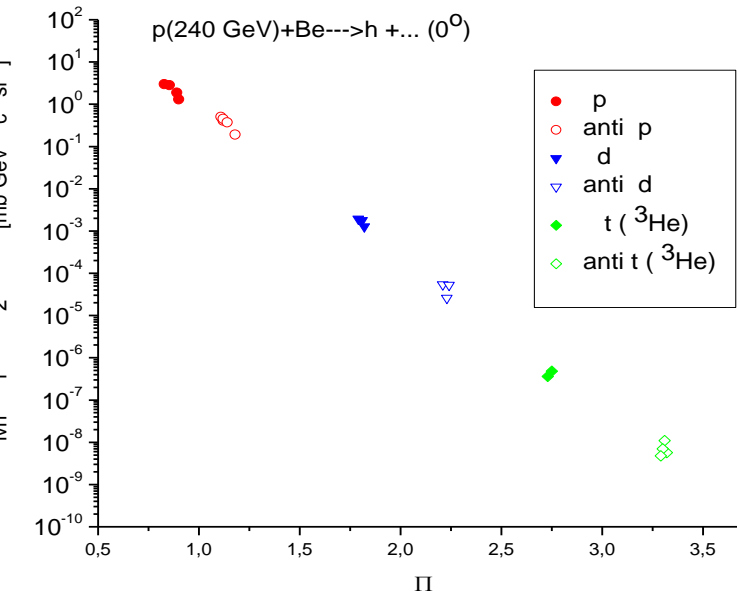
Twice cumulative processes.



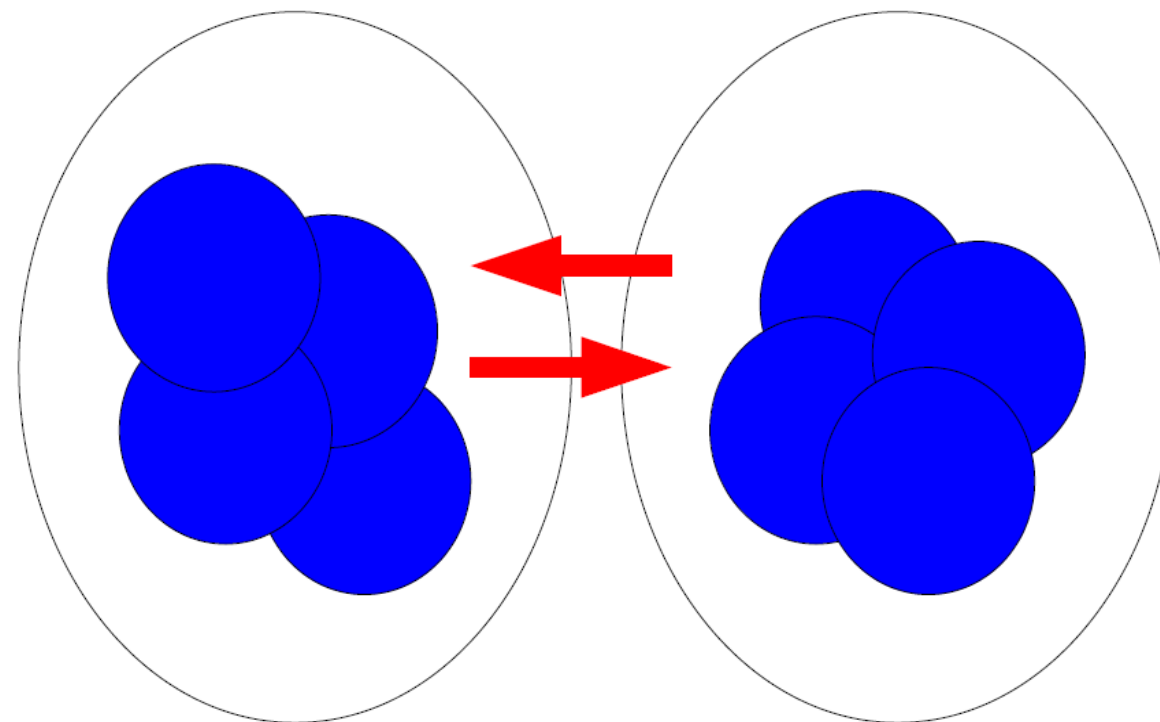
Twice cumulative deep subthreshold processes with heavy nuclei.



Antimatter production.

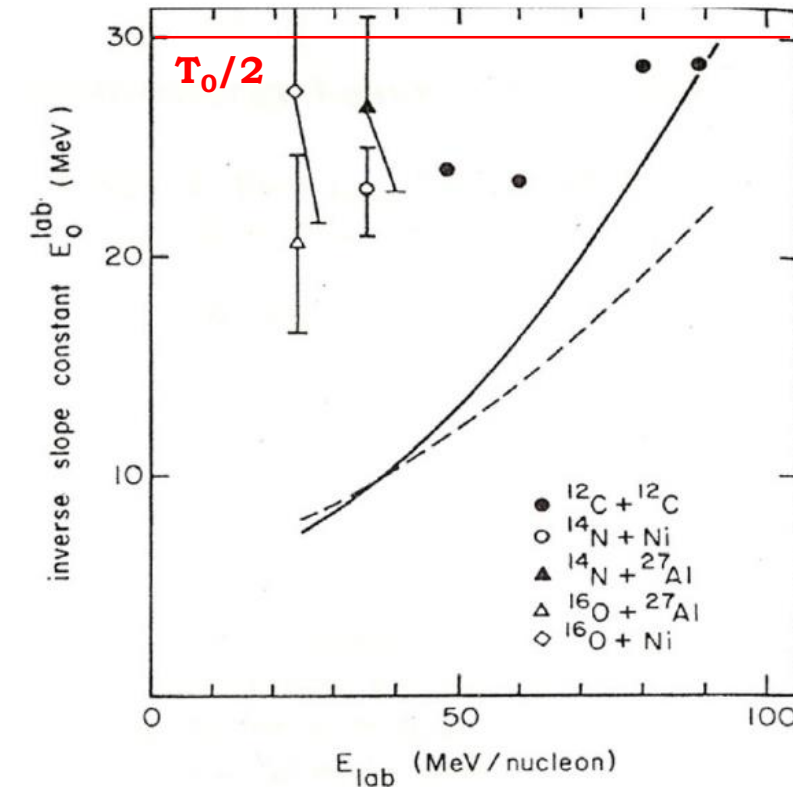
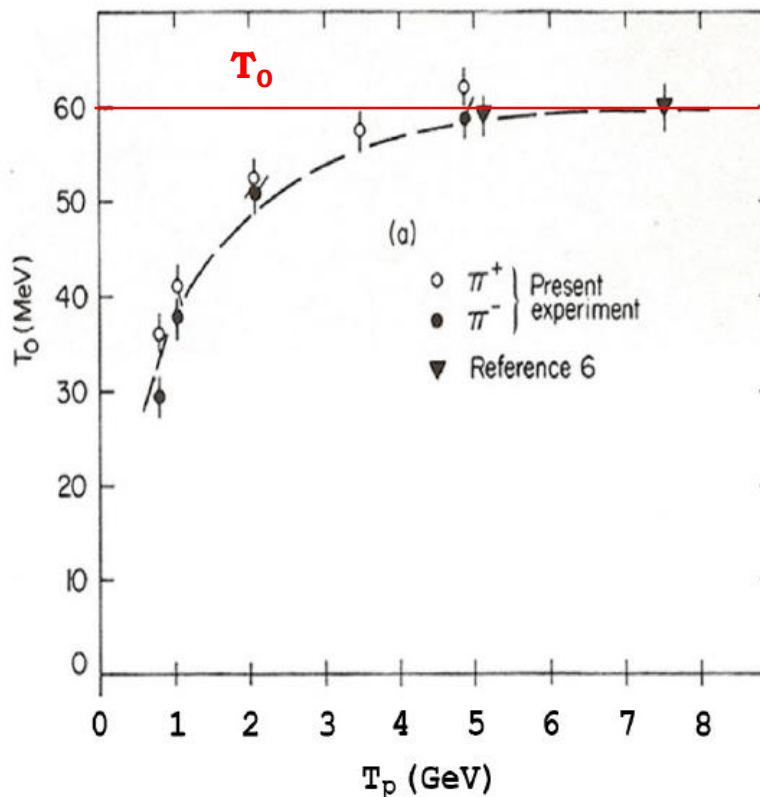


Subthreshold flucton-flucton production



$$\sigma_h \sim P_K^2 \cdot G_{h/K}^2(K)$$

Inverse slope for subthreshold production must be less than $T_0/2$
 (near the phase space border).



$$P_{cum} \sim \exp(-T/T_0) \quad \Rightarrow \quad P_{subthresh} \sim \exp(-T/T_0) \cdot \exp(-T/T_0) \sim \exp(-T/(T_0/2))$$

**DIS in the cumulative
region.**

K.Rith From Nuclei to Nucleons (Summary)

Nuclear Physics A532 (1991) 3c-14c

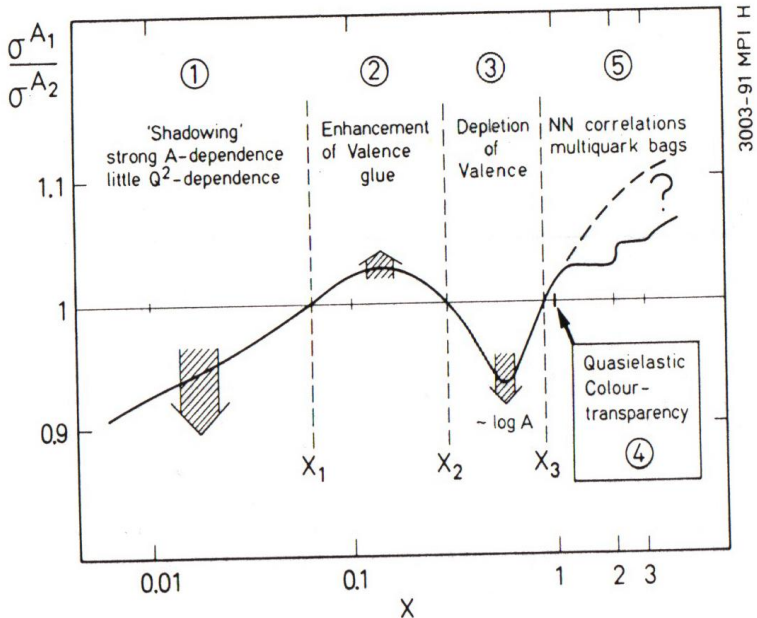


Figure 1. Global behaviour of nuclear effects in parton distributions

Region 1: $0 < x < x_1 \approx 0.06$ ($z > 3$ fm)

In this region the dominant contribution to the cross section comes from sea quarks, the essential longitudinal distances z involved in the deep inelastic interaction are $z > 3$ fm, much bigger than the size of individual nucleons. $R^A(x)$ is smaller

than one. The effect (historically called 'Shadowing') increases with decreasing x , it increases strongly with atomic mass A and depends very little on Q^2 . This behaviour is also observed in the antiquark distributions $\bar{q}(x)$, measured in the Drell-Yan process.

Region 2: $x_1 < x < x_2 \approx 0.3$ ($3 \text{ fm} > z > 0.7 \text{ fm}$)

$R^A(x)$ shows a small increase of a few percent above one. This enhancement varies very little with A and Q^2 , it is definitely not due to seaquarks alone but probably dominantly a valence quark effect. There are indications that also the gluon distribution $g(x)$ is enhanced in this region.

Region 3: $x_2 < x < x_3 \approx 0.8$ ($z < 0.7$ fm)

In this region the sea quark distribution is essentially negligible and $R^A(x)$ reflects the behaviour of the valence-quark distributions. $R^A(x)$ is smaller than one with a minimum at $x \approx 0.65$. The effect increases approximately like $\log A$ or the mean nuclear density $\bar{\rho}_A$.

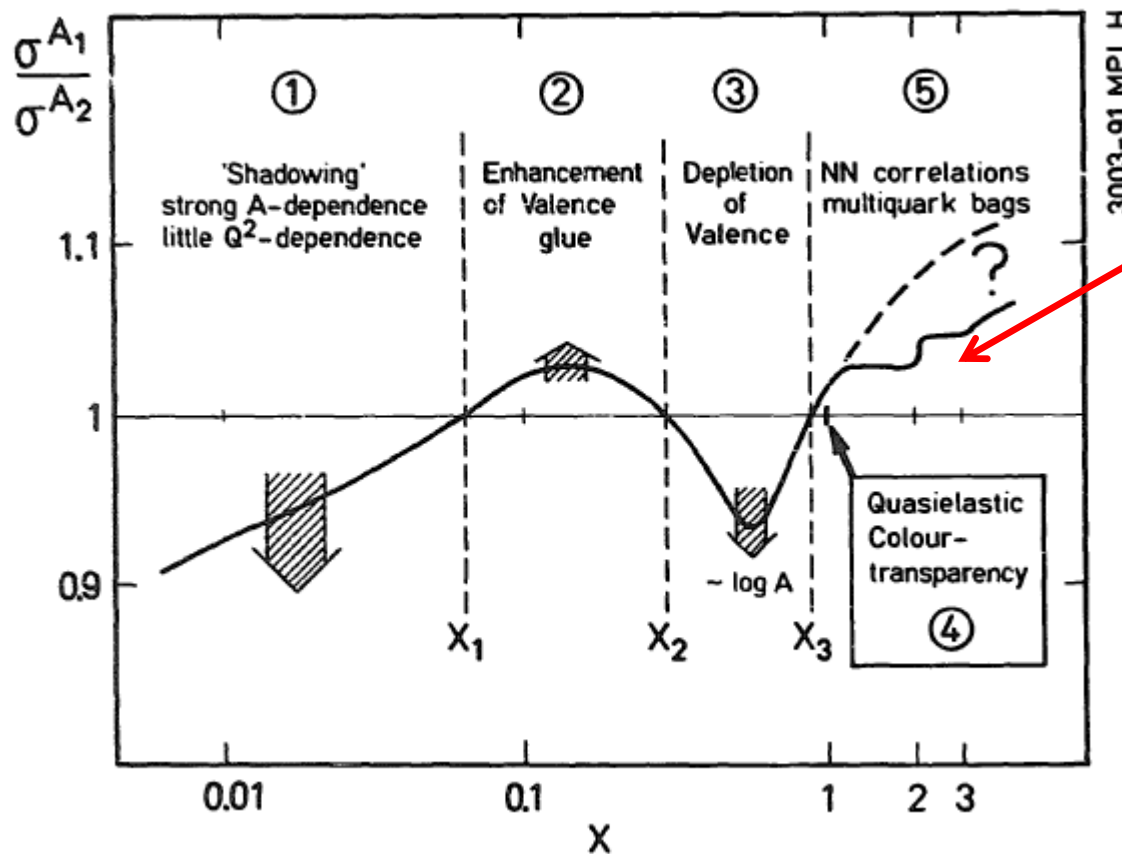
Region 4: $x = 1$

This is the special region of quasielastic scattering where possibly effects of 'colour-transparency' could be observed.

Region 5: $x_3 < x < x_A$

For a nucleus with atomic mass A the quark distributions can in principle extend to $x_A = A$. $R^A(x)$ is bigger than one. Its behaviour is strongly influenced by Fermi-motion, final state interactions, nucleon-nucleon correlations, or the formation of multiquark clusters. Experimentally this region is essentially unexplored.

Cumulative
kinematical
region



Region 5: $x_3 < x < x_A$

For a nucleus with atomic mass A the quark distributions can in principle extend to $x_A = A$. $R^A(x)$ is bigger than one. Its behaviour is strongly influenced by Fermi-motion, final state interactions, nucleon-nucleon correlations, or the formation of multiquark clusters. Experimentally this region is essentially unexplored.

Nuclear structure functions at $x > 1$

B. W. Filippone, R. D. McKeown, R. G. Milner,* and D. H. Potterveld[†]
Kellogg Radiation Laboratory, California Institute of Technology, Pasadena, California 91125

D. B. Day, J. S. McCarthy, Z. Meziani,[‡] R. Minehardt, R. Sealock, and S. T. Thornton
Institute of Nuclear and Particle Physics and Department of Physics, University of Virginia, Charlottesville, Virginia 22901

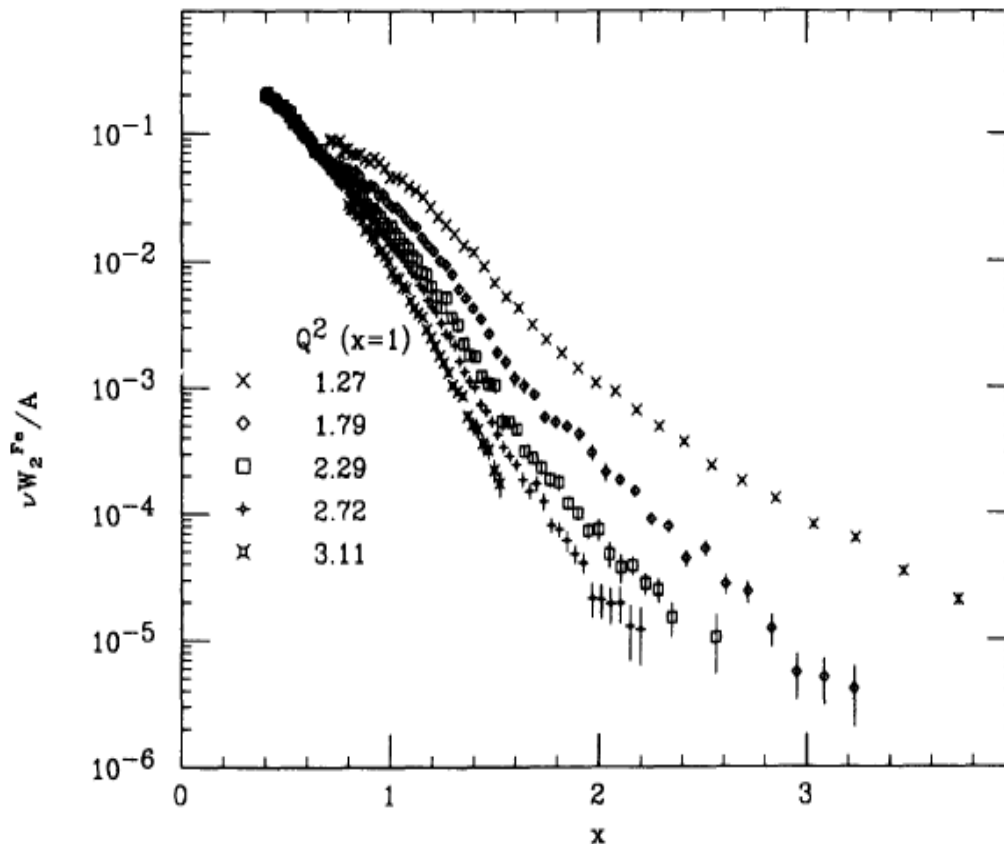


FIG. 1. Measured structure function per nucleon for Fe vs x . The Q^2 value at $x = 1$ is also listed for the different kinematics.

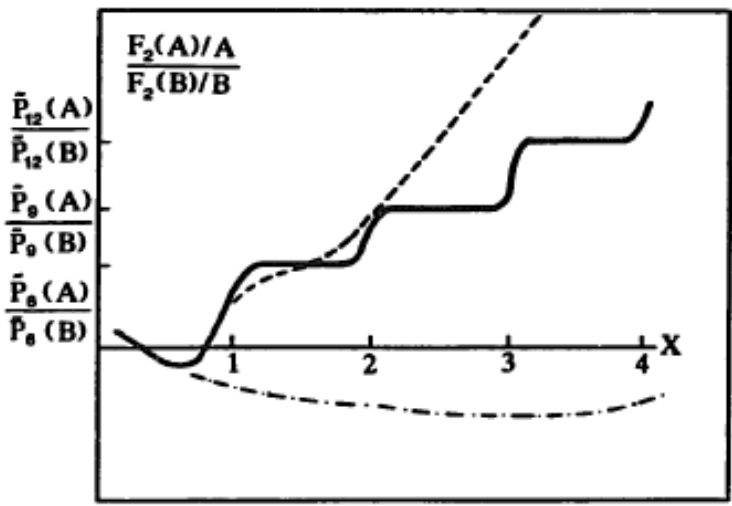


Figure 5. Theoretical predictions for nuclear structure functions at $x > 1$

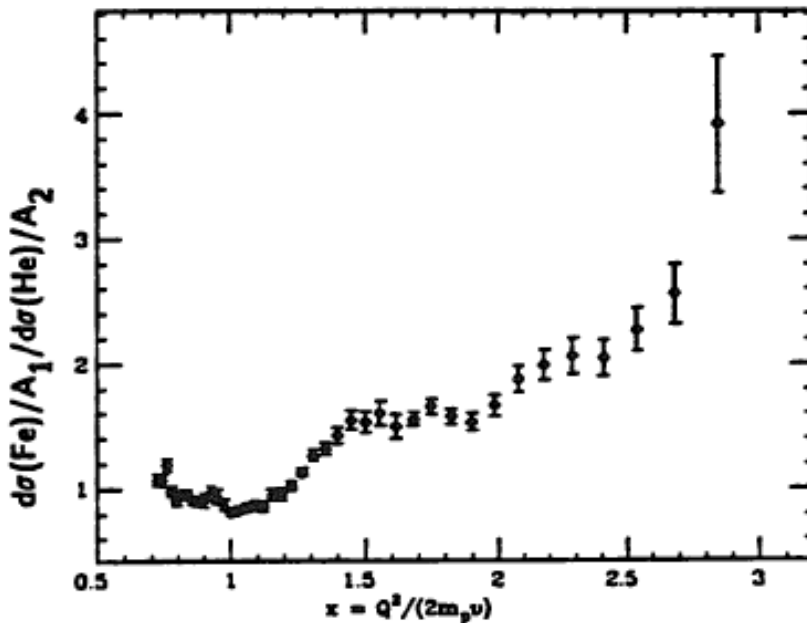


Figure 6. Preliminary results for σ^{Fe}/σ^{He} from NE-2 at SLAC

32 J. Vary, Proceedings of the 7th Int. Conf. on High Energy Physics problems,
Dubna 1984, 147.

N.P. Zotov, V.A. Saleev, V.A. Tsarev (Lebedev Inst.)

Published in JETP Lett. 40 (1984) 965-968, Pisma Zh.Eksp.Teor.Fiz. 40 (1984) 200-203

Nuclear structure functions in carbon near $x = 1$

BCDMS Collaboration

A.C. Benvenuti, D. Bollini, T. Camporesi¹, L. Monari*, F.L. Navarria

Dipartimento di Fisica dell'Università and INFN, Bologna, Italy

A. Argento², J. Cvach³, W. Lohmann⁴, L. Piemontese⁵

CERN, Geneva, Switzerland

V.I. Genchev⁶, J. Hladky³, I.A. Golutvin, Yu.T. Kiryushin, V.S. Kiselev, V.G. Krivokhizhi
S. Nemeček³, D.V. Peshekhonov, P. Reimer³, I.A. Savin, G.I. Smirnov, S. Sultanov⁶, A.G. Vo
Joint Institut for Nuclear Research, Dubna, Russia

D. Jamnik⁸, R. Kopp⁹, U. Meyer-Berkhout, A. Staude, K.-M. Teichert, R. Tirler¹⁰, R. Voss¹, Č
Sektion Physik der Universität, München, Germany¹¹

J. Feltesse, A. Misztajn, A. Ouraou, P. Rich-Hennion, Y. Sacquin, G. Smadja, P. Verrecchia, M
DAPNIA-SPP, Centre d'Etudes de Saclay, CEA, Gif-sur-Yvette, France

Received: 1 March 1994

Abstract. Data from deep inelastic scattering of 200 GeV muons on a carbon target with squared four-momentum transfer $52 \text{ GeV}^2 \leq Q^2 \leq 200 \text{ GeV}^2$ were analysed in the region of the Bjorken variable close to $x = 1$, which is the kinematic limit for scattering on a free nucleon. At this value of x , the carbon structure function is found to be $F_2^C \approx 1.2 \cdot 10^{-4}$. The x dependence of the structure function for $x > 0.8$ is well described by an exponential $F_2^C \propto \exp(-sx)$ with $s = 16.5 \pm 0.6$.

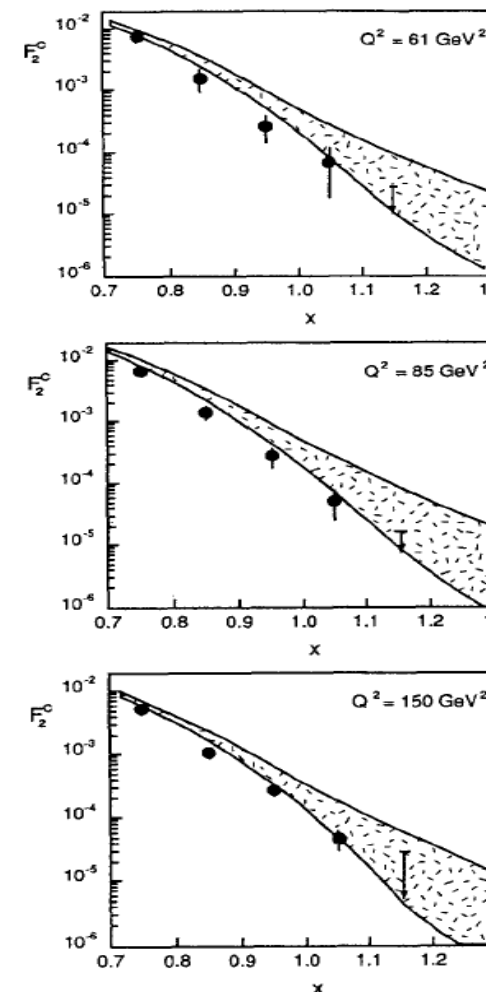


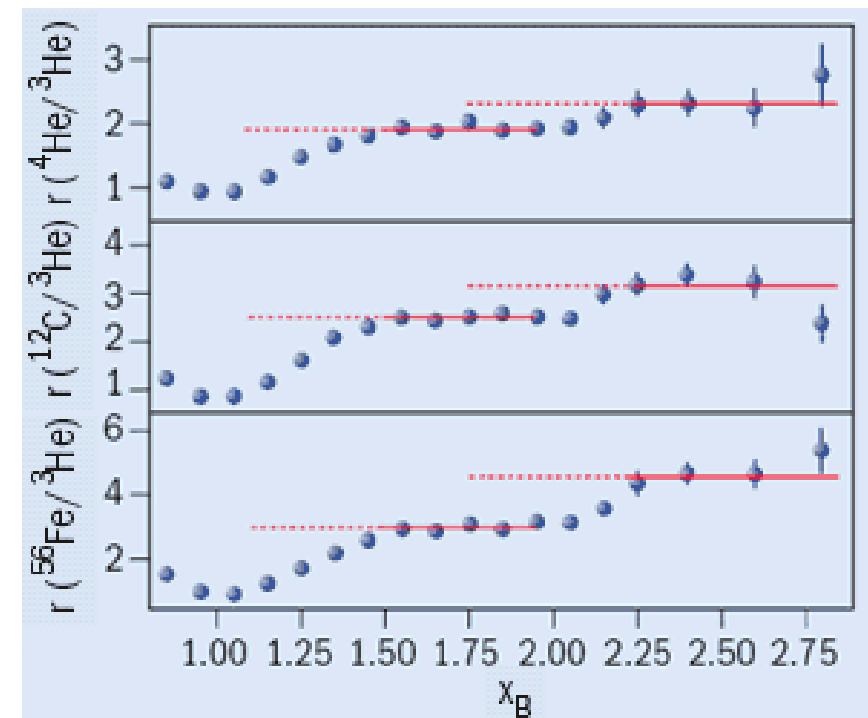
Fig. 7. The nuclear structure function $F_2^C(x)$ as a function of x , at three different values of Q^2 . The hatched regions show the range of predictions of [26]

Measurement of 2- and 3-Nucleon Short Range Correlation Probabilities in Nuclei

K.S. Egiyan,¹ N.B. Dashyan,¹ M.M. Sargsian,¹⁰ M.I. Strikman,²⁸ L.B. Weinstein,²⁷ G. Adams,³⁰ P. Ambrozewicz,¹⁰ M. Anghinolfi,¹⁶ B. Asavapibhop,²² G. Asryan,¹ H. Avakian,³⁴ H. Bagdasaryan,²⁷ N. Baillie,³⁸ J.P. Ball,²

$$r(A, {}^3\text{He}) = \frac{A(2\sigma_{ep} + \sigma_{en})}{3(Z\sigma_{ep} + N\sigma_{en})} \frac{3\mathcal{Y}(A)}{A\mathcal{Y}({}^3\text{He})} C_{\text{rad}}^A, \quad (2)$$

where Z and N are the number of protons and neutrons in nucleus A , σ_{eN} is the electron-nucleon cross section, \mathcal{Y} is the normalized yield in a given (Q^2, x_B) bin [30] and C_{rad}^A is the ratio of the radiative correction factors for A and ${}^3\text{He}$ ($C_{\text{rad}}^A = 0.95$ and 0.92 for ${}^{12}\text{C}$ and ${}^{56}\text{Fe}$ respectively). In our Q^2 range, the elementary cross section correction factor $\frac{A(2\sigma_{ep} + \sigma_{en})}{3(Z\sigma_{ep} + N\sigma_{en})}$ is 1.14 ± 0.02 for C and ${}^4\text{He}$ and 1.18 ± 0.02 for ${}^{56}\text{Fe}$. Fig. 1 shows the resulting ratios integrated over $1.4 < Q^2 < 2.6 \text{ GeV}^2$.



Having these data, we know almost full ($\approx 99\%$) nucleonic picture of nuclei with $A \leq 56$

Fractions Nucleus	Single particle (%)	2N SRC (%)	3N SRC (%)
^{56}Fe	76 $\pm 0.2 \pm 4.7$	23.0 $\pm 0.2 \pm 4.7$	0.79 $\pm 0.03 \pm 0.25$
^{12}C	80 $\pm 02 \pm 4.1$	19.3 $\pm 0.2 \pm 4.1$	0.55 $\pm 0.03 \pm 0.18$
^4He	86 $\pm 0.2 \pm 3.3$	15.4 $\pm 0.2 \pm 3.3$	0.42 $\pm 0.02 \pm 0.14$
^3He	92 ± 1.6	8.0 ± 1.6	0.18 ± 0.06
^2H	96 ± 0.8	4.0 ± 0.8	-----

Using the published data on (p,2p+n) [PRL,90 (2003) 042301] estimate the isotopic composition of 2N SRC in ^{12}C

$$\begin{aligned}
 a_{pp}(^{12}\text{C}) &\approx 4 \pm 2 \% \\
 a_{2N}(^{12}\text{C}) \approx 20 \pm 0.2 \pm 4.1 \% &\xrightarrow{\hspace{1cm}} a_{pn}(^{12}\text{C}) \approx 12 \pm 4 \% \\
 a_{nn}(^{12}\text{C}) \approx 4 \pm 2 \%
 \end{aligned}$$

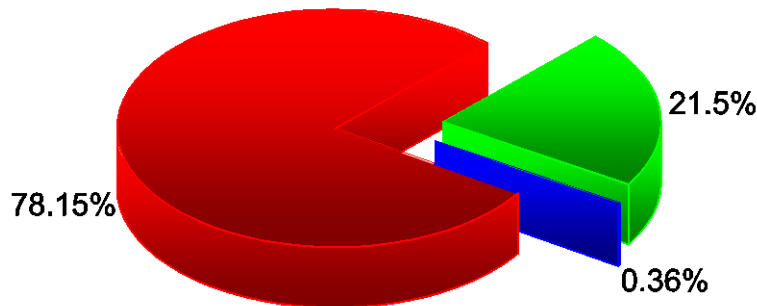
^{12}C - structure

RNP - program at JINR

V.V.Burov, V.K.Lukyanov, A.I.Titov, PLB, 67, 46(1977)

JINR - 1977

NN
6q
9q

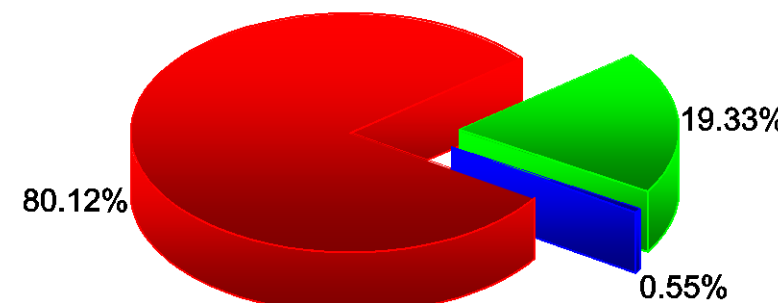


eA - program at JLab

R.Subedi et al., Science 320 (2008) 1476-1478
e-Print: arXiv:0908.1514 [nucl-ex]

JLab - 2008

NN
2N SRC
3N SRC



Кумулятивные процессы при больших p_T

E850/EVA (BNL)

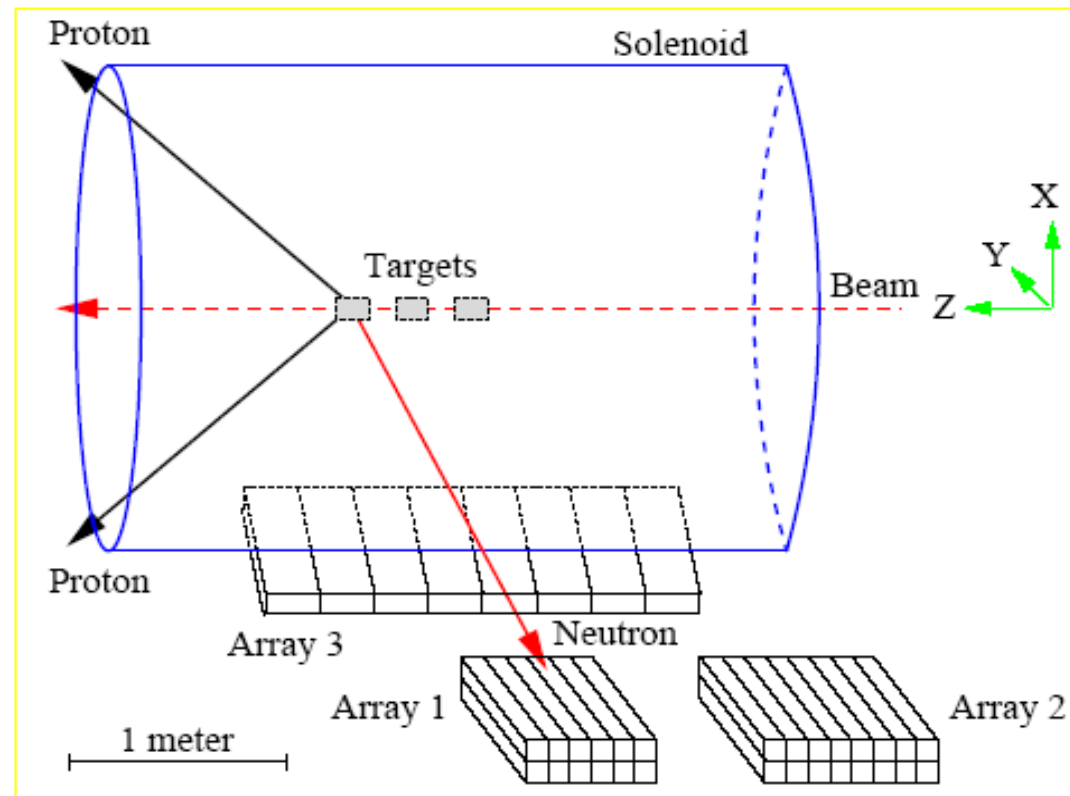


Figure I.3: A schematic view of the EVA solenoid and the neutron counters in the 1998 measurement.

***n-p* Short-Range Correlations from (*p*, 2*p* + *n*) Measurements**

A. Tang,¹ J. W. Watson,¹ J. Aclander,² J. Alster,² G. Asryan,^{4,3} Y. Averichev,⁸ D. Barton,⁴ V. Baturin,^{6,5} N. Bukhtoyarova,^{4,5} A. Carroll,⁴ S. Gushue,⁴ S. Heppelmann,⁶ A. Leksanov,⁶ Y. Makdisi,⁴ A. Malki,² E. Minina,⁶ I. Navon,² H. Nicholson,⁷ A. Ogawa,⁶ Yu. Panebratsev,⁸ E. Piasetzky,² A. Schetkovsky,^{6,5} S. Shimanskiy,⁸ and D. Zhalov⁶

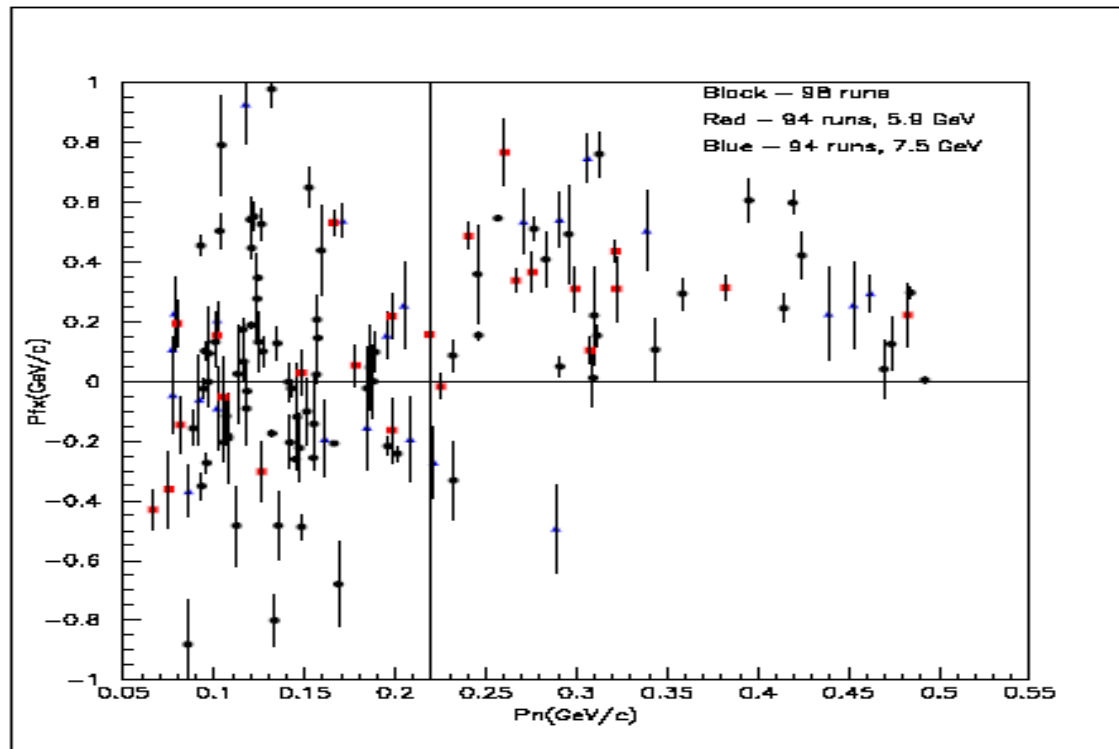
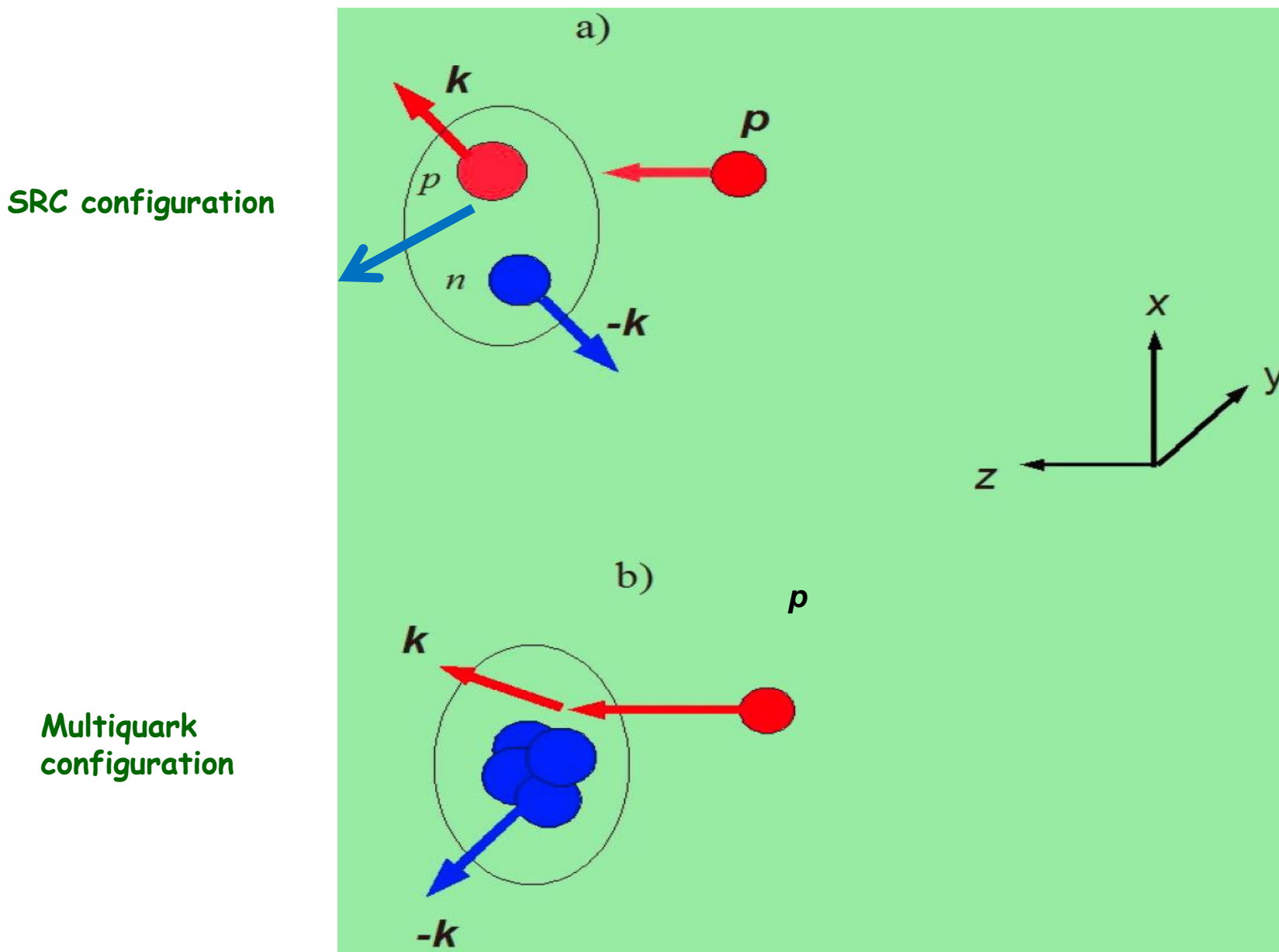


Figure I.5: The vertical component of the target nucleon momentum vs. the total neutron momentum. The positive vertical axis is the upward direction. The events shown are for triple coincidences of the neutron with the two high energy protons emerging from the QE C(p , 2*p*) reaction. The squares are for the 5.9 GeV/c incident beam and the triangles are for 7.5 GeV/c. The dots are preliminary unpublished data from the 1998 running period. We associate the events in the upper right corner with NN SRC.

Knot out cold dense nuclear configurations

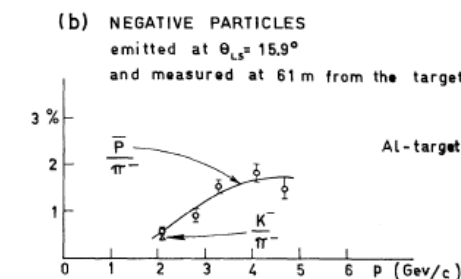
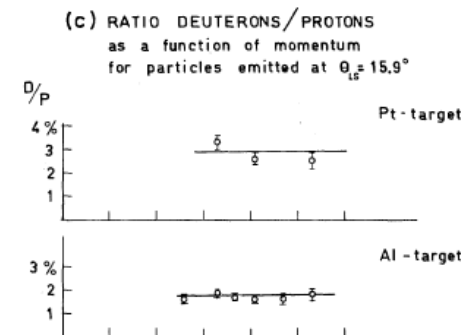
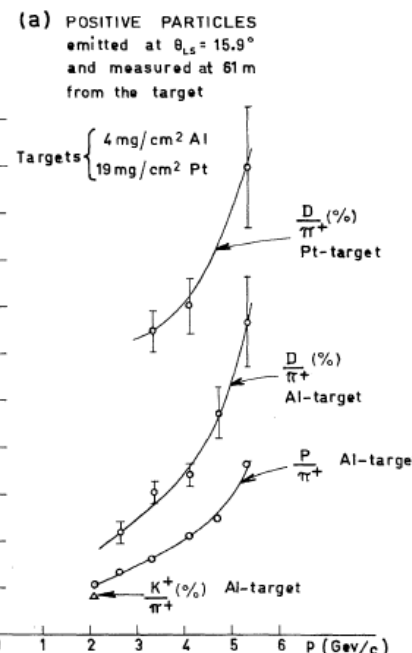


MASS ANALYSIS OF THE SECONDARY PARTICLES PRODUCED
BY THE 25-GEV PROTON BEAM OF THE CERN PROTON SYNCHROTRON

V. T. Cocconi,* T. Fazzini, G. Fidecaro, M. Legros,[†] N. H. Lipman, and A. W. Merrison
CERN, Geneva, Switzerland

(Received June 1, 1960)

We present here some results of a mass analysis of the secondary particles produced at 15.9° to the circulating beam in an aluminum target bombarded by 25-Gev protons in the CERN proton synchrotron.



Particle Production at Large Angles by 30- and 33-Bev Protons Incident on Aluminum and Beryllium*

V. L. FITCH, S. L. MEYER,[†] AND P. A. PIROUÉ
Palmer Physical Laboratory, Princeton University, Princeton, New Jersey
(Received February 12, 1962)

A mass analysis has been made of the relatively low momentum particles emitted from Al and Be targets when struck by 30- and 33-Bev protons. Measurements were made at 90°, 45°, and 13½° relative to the direction of the Brookhaven AGS proton beam. Magnetic deflection and time-of-flight technique were used to determine the mass of the particles.

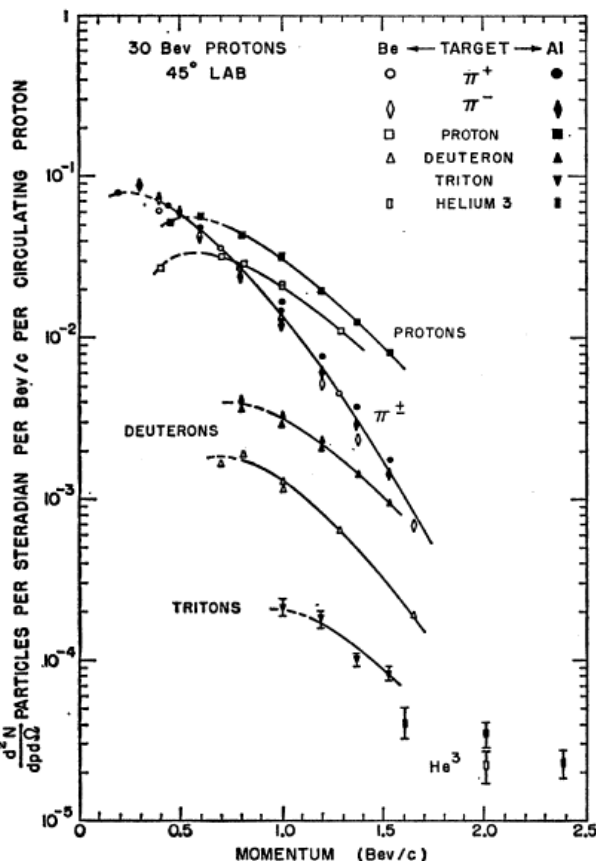


FIG. 3. Momentum spectra of particles emitted at 45° from aluminum and beryllium targets when struck by 30-Bev protons. Tritons from Be were not measured. For general remarks refer to Fig. 2 caption.

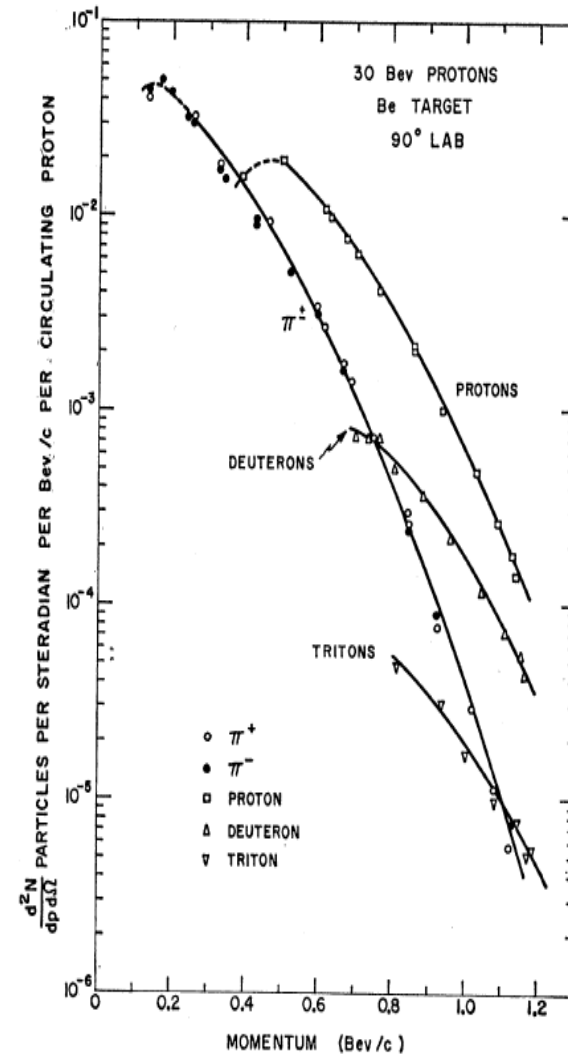


FIG. 2. Momentum spectrum of particles emitted at 90° from a beryllium target struck by 30-Bev protons. The ordinate is the number of particles produced at the target per steradian per Bev/c per circulating proton. The dashed portions of the curves indicate regions where the corrections due to multiple scattering exceed 15%. At the time these data were taken no effort was made to detect He^3 .

Production of hadrons at large transverse momentum at 200, 300, and 400 GeV *

J. W. Cronin, H. J. Frisch, and M. J. Shochet

The Enrico Fermi Institute, University of Chicago, Chicago, Illinois 60637

J. P. Boymond, P. A. Piroué, and R. L. Sumner

Department of Physics, Joseph Henry Laboratories, Princeton University, Princeton, New Jersey 08540

(Received 5 December 1974)

We have measured, as a function of transverse momentum (p_{\perp}), the invariant cross section $E d\sigma/d^3p$ for the production of π^\pm , K^\pm , p , \bar{p} , d , and \bar{d} in proton collisions with a tungsten (W) target at incident proton energies of 200, 300, and 400 GeV. The measurements were made in the region of 90° in the c.m. system of the incident proton and a single nucleon at rest. Measurements were also made with 300-GeV protons incident on Be, Ti, and W targets of equal interaction length. These p -nucleus measurements, which show a strong dependence on atomic number at high p_{\perp} , were used to extract effective proton-nucleon cross sections by extrapolation to atomic number unity. At large values of the scaling variable $x_{\perp} = 2p_{\perp}/\sqrt{s}$, where s is the square of the c.m. energy, the pion data are found to be well represented by the expression $(\sqrt{s})^{-n} e^{-ax_{\perp}}$, with $n = 11.0 \pm 0.4$ and $a = 36.0 \pm 0.4$. At $x_{\perp} < 0.35$, where similar measurements have been made at the CERN ISR, our data are in good agreement with the ISR data.

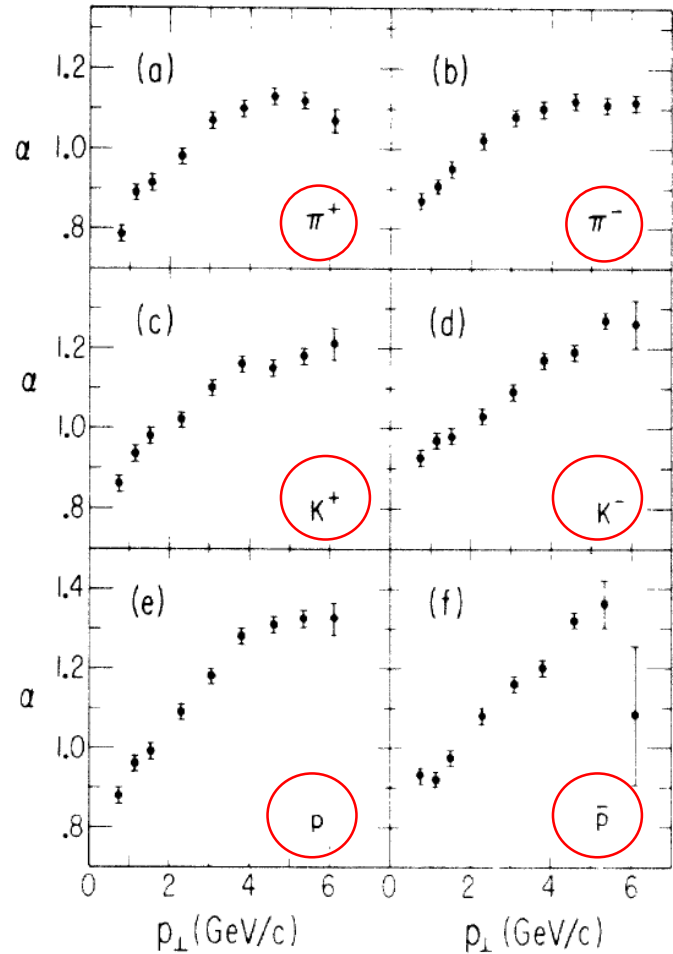
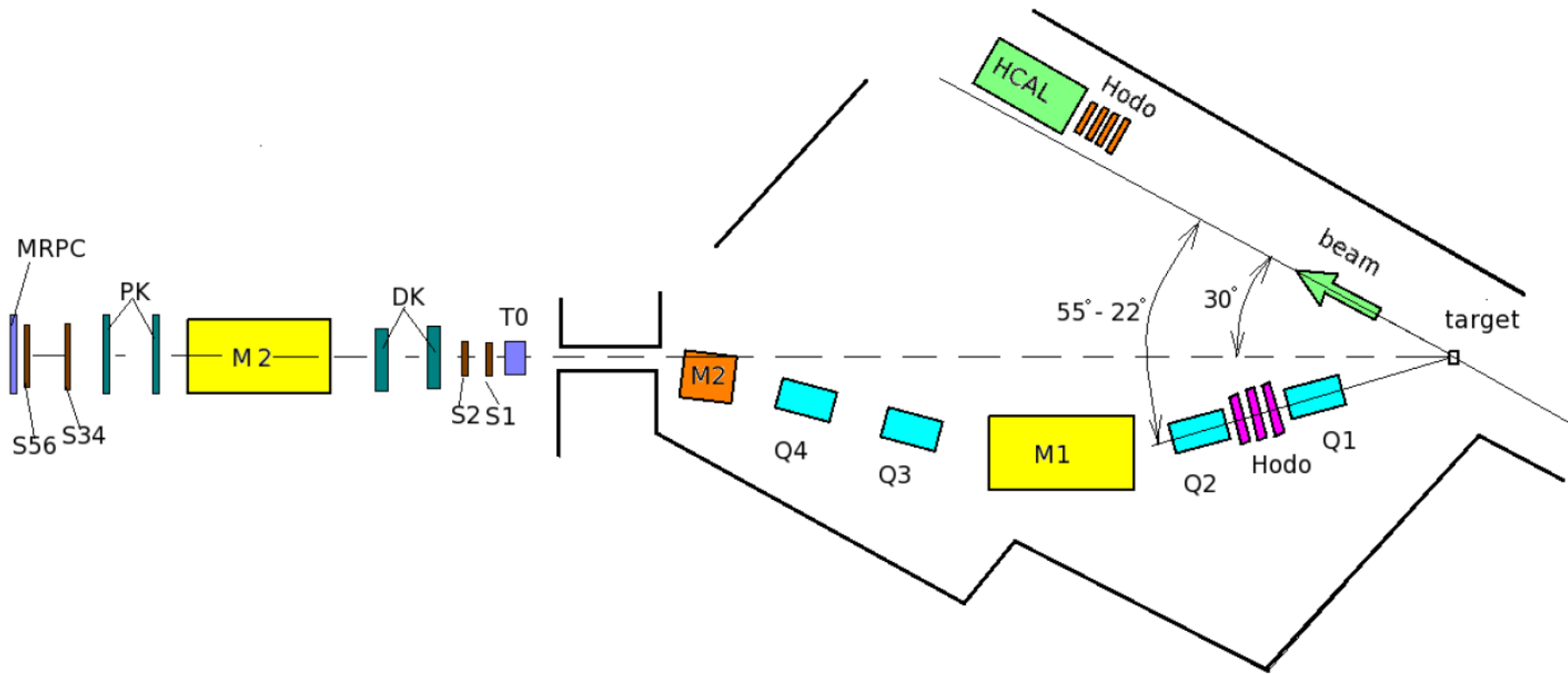
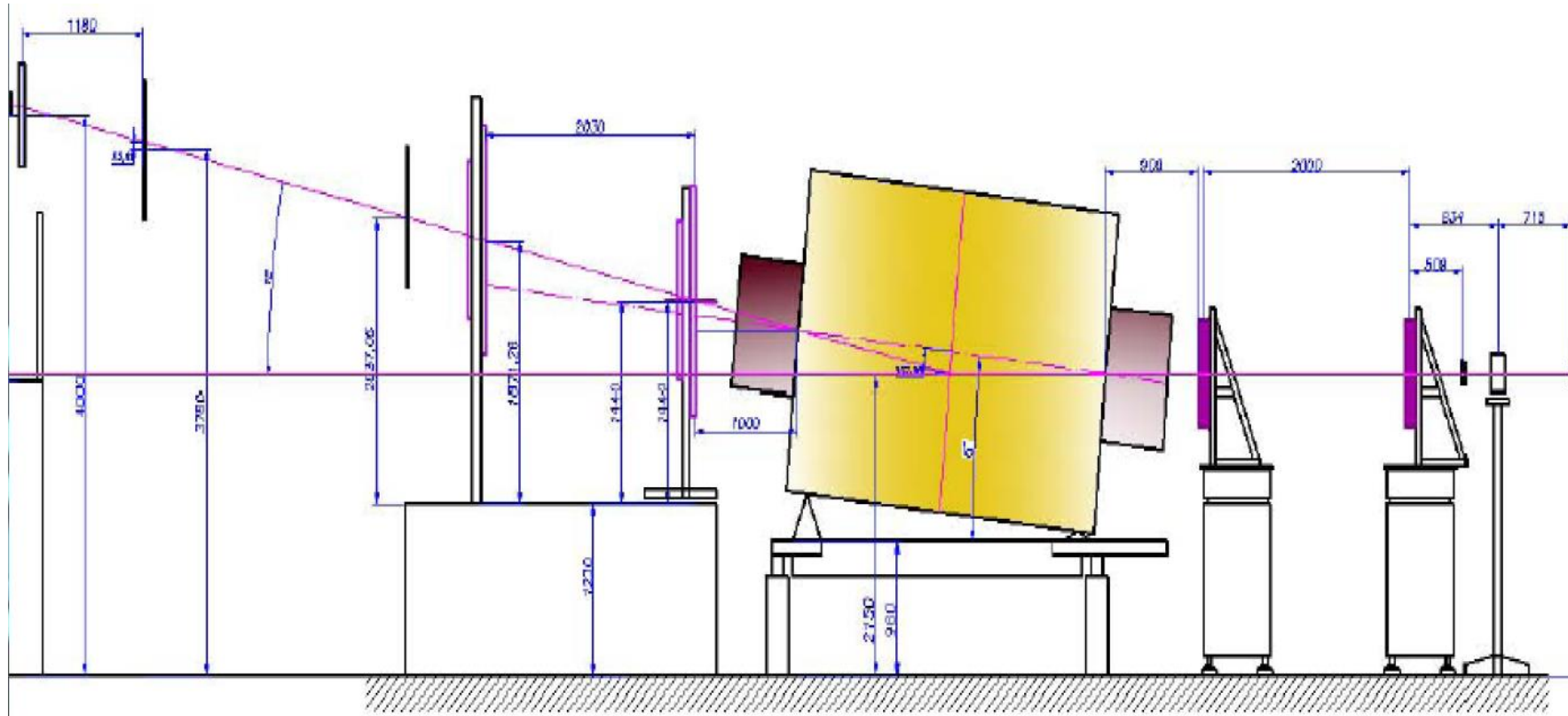


FIG. 17. Plots of the power α of the A dependence versus p_{\perp} for the production of hadrons by 300-GeV protons; (a) π^+ , (b) π^- , (c) K^+ , (d) K^- , (e) p , and (f) \bar{p} .

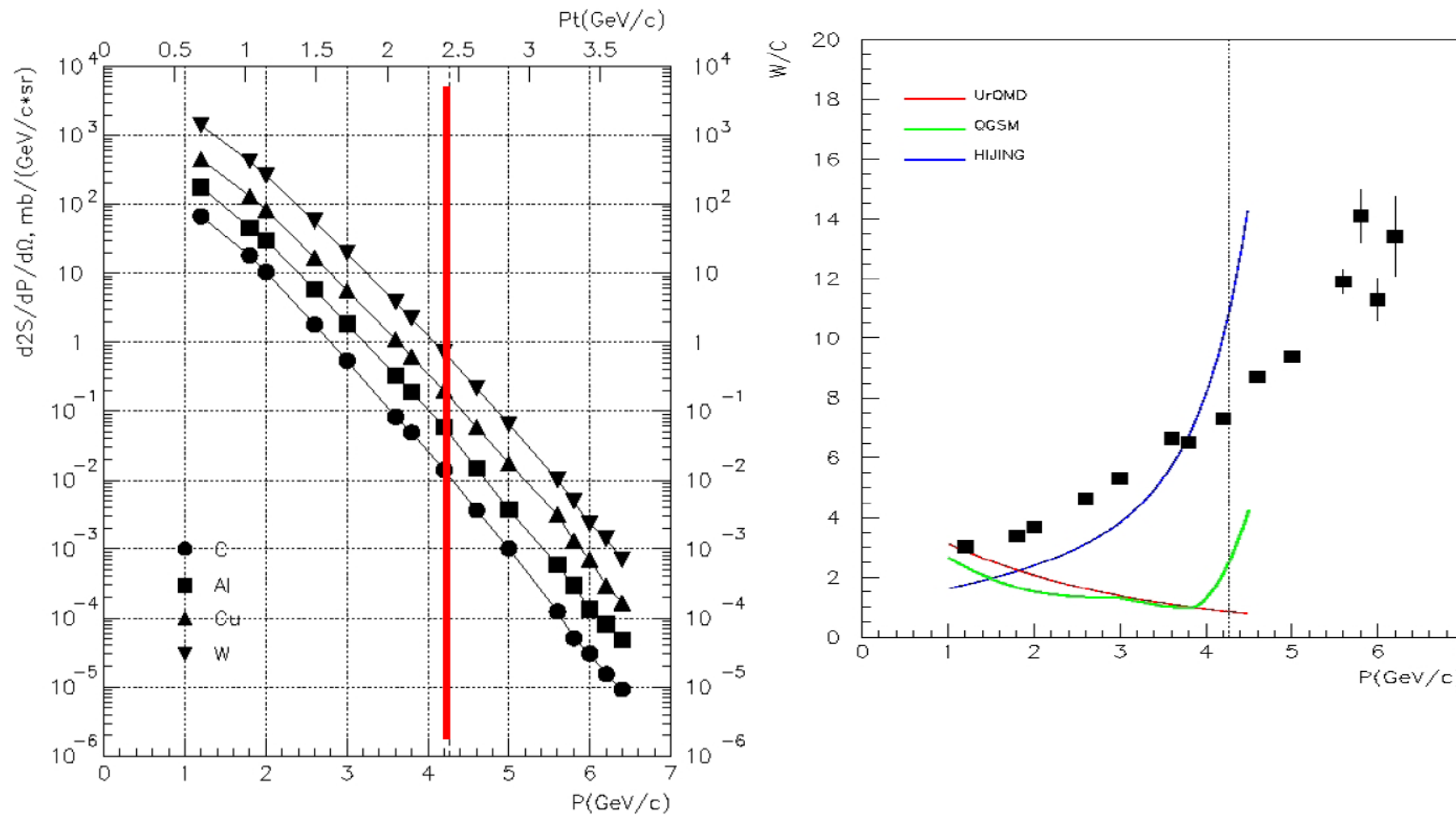
Установка СПИН в ИФВЭ (Протвина)



SPIN

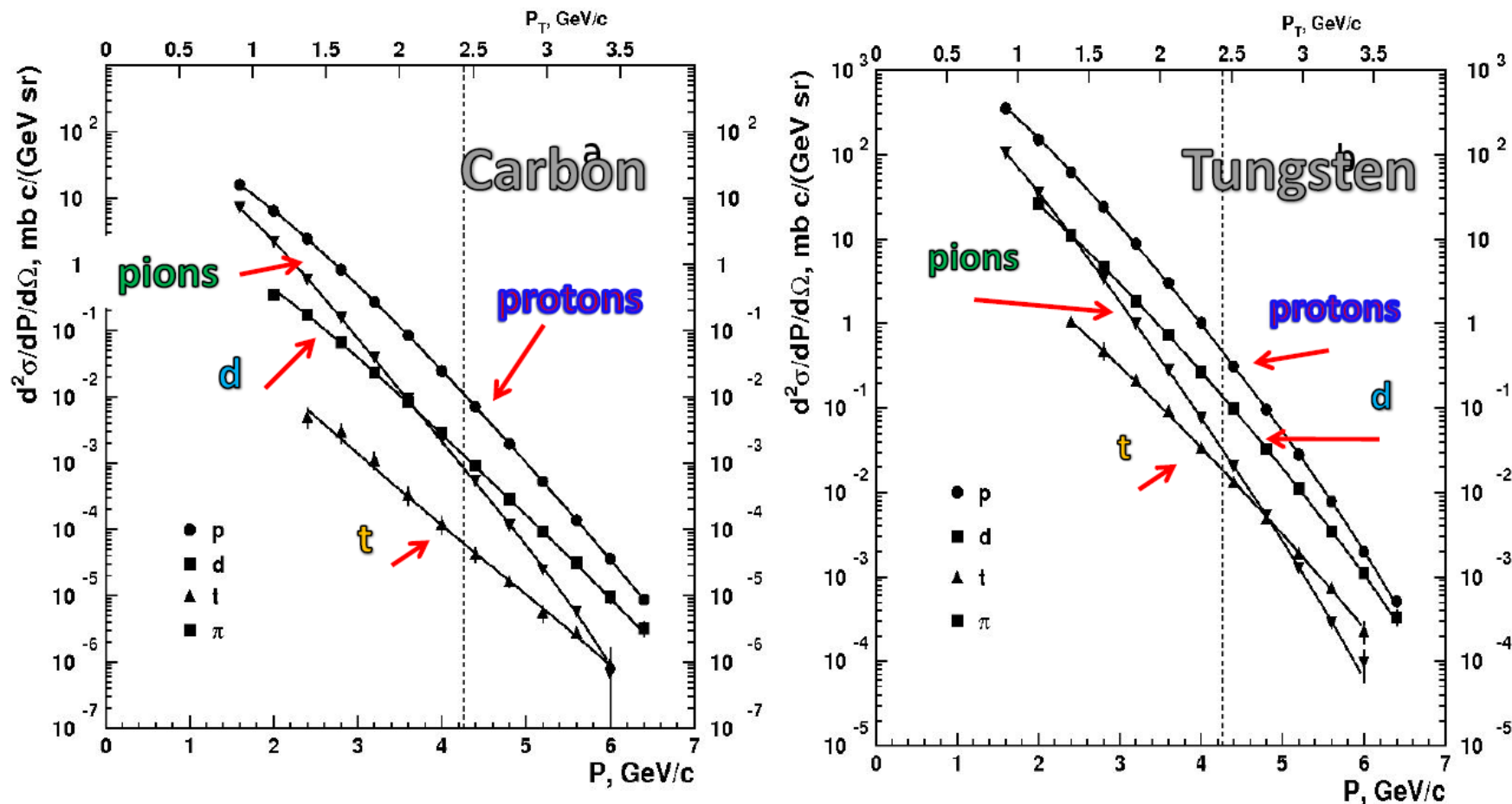


Предварительные данные установки СПИН реакция $p + A \rightarrow h(35^\circ) + X$



SPIN data

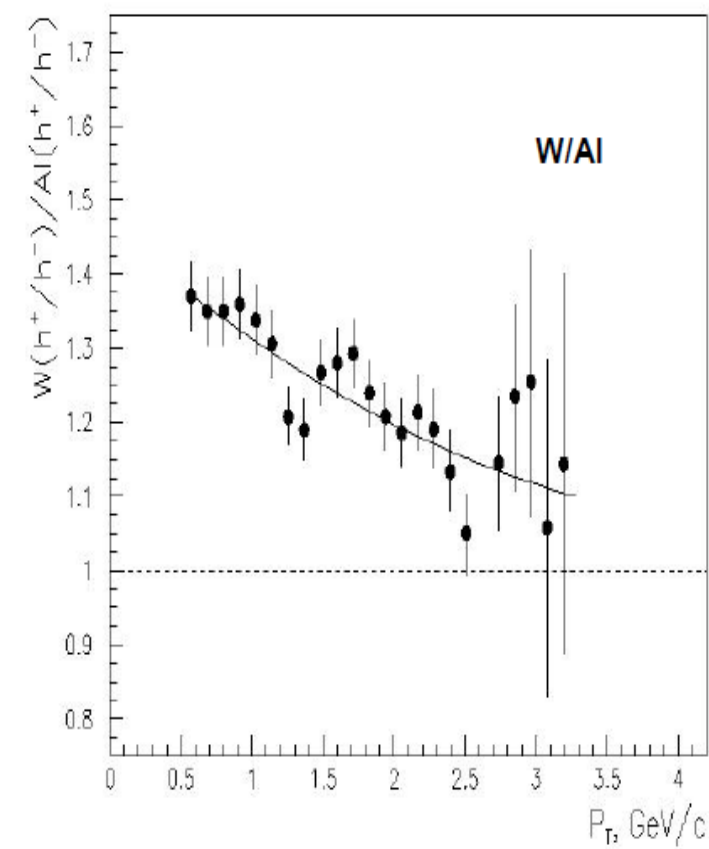
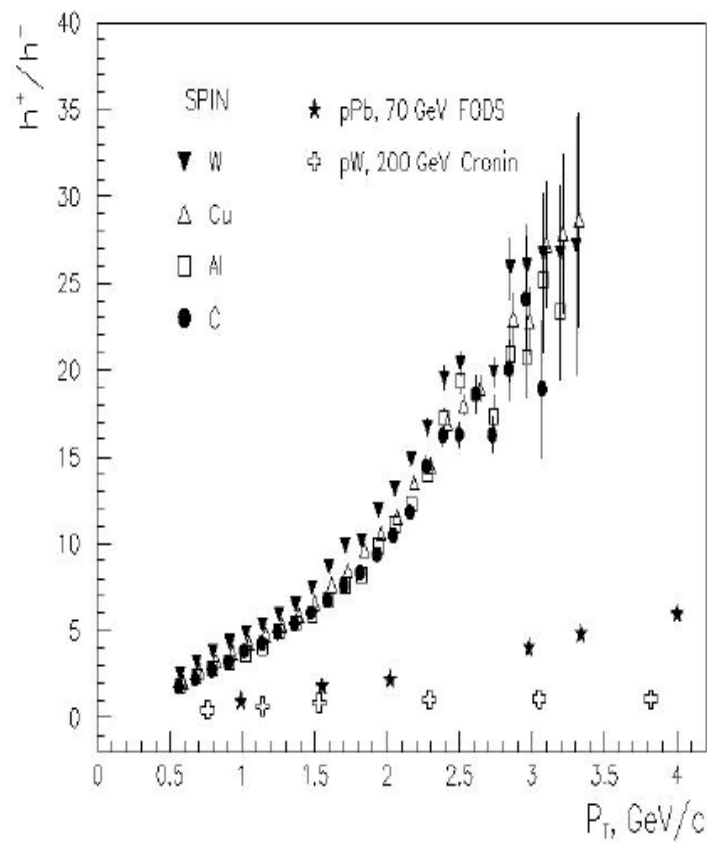
N.N. Antonov et al., *JETP Letters*, Vol.101, No.10,
pp.670-673(2015)



Invariant function found for positive pion, proton, deuteron and triton.

The vertical dashed lines indicate the kinematical limit for elastic nucleon-nucleon scattering. The upper horizontal scale shows values of the transverse momentum p_T .

Ratios

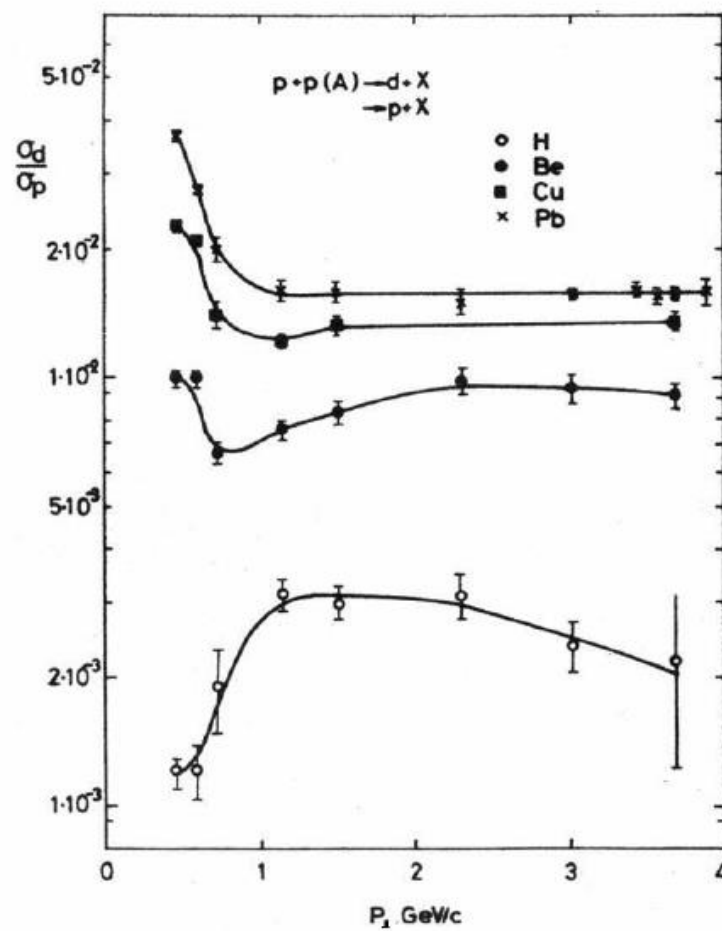
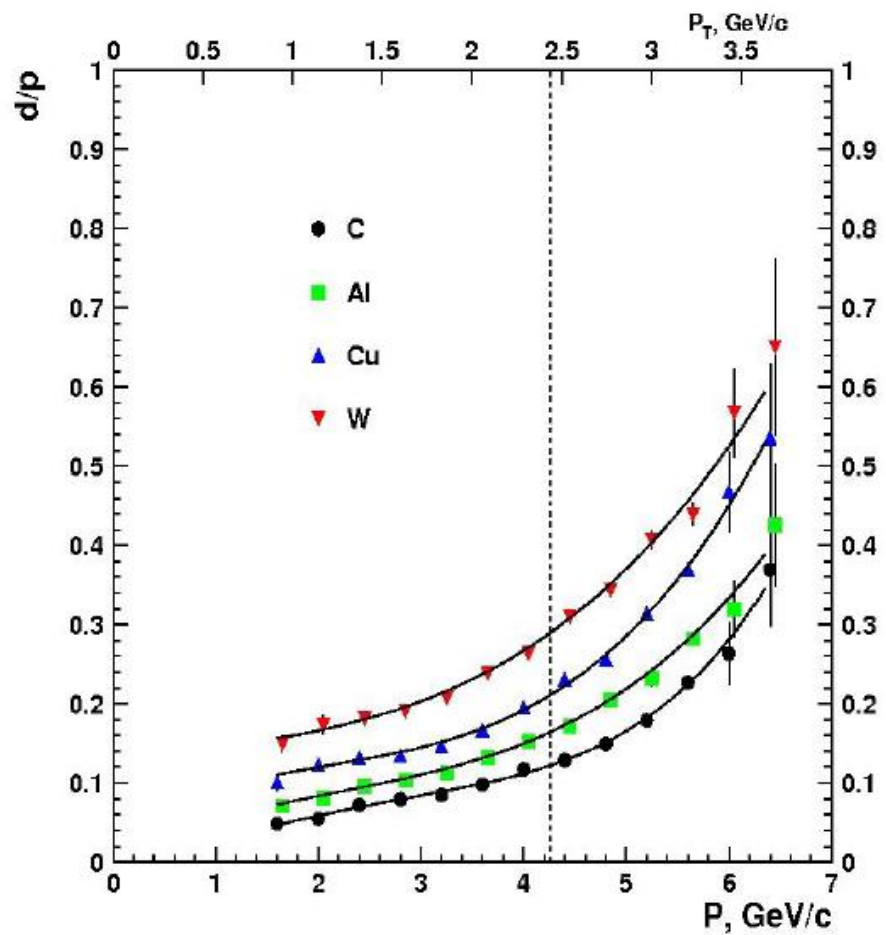


Ratio d/p

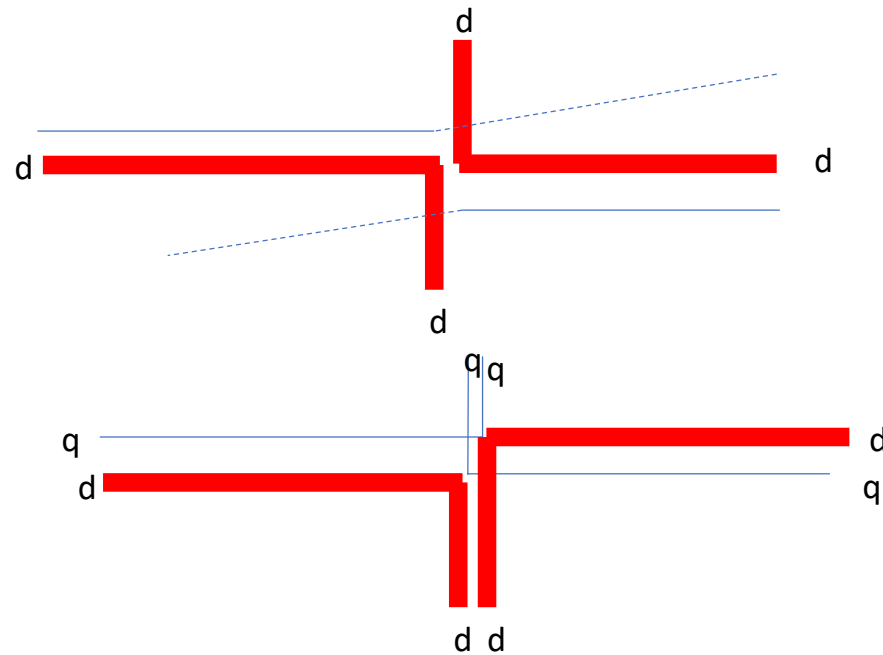
SPIN data

ФОДС

В.В.Абрамов и др.,
ЯФ 45(5) (1987), 845–851

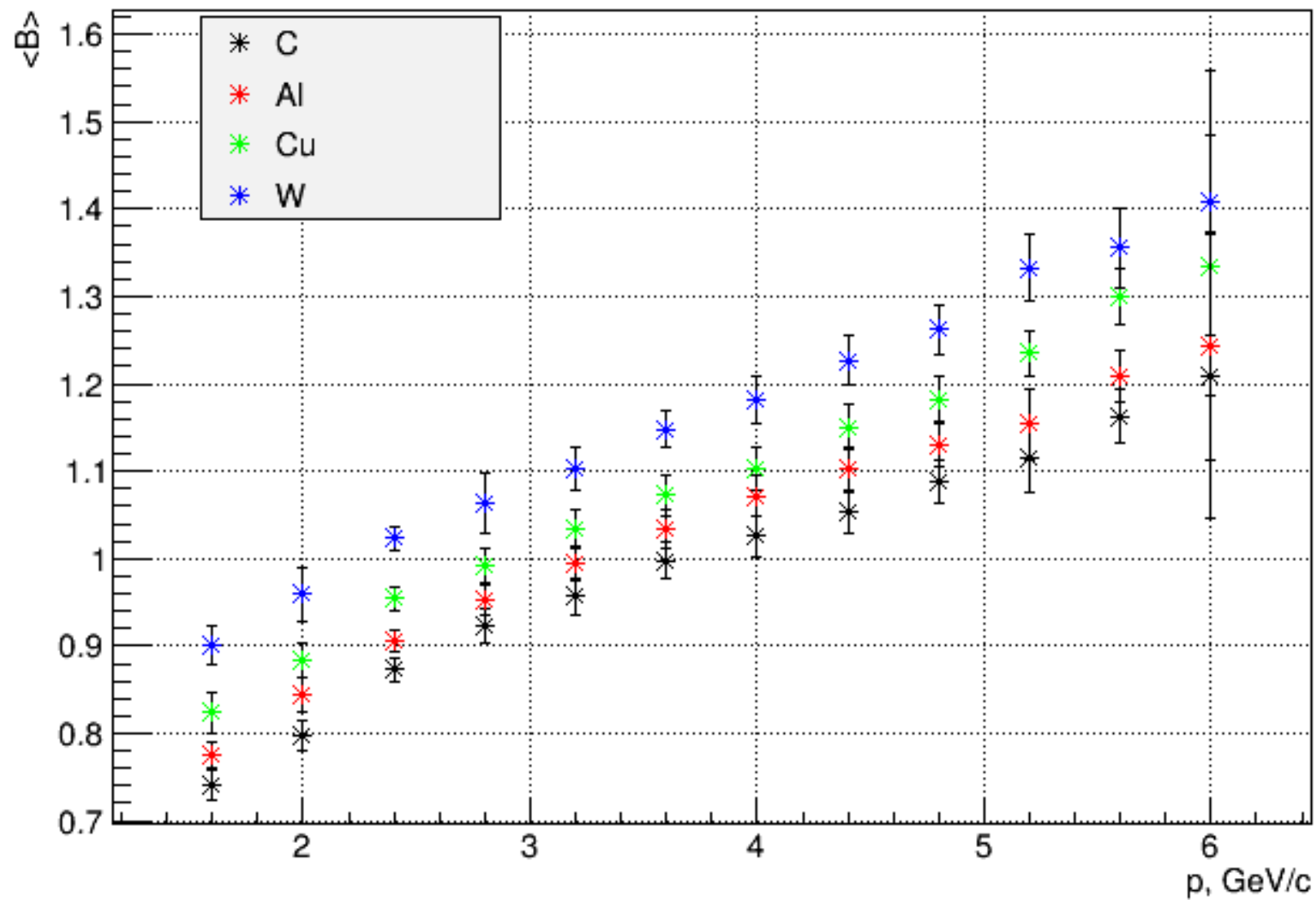


$pp \rightarrow p + X$, $pp \rightarrow D + X$ reactions with diquarks



Kim's mechanisms

Average baryon number $\langle B \rangle$



Knockout of Deuterons and Tritons with Large Transverse Momenta in pA Collisions Involving 50-GeV Protons

N. N. Antonov^a, A. A. Baldin^b, V. A. Viktorov^a, V. A. Gapienko^{a, *}, G. S. Gapienko^a,
V. N. Gres'^a, M. A. Ilyushin^a, V. A. Korotkov^a, A. I. Mysnik^a, A. F. Prudkoglyad^a,
A. A. Semak^a, V. I. Terekhov^a, V. Ya. Uglekov^a, M. N. Ukhanov^a,
B. V. Chuiko^{a†}, and S. S. Shimanskii^b

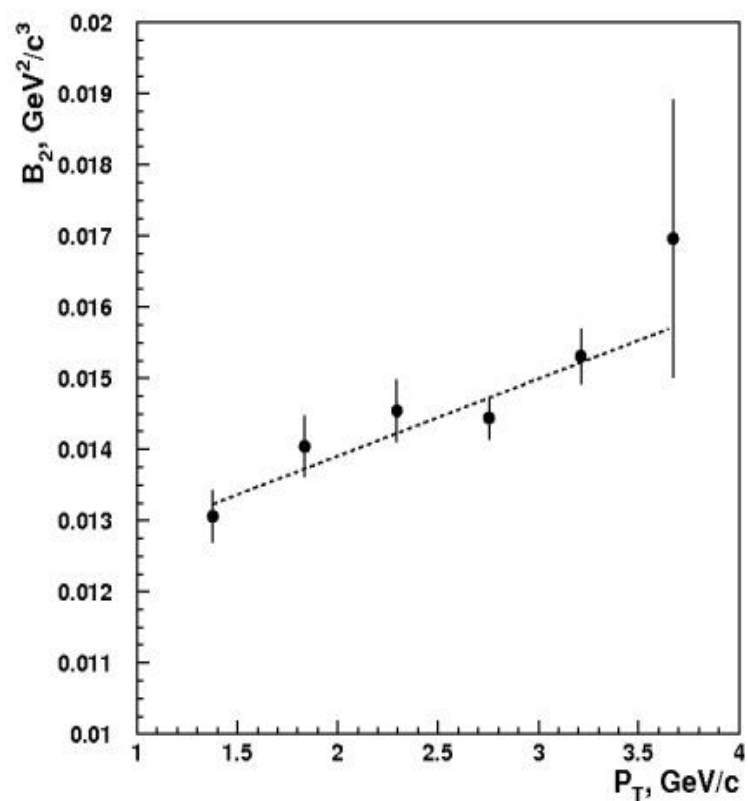
$$\frac{E_d}{\sigma_{inel}} \frac{d^3 \sigma_A}{dp_A^3} = B_A \times \left(\frac{E_p}{\sigma_{inel}} \frac{d^3 \sigma_p}{dp_p^3} \right)^A$$

Mean values of the B_2 parameter

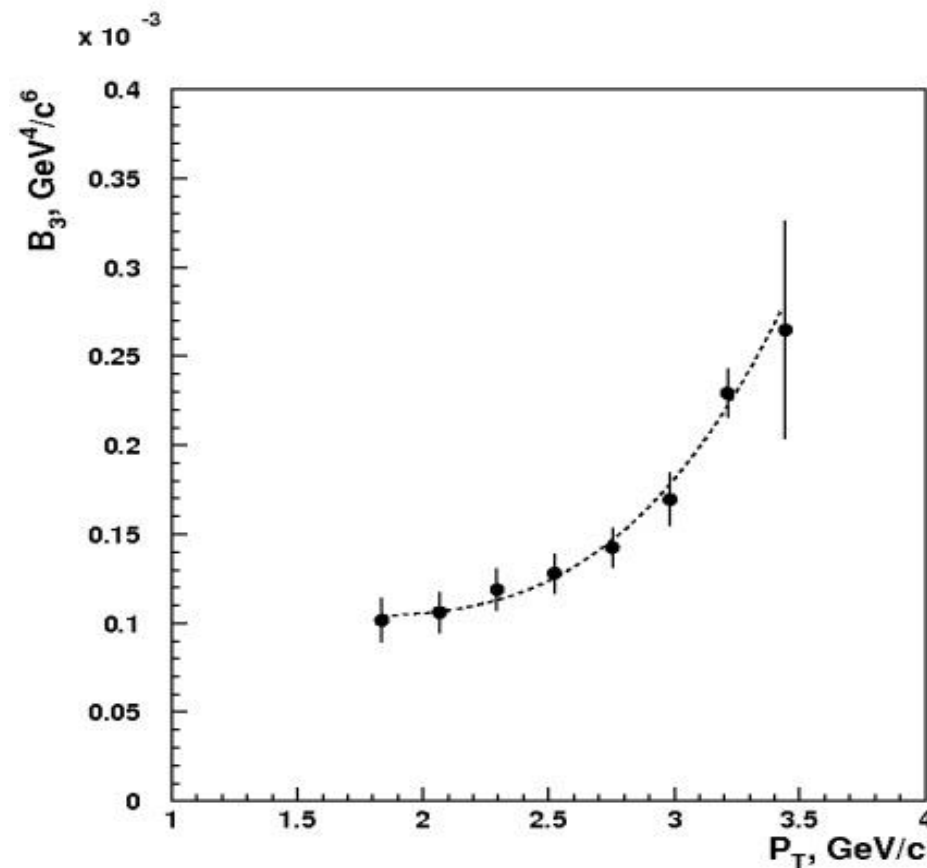
Target	C	Al	Cu	W
$B_2 \times 10^2, \text{GeV}^2/c^3$	1.41 ± 0.10	1.56 ± 0.08	1.51 ± 0.07	1.41 ± 0.06

SPIN data

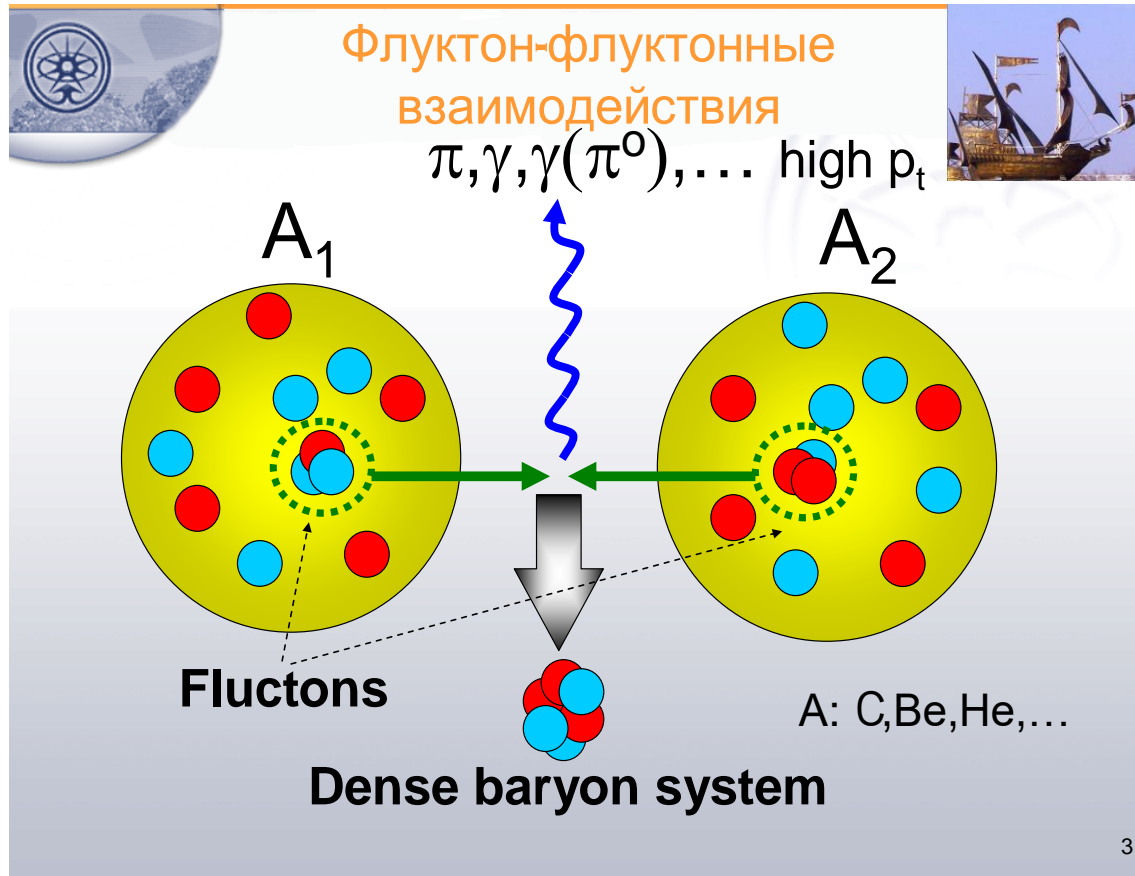
$$B_2 \sim V^1$$



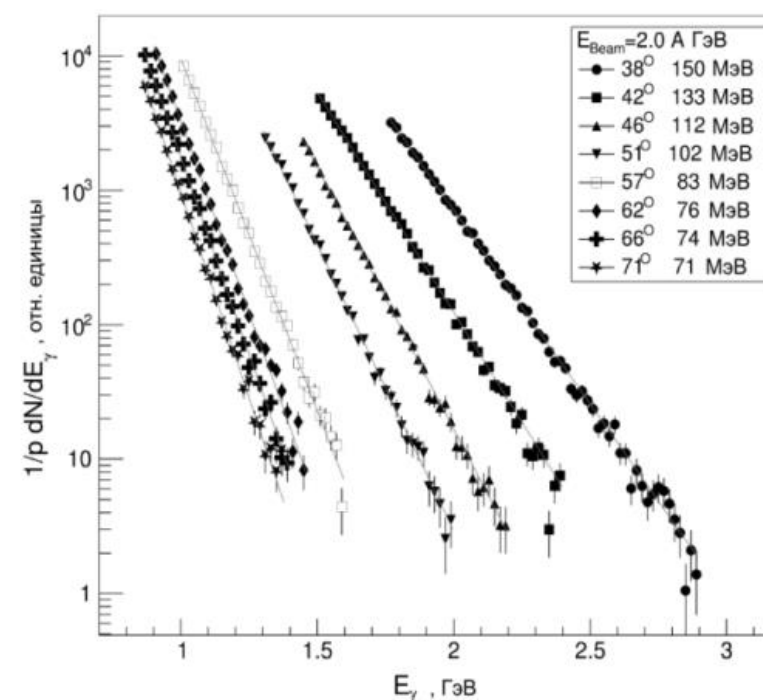
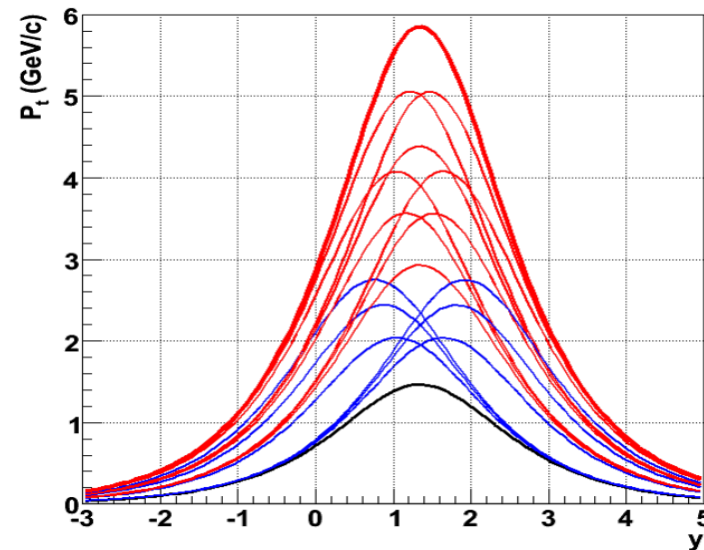
$$B_3 \sim V^2)$$



ITEP high p_T data



I.G.Alekseev et.al.(FLINT), ЯФ
 71(2008)1;
 A.Stavinskiy, EPJ Web Conf. 71
 (2014) 00125;
 K.R. Mikhailov et al.,
 Phys. Atom. Nucl. 77 (2014) 576;
 ЯФ 77 (2014) 610



CsDBM

1. **Cold** - exists inside ordinary nuclear matter as a quantum component of the wave function (with some probability and life time).
2. **superDense** - several nucleons can be in a volume less than the nucleon volume. The mass will be several nucleon masses. The small size means that the multinucleon(multiquark) configuration seeing as point like objects in processes with high transfer energy.
3. **Baryonic Matter** - enhancement of baryonic states and suppression of sea and gluon degrees of freedom (mesons and antiparticles production).

New DETECTOR Generation

“New directions in science are launched by new tools much more often than by new concepts.

The effect of a concept-driven revolution is to explain old things in new ways.

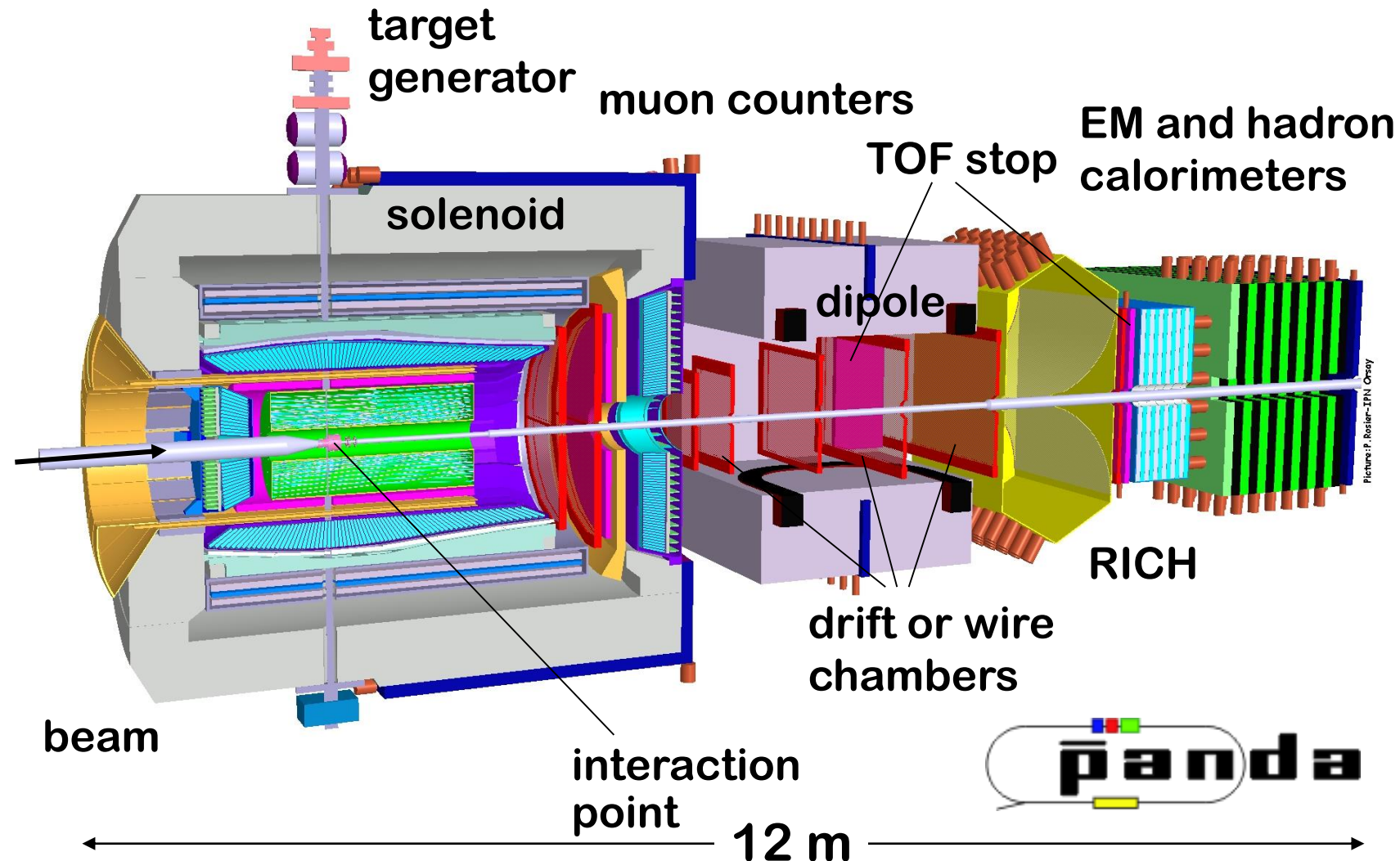
The effect of a tool-driven revolution is to discover new things that have to be explained”

From Freeman Dyson ‘Imagined Worlds’

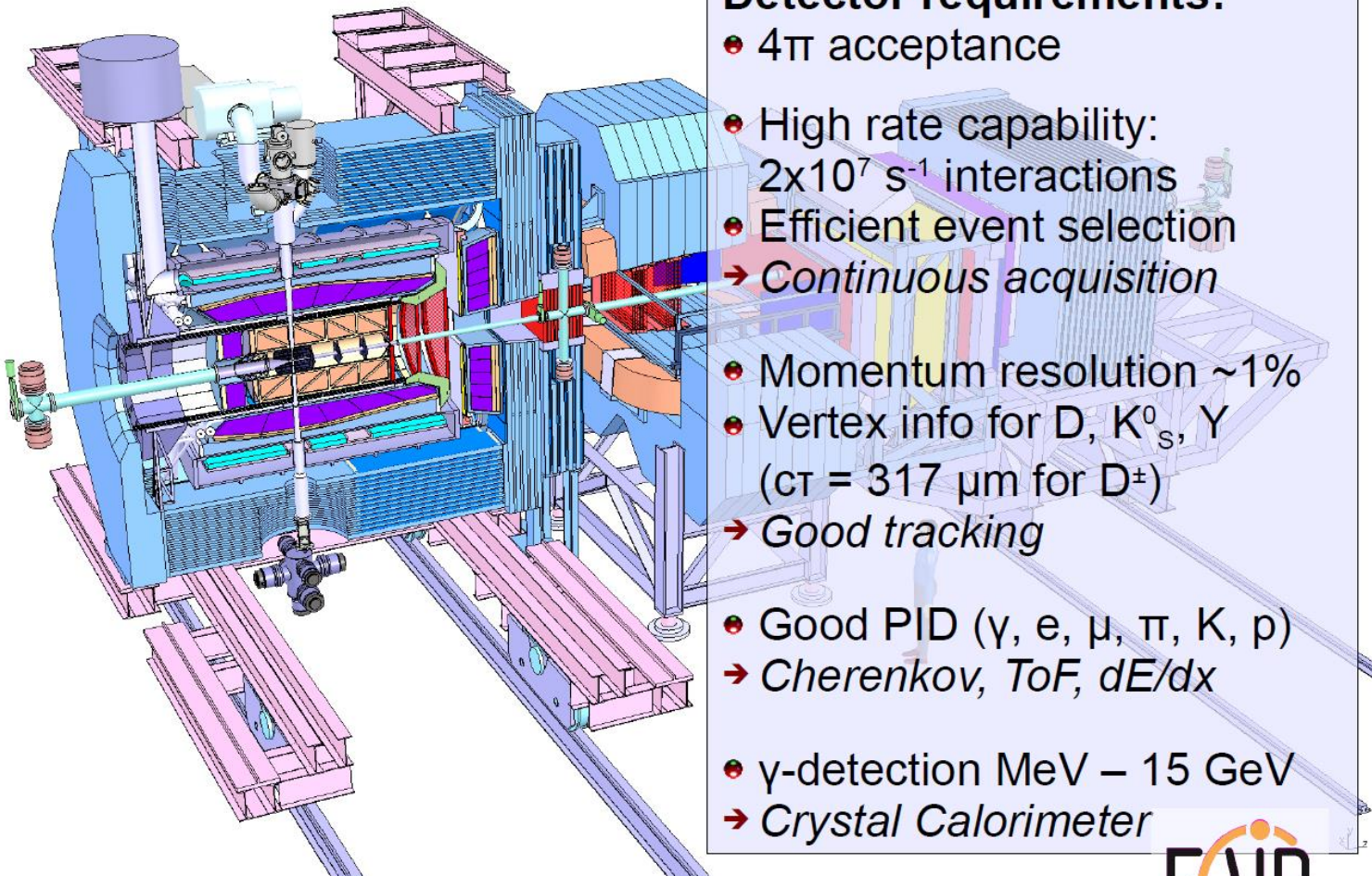


The PANDA Detector (antiproton beams 1-15 GeV)

$$\bar{p} + A \rightarrow \bar{p}' + \{X\}$$



PANDA Spectrometer



Detector requirements:

- 4π acceptance
- High rate capability:
 $2 \times 10^7 \text{ s}^{-1}$ interactions
- Efficient event selection
- Continuous acquisition
- Momentum resolution $\sim 1\%$
- Vertex info for D , K_s^0 , Υ
($c\tau = 317 \mu\text{m}$ for D^\pm)
- Good tracking
- Good PID (γ , e , μ , π , K , p)
- Cherenkov, ToF, dE/dx
- γ -detection MeV – 15 GeV
- Crystal Calorimeter



J-PARC HI -2016

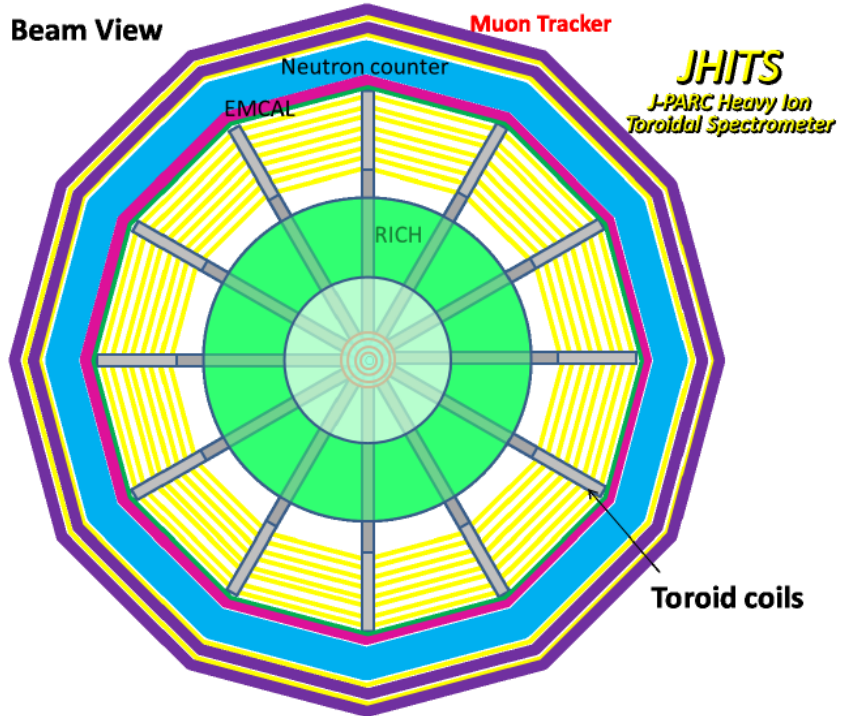


Figure 31: The beam view of the toroidal spectrometer (JHITS; J-PARC Heavy-Ion Toroidal Spectrometer).

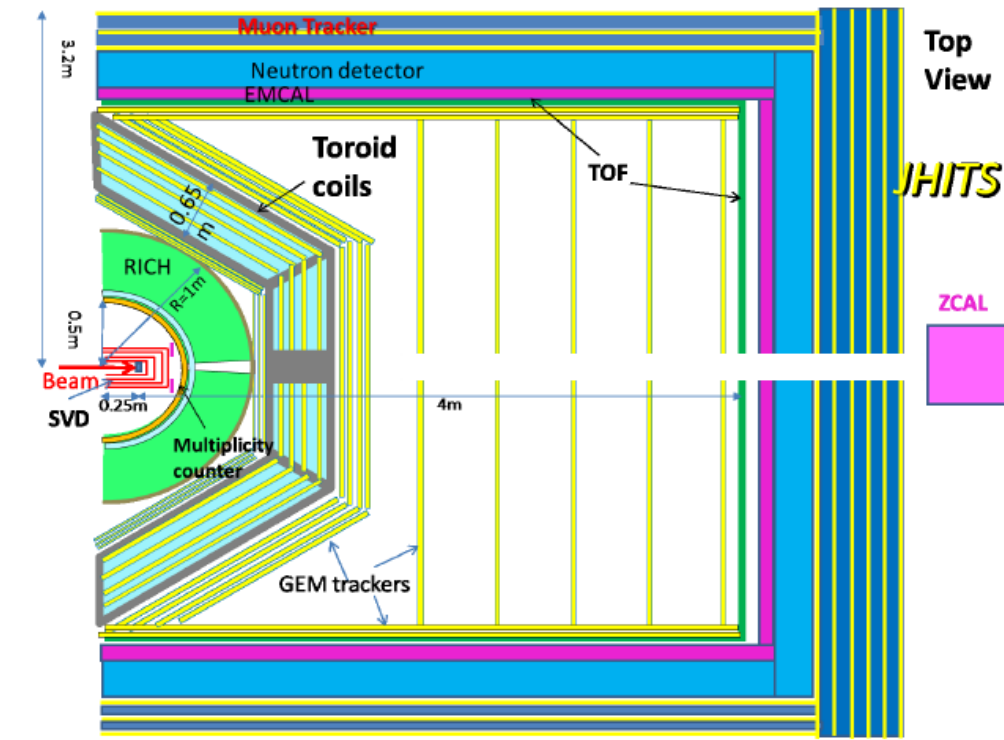


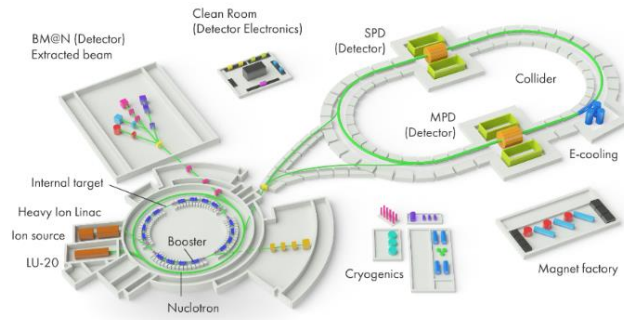
Figure 32: The top view of the toroidal spectrometer (JHITS; J-PARC Heavy-Ion Toroidal Spectrometer).

Main advantages

The unique beams: - wide range of kind of the beam particles (antiproton and polarization) and $\Delta p/p$ up to 10^{-5} .

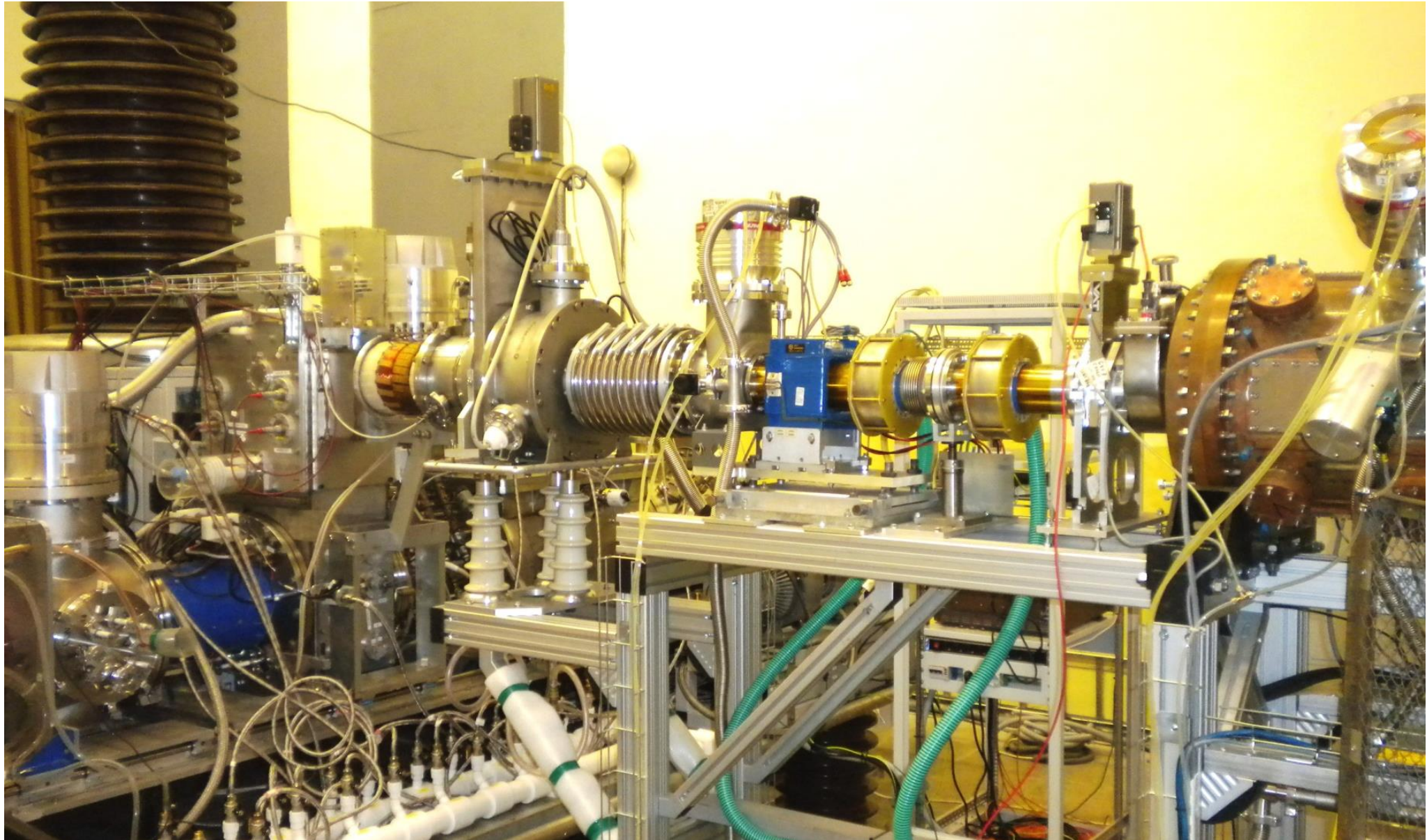
The unique detectors: $\Delta\Omega \sim 4\pi$ (exclusive reactions, correlations, backward range); detection all kinds of particles; working at luminosity $\sim 10^{32} \text{ cm}^{-2} \text{ s}^{-1}$ (the rare event can be investigated); PID - close to full energy range and high momentum resolution.

Requirements for the SPD

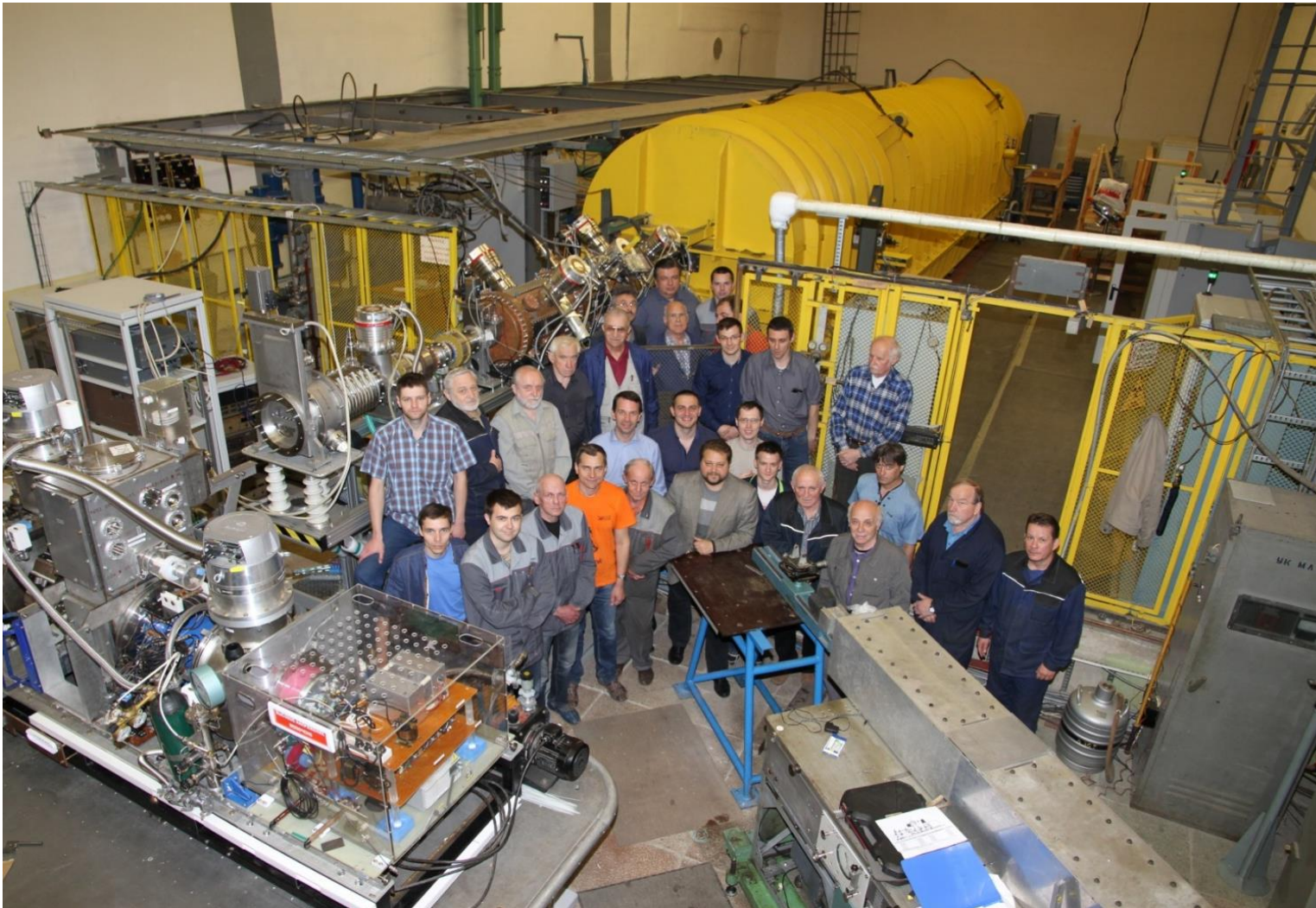


- close to 4π geometrical acceptance;
- high-precision ($\sim 50 \mu\text{m}$) and fast vertex detector;
- high-precision ($\sim 100 \mu\text{m}$) and fast tracker,
- good particle ID capabilities;
- efficient muon range system,
- good electromagnetic calorimeter,
- low material budget over the track paths,
- trigger and DAQ system able to cope with event rates at luminosity of $10^{32} (\text{cm.s})^{-1}$,
- modularity and easy access to the detector elements, that makes possible further reconfiguration and upgrade of the facility.

Implementation of polarized beam program



New for-injector LU-20 & SPI



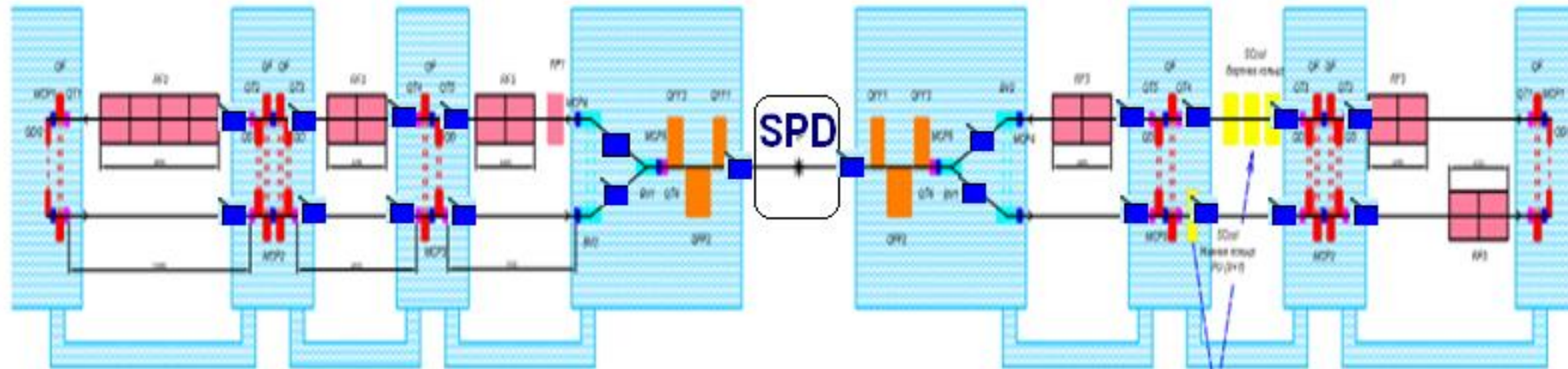
RUN #52, d+
Energy 750 MeV/u, intensity 10^9

May 16 2016: 1st beam in LU-20
June 12 2016: 1st beam from the SPI

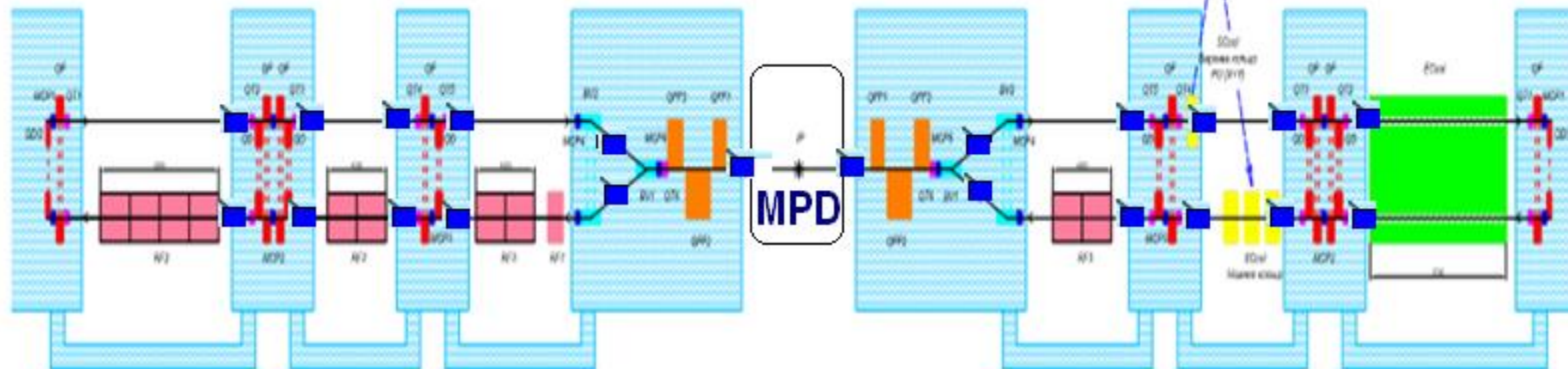
Polarization control in the Collider at $v_s = 0$

option 1: combination of the solenoids and RF

Южный промежуток (SPD)

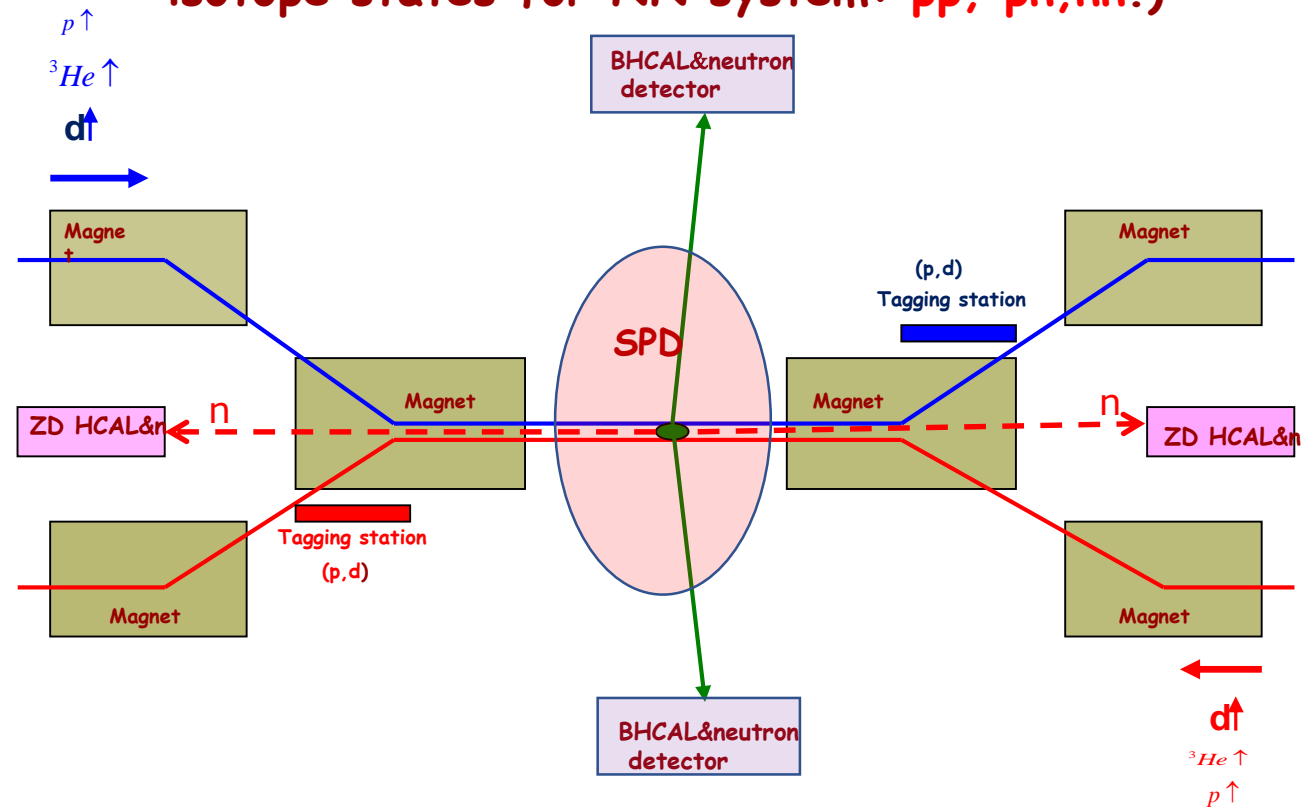


Северный промежуток (MPD)



- polarization control equipment

NICA Collision place for SPIN physics (deuteron and other beams, the first time all isotope states for NN system: pp, pn, nn.)

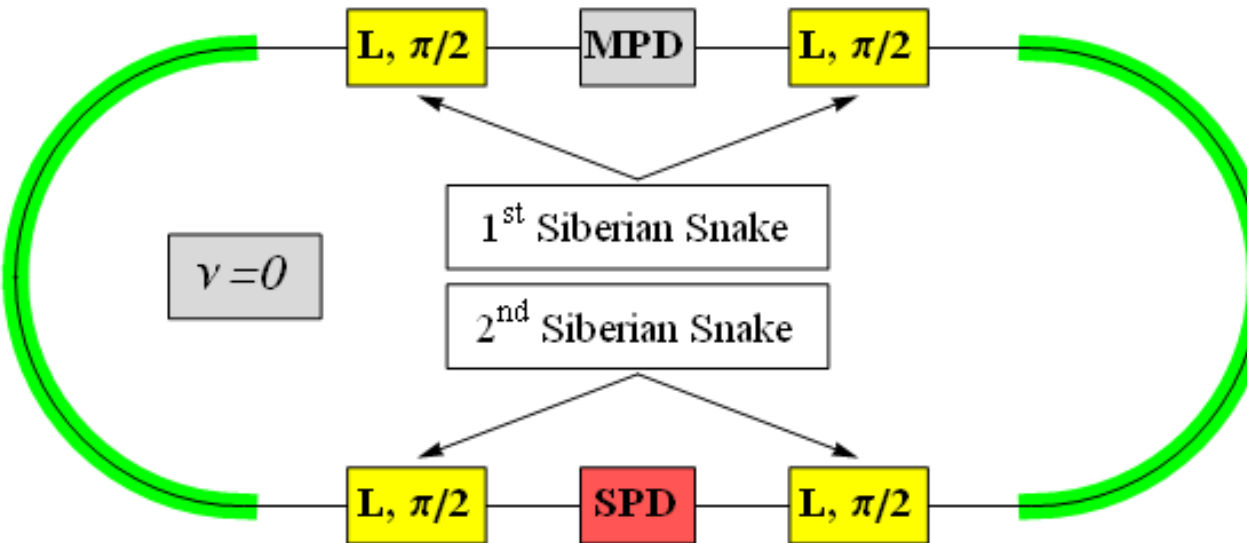


The tagging stations can be used as polarimeter!

Polarization control in the Collider at $v_s = 0$ (1)

Solenoidal Snake
at particle
momentum:

$$p = (2.5 \div 13) \text{ GeV}/c$$



Necessary integral of the magnetic field

protons:

$$(B_{||}L)_{\max} = 4 \times (5 \div 25) \text{ T}\cdot\text{m}$$

deuterons:

$$(B_{||}L)_{\max} = 4 \times (15 \div 80) \text{ T}\cdot\text{m}$$

Colliders with polarized ions

Collider	Momentum range, GeV/c	Colliding particles	Spin Tune	Spin Transparency
RHIC <i>(BNL)</i>	25-250	pp	1/2	—
JLEIC (<i>JLAB</i>) (figure-8)	25-100	eN	0	+
NICA <i>(JINR)</i>	2.5-13.5	NN	0	+

Ion Polarization Control

Collider	Spin Rotators based on	Polarization Direction at IP	Spin Flipping	
			Reversal Time	Orbital Parameters
RHIC <i>(BNL)</i>	‘strong’ magnetic fields	Transversal Longitudinal (w/o deuterons)	Few min	Change
JLEIC <i>(JLAB)</i>	‘weak’ solenoids	Any directions (any particles: p, d, He^3, \dots)	Few ms	Do not change
NICA <i>(JINR)</i>	‘weak’ solenoids	Any directions (any particles: p, d, He^3, \dots)	Few ms	Do not change

Spin Flipping System allows one to make spin reversal during an experiment (high precision experiments with polarized ions).

Spin Flipping System at the NICA collider

New regimes of filling the rings: all bunches with the same polarization in both rings. New modes of operation (spin-flippers are turned on by turns):

1-st ring	+++ ...	xxx	- - - ...	----	- - - ...	xxx	+++	----	+++ ...
2-nd ring	+++ ...	----	+++ ...	xxx	- - - ...	----	- - -	xxx	+++ ...
	(+ +)		(- +)		(- -)		(+ -)		(+ +)

|xxx| — spin-flipper is turned on. There is no data collection.

|----| — spin-flipper is not turned on. There is no data collection.

- The measurement of the luminosity between the bunches is resolved
- Operation with the same polarized ion mode in all bunches during the filling ring

SPD Hybrid system

$\frac{1}{2}$ model symmetry

$$B^{(z)}(x, y, 0) = 0.$$

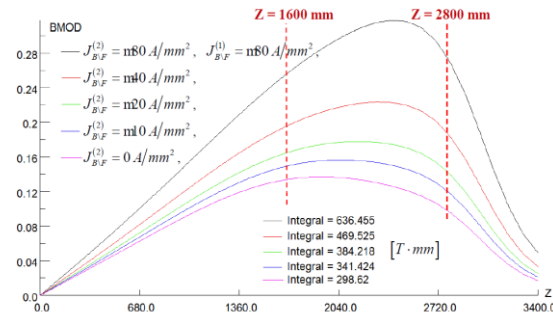
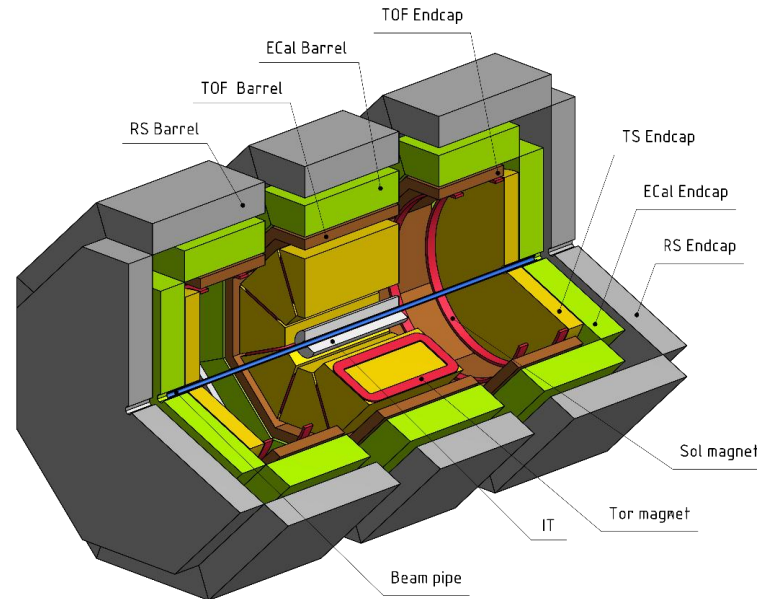
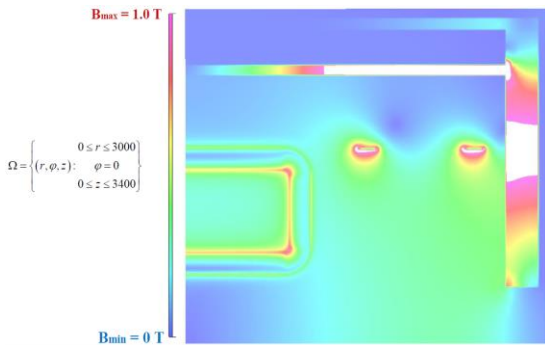
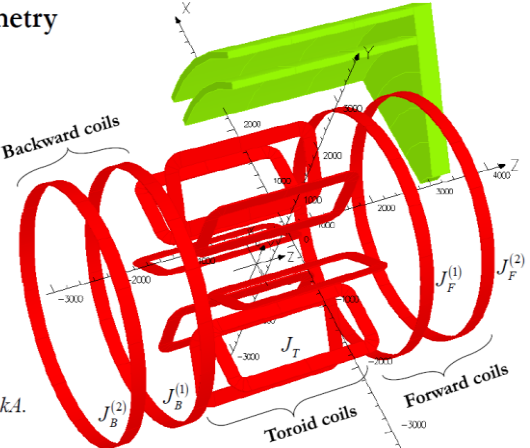
$$J_T = 40 \frac{A}{mm^2},$$

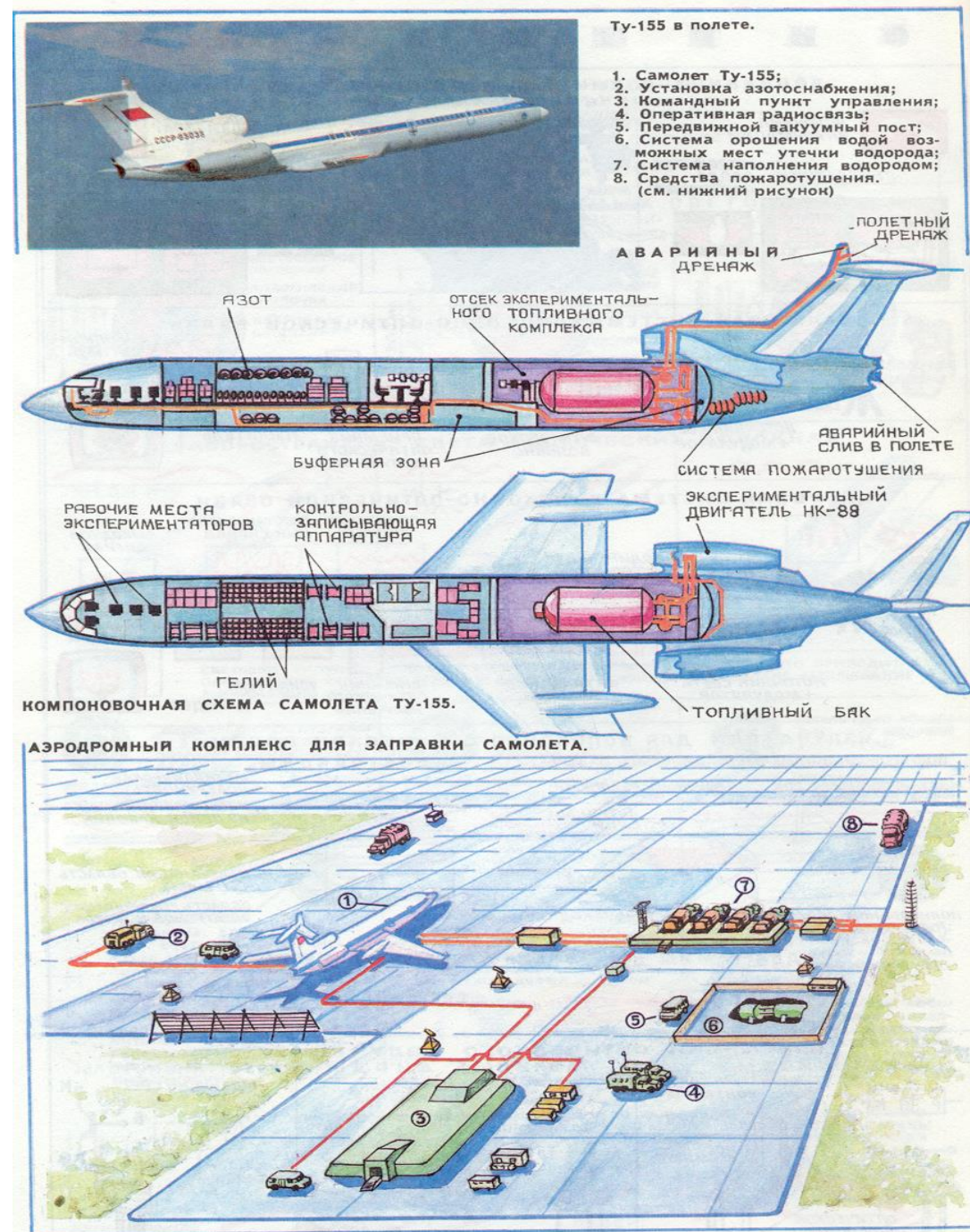
$$J_{B,F}^{(1,2)} = m80 \frac{A}{mm^2},$$

$$S = 200 \times 20 mm^2,$$

$$I_T = J_T \cdot S = 160 kA,$$

$$I_{B,F} = J_{B,F} \cdot S = m800 kA.$$





END